

## **General Disclaimer**

### **One or more of the Following Statements may affect this Document**

- This document has been reproduced from the best copy furnished by the organizational source. It is being released in the interest of making available as much information as possible.
- This document may contain data, which exceeds the sheet parameters. It was furnished in this condition by the organizational source and is the best copy available.
- This document may contain tone-on-tone or color graphs, charts and/or pictures, which have been reproduced in black and white.
- This document is paginated as submitted by the original source.
- Portions of this document are not fully legible due to the historical nature of some of the material. However, it is the best reproduction available from the original submission.

**NASA CR-**

CR-170435

METHODS OF SEQUENTIAL ESTIMATION FOR DETERMINING INITIAL DATA  
IN NUMERICAL WEATHER PREDICTION

STEPHEN E. COHN ✓  
NEW YORK UNIVERSITY  
COURANT INSTITUTE FOR MATHEMATICAL SCIENCES  
251 MERCER STREET  
NEW YORK, NY 10012

JUNE 1982

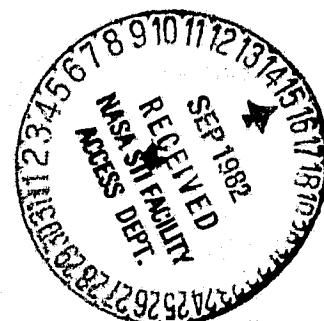
(NASA-CR-170435) METHODS OF SEQUENTIAL  
ESTIMATION FOR DETERMINING INITIAL DATA IN  
NUMERICAL WEATHER PREDICTION Ph.D. Thesis  
(New York Univ., New York.) 190 p  
HC A09/MF A01

N82-32937

Unclas  
CSCL 04B G3/47 33554

A DISSERTATION IN THE DEPARTMENT OF MATHEMATICS SUBMITTED TO THE  
FACULTY OF THE GRADUATE SCHOOL OF ARTS AND SCIENCE IN PARTIAL  
FULFILLMENT OF THE REQUIREMENTS FOR THE DEGREE OF DOCTOR OF PHILOSOPHY  
AT NEW YORK UNIVERSITY.

GRANTS: NSG 5034 ✓  
NSG 5130



**METHODS OF SEQUENTIAL ESTIMATION FOR DETERMINING INITIAL DATA  
IN NUMERICAL WEATHER PREDICTION**

**STEPHEN E. COHN**

**June 1982**

A dissertation in the Department of Mathematics submitted to the faculty of the Graduate School of Arts and Science in partial fulfillment of the requirements for the degree of Doctor of Philosophy at New York University.

Approved: Michael Ghil  
Michael Ghil  
Advisor

Approved: Eugene Isaacson  
Eugene Isaacson  
Advisor

METHODS OF SEQUENTIAL ESTIMATION FOR DETERMINING INITIAL DATA  
IN NUMERICAL WEATHER PREDICTION

Stephen E. Cohn

Advisors: Michael Ghil and Eugene Isaacson

ABSTRACT

Numerical weather prediction (NWP) is an initial-value problem for a system of nonlinear partial differential equations, in which initial values are known incompletely and inaccurately. Observational data available at the initial time must therefore be supplemented by data available prior to the initial time, a problem known as meteorological data assimilation.

A further complication in NWP is that solutions of the governing equations evolve on two different time scales, a fast one and a slow one, whereas fast scale motions in the atmosphere are not reliably observed. This leads to the so-called initialization problem: initial values must be constrained to result in a slowly evolving forecast.

The theory of estimation of stochastic-dynamic systems provides a natural approach to such problems. For linear stochastic-dynamic models, the Kalman-Bucy (KB) sequential filter is the optimal data assimilation method. We show that, for linear models, the optimal combined data assimilation-initialization method is a modified version of the KB filter. This modified KB filter combines the standard KB filter with a projection onto the slow solution subspace.

The shallow-water equations are a simple system whose solutions exhibit many features of large-scale atmospheric flow important in NWP.



We implement the standard and modified KB filters for a linearized version of these equations, given a simple observational pattern. The numerical results show that the modified filter produces a slowly evolving forecast, at the expense of forecast errors only slightly larger than those incurred by using the standard KB filter.

A statistical data assimilation method widely used at NWP centers is known as optimal interpolation (OI). We implement OI for the shallow-water model, and we use the estimation-theoretic framework to compare the performance of OI with that of the standard and modified KB filters.

Numerical results show that the simplifying assumptions involved in OI lead to relatively large errors near boundaries separating data-dense and data-sparse regions, and that proper initialization is a partial cure for this boundary effect. We show also how estimation theory can be used to tune the free parameters involved in OI, in such a way that the tuned scheme performs roughly as well as the modified KB filter.

## ACKNOWLEDGEMENTS

I wish to thank my thesis advisors, Professors Michael Ghil and Eugene Isaacson, for their excellent guidance, for their constant encouragement, and for their individual investments of time and energy in sharing their expertise with me.

I am very grateful to the faculty of the Courant Institute for providing outstanding instruction, and I am indebted to numerous researchers whose work I have drawn upon. I am particularly grateful to Professor Cecil Leith, for helping clarify several aspects of this dissertation during his recent stay at the Institute. I also want to thank Dr. Kenneth Bube and Dr. John Tavantzis, whose research provided much of the foundation for this work, and Dr. Amnon Dalcher, with whom I have had the benefit of many enlightening discussions.

The manuscript was cheerfully typed by Connie Engle, whose support is very much appreciated. Computations were carried out on the CDC 6600 of the Courant Mathematics and Computing Laboratory, under Contract DEAC0276ER03077-V with the U. S. Department of Energy; I am grateful to the CMCL staff for their assistance. I wish to acknowledge the generous financial support of the Laboratory for Atmospheric Sciences, Goddard Space Flight Center, which funded this work under NASA Grants NSG-5034 and NSG-5130.

I want to thank Mary Santi for her patience and encouragement during the writing of this dissertation. Finally, I am deeply grateful to my family, whose unflagging support has been essential to the completion of this work.

## CONTENTS

1.	Introduction	1
1.1.	Description of the problem and outline of results	1
1.2.	Background on numerical weather prediction	8
2.	Estimation Theory and Meteorological Data Assimilation	20
2.1.	The stochastic-dynamic models	20
2.2.	Unbiased linear data assimilation methods	24
2.3.	Assessing the performance of data assimilation methods	27
2.4.	Derivation of the Kalman-Bucy filter	29
2.5.	Optimality properties of the Kalman-Bucy filter	35
2.6.	Further remarks on estimation theory	36
3.	Slow Solutions of the Linear Shallow-Water Equations	40
3.1.	The equations	40
3.2.	Fourier series	43
3.3.	Solution of the initial-value problem	45
3.4.	The slow-wave subspace	47
3.5.	The eigenfrequencies and phase speeds	48
3.6.	Approximate slow initial data	53
4.	Slow Solutions of Discrete Linear Shallow-Water Equations	57
4.1.	The discrete equations	57
4.2.	The discrete Fourier transform	61
4.3.	Solution of the initial-value problem	65
4.4.	The eigenfrequencies and phase speeds	68
4.5.	The discrete slow-wave subspace	70

5. Estimation Theory and Initialization	73
5.1. Introduction	73
5.2. Projection matrices	75
5.3. The modified Kalman-Bucy filter	84
5.4. Computation of projections onto the slow-wave subspace	92
5.5. Choice of the weighting matrix	100
6. Experiments with the Standard and Modified Kalman-Bucy Filters	113
6.1. Observing pattern, noise covariances and initial data	113
6.2. Numerical results	122
7. Comparison with Optimal Interpolation	129
7.1. The optimal interpolation filter	129
7.2. Numerical results	134
References	140
Appendix. Proofs of Results in Chapter 5	145
Tables	167
Figure Captions	172
Figures	175

## CHAPTER ONE

### INTRODUCTION

#### 1.1. Description of the Problem and Outline of Results

One of the main reasons why we cannot tell what the weather will be tomorrow is that we do not know what the weather is today. In other words, numerical weather prediction (NWP) is an initial-value problem for which initial data are not available in sufficient quantity or with sufficient accuracy.

Numerical forecasts are now produced routinely by weather services in many countries. The models used in NWP are discretized versions of the partial differential equations which govern large-scale atmospheric flow. The spatial domain of many models surrounds either the entire globe or at least an entire hemisphere. Values of the atmospheric variables must be specified over a regular three-dimensional mesh at each initial forecast time.

Observational data, collected from a variety of ground-based, airborne and space-borne observing systems, are distributed very irregularly in space and time. At any single time, the data are too sparse over most of the globe to determine a complete set of initial values. Observational data are also subject to significant random, systematic and correlated errors.

Data available at the initial time of each forecast must therefore be supplemented with information from previous observations. The attempt to provide initial values for NWP models by use of all available data is known as four-dimensional data assimilation. The

adjective "four-dimensional" emphasizes that data distributed in both time and space must be used.

The current data assimilation practice at NWP centers is to linearly combine observations available at the initial time with a forecast issued from previous observations. A new forecast is then issued, and the process is repeated as further observations become available: the forecast model assimilates the data. The problem of four-dimensional data assimilation is essentially that of determining the best way to combine forecast and observed values.

The peculiar dynamics of the earth's atmosphere present a further difficulty in the determination of initial values. Namely, NWP is a problem with two time scales, in which motion on the fast time scale is not reliably observed.

The system of nonlinear partial differential equations which governs the atmosphere's dynamics admits two types of solutions: rapidly evolving solutions, which in the earth's atmosphere consist mostly of inertia-gravity waves, and slowly evolving solutions, consisting mostly of Rossby waves. In the earth's atmosphere, the fast-scale motions occur mainly on small spatial scales which are resolved neither by the observational network nor by global NWP models. Fortunately, the fast-scale components of motion typically carry much less energy than the slow-scale components. On spatial scales which NWP models are designed to resolve, the slow motions are the significant ones.

Initial data for NWP models must be chosen accordingly: the data must be constrained to result in a slowly evolving forecast. Improperly chosen initial data lead to spurious fast waves which appear

as large, transient errors in the forecast of every meteorological variable. Forecasts of vertical motion, and therefore precipitation forecasts, are particularly affected by the spurious waves.

The process of adjusting initial data so that a slowly evolving forecast ensues is known as initialization. Customarily, a data assimilation method provides "first guess" initial data, which are then adjusted by application of an initialization scheme.

The estimation theory of stochastic-dynamic systems provides a natural framework for studying the data assimilation-initialization problem. In the approach of estimation theory, the evolution of the atmosphere is assumed to differ from that of a given NWP model by random increments; the random increments are meant to account for modeling errors. Thus, the "true" atmospheric state is governed by a stochastic-dynamic model. Observations are treated similarly: they are noisy "output" of the stochastic-dynamic atmospheric model.

In the context of estimation theory, the data assimilation problem is that of estimating the "true" state, given the unperturbed, imperfect NWP model, and given inaccurate, incomplete observations of the "true" state. The initialization problem is that of constraining the state estimates, or forecast, to evolve slowly.

In this dissertation, we apply estimation theory to study the data assimilation-initialization problem, in two ways. First, we formulate a combined data assimilation-initialization method which is statistically optimal for linear stochastic-dynamic models. Second, by means of numerical experiments with a simple linear model, we compare this method with the method of "optimal interpolation" which is widely used at NWP centers.

For linear stochastic-dynamic models, the discrete Kalman-Bucy (KB) filter of estimation theory is the statistically optimal data assimilation method. The KB filter is optimal in that it simultaneously minimizes all quadratic measures of the estimation error, i.e., all quadratic functionals of the difference between the estimated state and the true state. Like data assimilation methods in operational use at NWP centers, the KB filter processes data sequentially: observations are discarded once they have been processed, so that past observations are used only in the form of a forecast issued from them. The optimality and sequential nature of the KB filter has led to its successful use in a wide variety of engineering problems.

The KB filter does not automatically provide slowly evolving state estimates, however, and therefore it is not directly applicable to NWP. To find a combined data assimilation-initialization algorithm, we solve a constrained minimization problem. Namely, we require that a quadratic functional of the estimation error be minimized, subject to the constraint that the ensuing state estimates will evolve slowly.

The solution turns out to be a modified form of the standard KB filter. It is given by multiplying the usual KB gain matrix, which specifies the linear combination of forecast and observed values, by a matrix which projects onto the set of data which lead to slowly evolving forecasts. That is, the KB gain matrix is multiplied by a projection matrix onto the model's slow-wave subspace. The projection matrix depends on the choice of error functional, and thus a tradeoff is involved in constraining the estimates to evolve slowly: the modified filter depends on the choice of error functional, whereas the



standard KB filter does not. When using the modified KB filter, one must choose the error functional to be minimized.

The modified KB filter is equivalent to combining the standard KB filter with the method of variational linear normal mode initialization which is used at NWP centers. In this initialization method, the first guess estimate provided by a data assimilation scheme is projected onto the slow-wave subspace, in such a way as to minimize a quadratic functional of the difference between the first guess and the initialized estimate. Inasmuch as the first guess in our case is provided by the KB filter, the modified filter minimizes also a functional of the difference between the true state and the initialized estimate. This property is important in deciding upon an appropriate error functional to be minimized.

A simple model whose solutions exhibit many features of large-scale atmospheric flow, including the two time-scale behavior, is the one governed by the shallow-water equations. We implement the standard and modified filters for a linear, one-dimensional version of the shallow-water equations. We use a simplified observing pattern based on the conventional meteorological observing network.

One of the advantages of the estimation-theoretic framework is that it provides a way of assessing the performance of data assimilation schemes: the estimation error variances evolve in a known way. We make use of this fact to compare the performance of the standard and modified filters in our shallow-water model. The results show that the modified filter does indeed produce slowly evolving estimates, and at the expense of estimation errors only slightly larger than those of the standard KB filter.

Our numerical experiments also demonstrate that the two filters automatically determine observational weights in accordance with local data density and with the amount of information advected between data-dense and data-sparse regions. In particular, the filters are able to discern between data-sparse regions located upstream and downstream from a data-dense region.

For our second application of estimation theory, we implement a version of optimal interpolation (OI) for our shallow-water model. This data assimilation method is in use at a number of NWP centers and is under development at several others. Optimal interpolation is based on a number of assumptions concerning forecast error correlations and the evolution of forecast error variances.

We use the estimation-theoretic framework to assess the performance of OI in our model, and we compare the performance of OI with that of the standard and modified KB filters. Our numerical results suggest that the simplifying statistical assumptions involved in OI lead to relatively large errors near boundaries separating data-dense and data-sparse regions. We show that proper initialization is a partial cure for this boundary effect, in that initialization helps keep estimation errors localized.

A number of free parameters, such as forecast error variance growth rates over different regions, are specified in OI schemes. We show that, by monitoring the size of estimation errors, these parameters may be adjusted, or tuned. The results show that, when the growth rates are properly tuned, the performance of an initialized version of OI is roughly comparable to that of the modified KB filter.

The tuning is a way of allowing the OI scheme to make some use of advected information.

We hope that our results, both theoretical and numerical, lead to a better understanding of the interaction between initialization and four-dimensional data assimilation.

In Section 1.2, we review several aspects of NWP models and meteorological observing systems, in order to acquaint the reader with some of the practical considerations involved in numerical weather prediction. We also discuss the general formulation of data assimilation methods and we discuss normal mode initialization methods in some detail.

In Chapter 2, we review the relevant aspects of estimation theory. We show, in particular, how estimation theory can be used to assess the performance of data assimilation schemes. A simple derivation of the KB filter is presented also.

In Chapter 3, we introduce the linearized shallow-water equations, and we formulate and discuss their slow-wave subspace. The discrete version of the shallow-water equations upon which our numerical experiments are based is given in Chapter 4, where we also define the slow-wave subspace of the discrete shallow-water model. The modified filter will depend upon the slow-wave subspace of the discrete model, rather than upon that of the original differential equations.

Our main theoretical results appear in Chapter 5. After preliminary remarks in Section 5.1 and a review of projection matrices in Section 5.2, the modified KB filter is presented in Section 5.3; it is given by Theorem 1. An efficient method for computing the projection matrix upon which the modified filter depends is given by Theorem 2 of

Section 5.4. We describe a variety of choices for the error functional, and the corresponding projection matrices, in Section 5.5.

The description and results of our numerical experiments with the standard and modified KB filters are given in Chapter 6; the OI experiments are described in Chapter 7. A preliminary version of the experiments in Chapter 6 was reported in Ghil et al. (1981). The results in Chapter 7 are summarized in Cohn et al. (1981).

Theorems 1 and 2 of Chapter 5, and also the lemmas of Sections 5.2 and 5.4, are proven in the Appendix.

## 1.2. Background on Numerical Weather Prediction

Most forecast models used in NWP are discretized versions of the so-called primitive equations, which are the Eulerian hydrodynamical equations modified by the hydrostatic assumption. Finite difference and spectral methods are used most often for the discretization; finite element methods are used to a much lesser extent. The models are fully three-dimensional, depending on a vertical coordinate and on two horizontal coordinates. Global, hemispherical and limited-area models are all in use. See Haltiner and Williams (1980) for a full treatment of numerical modeling in NWP.

The highest resolution global and hemispherical models have  $10^5$ - $10^6$  degrees of freedom -- a large number even by present computational standards. Still, this resolution corresponds to a horizontal mesh spacing of 100-200 km, which is not adequate for local prediction. Local forecasts are carried out by use of limited-area fine-mesh models and by subjective judgement. In any case, local

forecasts are based upon forecasts provided by global (or hemispherical) models.

Errors are incurred at each step of the prediction process. Some error is made at the local level. The global models are another source of error, primarily due to discretization and improper modeling of physical processes. Finally, there is error in the determination of global initial values.

Initial error is important, especially because the resulting forecast error grows rapidly. This growth is a consequence of the atmosphere's nonlinear dynamics, and is not an artifact of the model. In stable linear systems, the effect of an initial perturbation tends to zero with time. The atmosphere is nonlinear and has locally unstable modes. Perturbations at small scales of motion are nonlinearly fed into the larger scales and eventually grow enough to completely contaminate a forecast. The atmosphere is in this sense unpredictable.

Three approaches have been used to determine the rate at which predictability of large-scale atmospheric flow is lost. Lorenz (1969a) examined a five-year observational data set for atmospheric "analogues", or pairs of similar states, and studied their divergence in time. In the second approach (Charney et al., 1966; Williamson and Kasahara, 1971), one studies instead the divergence of pairs of numerical forecasts issuing from slightly different initial states. In the third approach (Leith and Kraichnan, 1972; Lorenz, 1969b), the transfer of error between different scales of motion, based on a presumed atmospheric energy spectrum, is calculated by means of statistical theories of turbulence.

The three approaches give the same quantitative results. For scales of motion resolved by current NWP models, two atmospheric states differing initially by a small amount diverge exponentially at first, with an rms error-doubling time of about 2-3 days. Errors level off in about 2-3 weeks, after which time the two states become statistically uncorrelated.

Errors in initial states are due to the incompleteness and inaccuracy of data provided by the global observing network. Here we briefly describe the observing systems and the error structure of the data they provide. For a more complete discussion we refer to Bengtsson (1975) and Fleming et al. (1979a,b).

The largest number of observations made at a single time each day are made at the so-called synoptic times, 0000 and 1200 hours Greenwich Mean Time (GMT); the synoptic times are chosen as initial forecast times. Synoptic data are provided by the conventional observing network of surface stations and radiosondes. In Figure 1, in the panels marked "surface", "pilots" and "temps", we show the distribution of conventional observations available at 1200 GMT on January 9, 1979. The uneven spatial distribution of conventional data is clear: observations are concentrated over the continents, especially those of the Northern Hemisphere.

A number of additional observations, mostly surface observations, are provided by the conventional network at the subsynoptic times, 0600 and 1800 GMT. A much larger number of observations, exceeding by now that given by the conventional network, are made in an essentially time-continuous manner by polar-orbiting satellites, geostationary satellites and other nonconventional observing systems (remaining

panels in Fig. 1). Satellite observations greatly improve upon the spatial coverage of conventional observations, but their usefulness in providing initial data is limited by the fact that satellite coverage of the globe is incomplete at any one time.

Each observing system has its own particular error characteristics. The conventional network provides point values of pressure, temperature, horizontal velocity and humidity. These fields are highly variable, and hence point measurements are not representative of volume averages, as they should be for numerical models. Although instrumental errors are relatively small, the total observational errors of conventional data can be quite large.

Observational errors from nonconventional measurements are often even larger. Geostationary satellites ("satwind" in Fig. 1), for example, provide sequential cloud images from which horizontal wind velocities are deduced. Velocity errors in this case are large, primarily because of difficulty in determining the vertical location of the clouds being tracked.

Observational errors are also correlated in a number of ways. Errors from radiosonde measurements are spatially correlated, as the sondes rise through the atmosphere. Polar-orbiting satellites ("satems" in Fig. 1) measure radiances at different wavelengths, from which vertical temperature profiles are deduced. The errors in a given profile are vertically correlated; profile errors are also horizontally correlated along the satellite track. Sequences of measurements from any single instrument are also likely to have temporally correlated errors.

The inaccuracy and incompleteness of observational data available at any single time gives rise to the necessity of four-dimensional data assimilation. Bube (1978, 1981) has studied some theoretical aspects of data assimilation for general first-order linear hyperbolic systems. He gives conditions under which solutions of such equations are uniquely determined by nonstandard data, i.e., by data other than complete initial data. For the method of direct insertion of nonstandard data during an integration, he shows how the rate of convergence toward the solution depends on the frequency with which data are available for insertion. In a similar theoretical study, Talagrand (1977, 1981) has examined the convergence of direct insertion methods based on both forward and forward-backward integration, for linearized versions of the shallow-water equations and of the primitive equations. Both studies assume perfect observations.

Direct insertion, or replacement of forecast values with observed values, is not desirable in practice, because of observational error and forecast error. Rather, an appropriate combination of observed and forecast values is sought. The usual procedure is as follows.

At a given time when observations are available, differences are formed between the observed and forecast values, after an interpolation between grid points and observation locations. Thus, if  $\underline{w}^o$  is the vector of observations, if  $\underline{w}^f$  is the vector of forecast values at all the grid points, and if  $H$  is a matrix which interpolates from grid points to observation locations, then the observed-minus-forecast residual is given by  $\underline{w}^o - H\underline{w}^f$ . Once the residual vector has been determined, it is multiplied by a matrix  $K$  of weighting coefficients, and then added back to the forecast vector. The result,



$$\underline{w}^a = \underline{w}^f + K(\underline{w}^o - H\underline{w}^f), \quad (1.1)$$

is known as the analysis vector, since it represents an "analysis" of the available observations. The forecast then proceeds, using the analysis vector as initial data, and the entire process is repeated when new observations become available. Thus, the schemes are sequential, in that observations are discarded once they have been processed.

The central problem of four-dimensional data assimilation is to determine an appropriate choice for the matrix  $K$ , as this matrix characterizes an assimilation scheme. This matrix is known in estimation theory as a gain matrix. In global NWP, gain matrices are very large, on the order of  $10^6 \times 10^5$ , so that almost all elements must be zero in order to leave a tractable computational problem. In actual practice, data assimilation is always carried out locally, so that gain matrices are block diagonal and have rather small bandwidths.

Until very recently, most assimilation methods used relatively little statistical information. The most popular such method, known as the successive correction method, was developed by Bergthorsson and DBBs(1955) and by Cressman (1959). In this method, weights assigned to observational data surrounding a grid point are functions of radial distance only; scans of the data over successively smaller radii from each grid point are employed, so that a smoothly varying analysis field results. A complete review of assimilation methods, including the successive correction method, appears in Gustavsson (1981).

We have already seen that the error structure of satellite observations is quite different than that of conventional observations. Thus, as nonconventional, satellite-based observations became available, it was realized that nonstatistical procedures would no longer suffice.

Statistical assimilation was first suggested by Eliassen (1954) and by Gandin (1963). The statistical schemes in current use are known as "optimal interpolation" methods. In these methods, the gain matrix is based upon a presumed forecast error covariance matrix and its presumed evolution in time. Current formulations of OI are multivariate, in that forecast error correlations between different atmospheric variables are prescribed (Rutherford, 1973, 1976; Schlatter, 1975; Schlatter et al., 1976). Statistical assumptions based on the atmosphere's approximate dynamics are involved in specifying the correlations.

In Chapter 2 we will see that, like OI, the KB filter is a statistical, sequential data assimilation method. The difference is that the KB filter is based upon the correct evolution of the forecast error covariance matrix, which is known by virtue of a stochastic-dynamic atmospheric model.

We describe in Chapter 7 the statistical assumptions made in OI. Our implementation of OI will be based on that at the U. S. National Meteorological Center (NMC; Bergman, 1979; McPherson et al., 1979) and at the European Centre for Medium Range Weather Forecasts (ECMWF; Lorenc, 1981).

In actual practice, all data assimilation methods are intermittent, rather than continuous. That is, observational data are

grouped in intervals centered at the synoptic times, and sometimes at the subsynoptic times also, and data are assimilated only at those times. Assimilation is performed intermittently for two reasons. First, intermittent assimilation is more compatible with data-handling procedures such as cross-checking for gross errors. Second, intermittent assimilation allows some time for the dispersion and dissipation of transient fast waves induced by each assimilation.

Still, it is necessary to combine data assimilation with some form of initialization. The initialization methods which have dominated both research and practice in recent years are the normal mode initialization methods. We describe them briefly here; see Daley (1981) for a complete review of these methods. For a review of other initialization methods, see Bengtsson (1975).

Normal mode initialization is based on writing the unforced forecast equations in phase space, as

$$\dot{\underline{y}} = -i \Lambda_1 \underline{y} + \underline{E}_1(\underline{y}, \underline{z}), \quad (1.2a)$$

$$\dot{\underline{z}} = -i \Lambda_2 \underline{z} + \underline{E}_2(\underline{y}, \underline{z}); \quad (1.2b)$$

$\underline{y}(t)$  and  $\underline{z}(t)$  are the slow and fast mode expansion coefficients, respectively; the  $\Lambda_j$  are constant, diagonal matrices, and the  $\underline{E}_j$  are nonlinear terms which depend on both slow and fast mode coefficients. The eigenfrequencies  $\Lambda_1$  are generally small compared to the eigenfrequencies  $\Lambda_2$ , and the nonlinear terms are generally small compared to the linear terms.

Linear normal mode initialization was suggested by Dickinson and Williamson (1972); it was tested with a shallow-water equations model

by Williamson (1976), and with a primitive equations model by Williamson and Dickinson (1976). In this method, the "first guess" analysis vector provided by data assimilation is adjusted by setting to zero its fast components, while leaving its slow components unchanged. Thus, if  $y^a(0)$  and  $z^a(0)$  are the modal coefficients of the analysis vector at time  $t = 0$ , say, then the modal coefficients of the "corrected", initialized vector from which the forecast proceeds are given by

$$y^c(0) = y^a(0) , \quad z^c(0) = 0 . \quad (1.3a,b)$$

Were Eqs. (1.2) linear, the fast oscillations would thereby be eliminated for all time:  $z(t) \equiv 0$  if  $z(0) = 0$  and  $L_2 \equiv 0$ . The equations are not linear, however, and the nonlinear terms excite fast modes during the forecast. Indeed, at the initial time we have

$$\dot{z} = L_2(y^a, 0) , \quad (1.4)$$

whereby  $\dot{z}(0) \neq 0$ , since  $y^a(0) \neq 0$  generally.

Nonlinear normal mode initialization was introduced by Machenhauer (1977), and independently by Baer (1977) and Baer and Tribbia (1977). This method attempts to eliminate the nonlinear excitation of fast modes by adjusting the initial vector so that

$$\dot{z}(0) = 0 . \quad (1.5)$$

That is, the fast waves are required to be stationary at the initial time. The slow coefficients are not changed,

$$y^c(0) = y^a(0) . \quad (1.6a)$$

To satisfy Eq. (1.5), the fast coefficients  $z^a(0)$  are discarded, and replaced by

$$z^c(0) = -1 \Lambda_2^{-1} \Sigma_2(y^c(0), z^c(0)) ; \quad (1.6b)$$

a small, balancing fast component is introduced. In the Machenhauer formulation, the nonlinear equation (1.6b) is solved approximately, by one or two steps of functional iteration. The Baer-Tribbia method is slightly different, and is based on a careful nondimensionalization with respect to the two time scales involved.

An extension of the nonlinear schemes, known as variational nonlinear normal mode initialization, has been developed by Daley (1978). In this method, the fast coefficients are still required to satisfy Eq. (1.6b), but the slow coefficients are now altered also, to reflect the relative accuracy of different atmospheric variables provided by the assimilation scheme. Thus, a discrete version of an error functional

$$\eta = \int_A [q_u(u^c - u^a)^2 + q_v(v^c - v^a)^2 + q_\phi(\phi^c - \phi^a)^2] dA \quad (1.7)$$

is minimized, subject to Eq. (1.6b) as a constraint. Here  $u^a$  and  $v^a$  denote velocity components of the analysis vector, and  $\phi^a$  denotes the geopotential, while the minimization is with respect to corrected values  $u^c$ ,  $v^c$ ,  $\phi^c$ ; the integration is carried out over the entire atmosphere. The prescribed weighting factors  $q_u$ ,  $q_v$ ,  $q_\phi$  may vary in space and time; they reflect data density and accuracy. The weights

are taken to be large over data-dense regions, for example, so that most of the correction is over regions of sparse coverage where the analysis vector is not likely to be very accurate. The variational approach can also be applied, of course, to the linear initialization scheme.

The slow manifold concept of Leith (1980) has provided a framework for understanding the behavior of normal mode initialization methods. The slow manifold approximates the set of slowly evolving solutions of the forecast equations; nonlinear normal mode initialization is viewed as projection onto the slow manifold. The nonvariational method corresponds to one type of projection. In the variational approach, the type of projection depends upon the weighting functions  $q_u$ ,  $q_v$ ,  $q_\phi$ .

The Rossby manifold is the set of solutions of the forecast equations having  $\bar{z} \equiv 0$ ; linear normal mode initialization is projection onto the Rossby manifold. For linear models, such as the shallow-water equations model we will work with, the Rossby manifold and slow manifold coincide. For linear models, the slow, Rossby manifold is in fact a subspace, i.e., linear combinations of slow solutions are also slow solutions.

We will see in Chapter 5 that the modified KB filter corresponds to combining the standard KB filter with variational linear normal mode initialization. That is, the standard KB filter can be viewed as the underlying assimilation scheme, with the KB analysis vectors being projected onto the slow-wave subspace. Essentially, we prove rigorously that this is the best that can be done for linear models.

For the modified KB filter, one must still choose the variational weights which define the type of projection. We will show that, in addition to minimizing the functional (1.7), the modified filter also minimizes the expected value of

$$\eta' = \int_A [q_u(u^c - u^t)^2 + q_v(v^c - v^t)^2 + q_\phi(\phi^c - \phi^t)^2] dA, \quad (1.8)$$

where  $u^t$ ,  $v^t$ ,  $\phi^t$  are components of the "true" atmospheric state governed by a stochastic-dynamic model;  $\eta'$  is a functional of the actual error of the initialized state. In our numerical experiments, we therefore minimize the expected value of the total energy of the error, i.e., we choose constant weights  $q_u$ ,  $q_v$ ,  $q_\phi$ . The theory, however, is developed for the most general quadratic error functional.

## CHAPTER TWO

### ESTIMATION THEORY AND METEOROLOGICAL DATA ASSIMILATION

In this chapter, we review some of the aspects of estimation theory which apply to the problem of assimilating meteorological observations. The theory is presented only for the case of discrete-time, linear systems. Jazwinski (1970) rigorously treats both nonlinear and linear estimation theory, and Davis (1977) gives an elegant account of the linear case. An elementary treatment is available in Gelb (1974).

#### 2.1. The Stochastic-Dynamic Models

In the application of estimation theory to data assimilation, the atmosphere is assumed to be governed by a stochastic-dynamic model which is a randomly perturbed version of a given NWP model. The random perturbation is meant to account for the discrepancy between the evolution of the actual atmosphere and the evolution described by the given forecast model. The observation process is represented by a second stochastic-dynamic model: the observations are considered to be noisy "output" of the stochastic-dynamic atmospheric model. The assumptions on which the stochastic-dynamic models are based lead to a statistically optimal assimilation scheme, and to a method for assessing the performance of alternative schemes. The stochastic-dynamic models are described in this section, and their ramifications are discussed in subsequent sections.



We present only a simple special case of the theory: the given forecast model is linear, and hence does not represent an actual NWP model. The forecast model is expressed symbolically as

$$\underline{w}_k = \Psi_{k-1} \underline{w}_{k-1} , \quad (2.1)$$

for values of the discrete time  $k = 1, 2, 3, \dots$ . The vector  $\underline{w}_k$  has dimension  $n$  and the dynamics matrix  $\Psi_{k-1}$  is  $n \times n$ , where  $n$  is the number of degrees of freedom of the model:  $n$  is as large as  $10^6$  for actual NWP models. Interpreting Eq. (2.1) as a finite-difference model, the components of  $\underline{w}_k$  approximate at time  $k$  the values of the atmospheric variables at each grid point;  $\Psi_{k-1}$  consists of finite-difference coefficients and advances the forecast from time  $k-1$  to time  $k$ . Forcing terms are omitted from Eq. (2.1) for simplicity.

The model (2.1) is linear:  $\Psi$  does not depend on  $\underline{w}$ . The linearity assumption leads to substantial simplification of the theory reviewed in this chapter and extended in Chapter 5. Linearity does not obscure the main phenomenon of interest: linearized NWP models have solutions which evolve on two time scales.

Given the forecast model (2.1), it is assumed that the true atmospheric state evolves according to the stochastic-dynamic model

$$\underline{w}_k^t = \Psi_{k-1} \underline{w}_{k-1}^t + \underline{b}_{k-1}^t . \quad (2.2a)$$

The superscript  $t$  denotes that the state vector  $\underline{w}_k^t$  is an  $n$ -vector of the true, but unknown, values of the atmospheric variables. The random perturbation, or system noise, is the  $n$ -vector  $\underline{b}_{k-1}^t$ . In general, it is supposed to account for dynamical and physical processes improperly

modeled by the forecast equations (2.1), as well as for truncation errors due to discretization. Since the dynamics of Eq. (2.2a) are linear, we will want the noise to account in particular for the nonlinear effect of unpredictability.

The sequence  $\{\underline{b}_k^t: k = 0, 1, 2, \dots\}$  is assumed to be a white noise sequence with mean zero and known covariance matrix  $Q_k$ :

$$E\underline{b}_k^t = 0, \quad E(\underline{b}_k^t)(\underline{b}_l^t)^T = Q_k \delta_{kl}. \quad (2.2b, c)$$

The operator  $E$  indicates the expected value, or ensemble average, the superscript  $T$  denotes the vector or matrix transpose, and the symbol  $\delta_{kl}$  is the Kronecker delta,  $\delta_{kl} = 0$  if  $k \neq l$  and  $\delta_{kl} = 1$  if  $k = l$ . The mean-zero assumption (2.2b) is made for convenience, and is not essential to the theory.

Having described the state model, Eqs. (2.2), we now describe the observation model. Suppose that a vector of observations  $\underline{w}_k^o$  is available at a given time  $k$ . It is assumed that the observations can be modeled by the equation

$$\underline{w}_k^o = H_k \underline{x}_k^t + \underline{b}_k^o. \quad (2.3a)$$

The dimension  $p$  of the observation vector  $\underline{w}_k^o$  is the number of measurements available at time  $k$ :  $p = p(k)$ . The observation matrix  $H_k$  is a nonrandom  $p \times n$  matrix, and the observation noise  $\underline{b}_k^o$  is a random  $p$ -vector. Typically  $p \ll n$ .

The elements of the observation vector are the raw observational data themselves. We merely assume that they are related to the true atmospheric state, and hence to Eq. (2.2a), by Eq. (2.3a). The

observation model is assumed to be linear:  $H_k$  does not depend on  $\underline{w}_k^t$ . In other words, Eq. (2.3a) models noisy observations of linear combinations of elements of the state vector.

The linear combinations correspond to the fact that the observation matrix must interpolate from variables defined at grid points (the elements of  $\underline{w}_k^t$ ) to variables defined at observation locations (the elements of  $\underline{w}_k^o$ ). The two sets of variables need not represent the same meteorological fields. For example, part of the observation matrix could contain linear regression coefficients for converting between temperature components of  $\underline{w}_k^t$  and satellite-measured radiances in  $\underline{w}_k^o$ .

The random vector  $\underline{b}_k^o$  models observational error, which includes both instrumental error and the sampling error inherent in point measurements of fields with considerable spatial variability. The observational noise is assumed to be white, with mean zero and known covariance matrix  $R_k$ :

$$E\underline{b}_k^o = 0, \quad E(\underline{b}_k^o)(\underline{b}_\ell^o)^T = R_k \delta_{k\ell}, \quad (2.3b,c)$$

and is assumed to be uncorrelated with the state noise:

$$E(\underline{b}_k^o)(\underline{b}_\ell^t)^T = 0. \quad (2.3d)$$

Assumptions similar to (2.3b,c,d) are also implicit in the data assimilation schemes in use at NMC (Bergman, 1979) and at ECMWF (Lorenc, 1981).

The stochastic-dynamic models (2.2, 2.3) express the basic assumptions involved in our application of estimation theory to NWP. Next, we introduce the class of data assimilation methods to be considered, and then we discuss the implications of the models for the data assimilation problem.

## 2.2. Unbiased Linear Data Assimilation Methods

Suppose that at some time  $k-1$ , observational data  $\underline{w}_{k-1}^o$  have been used to provide an estimate  $\underline{w}_{k-1}^a$  of the true atmospheric state  $\underline{w}_{k-1}^t$ . The superscript a is used for the estimate because the estimate is known in meteorological practice as the analysis vector: it represents an "analysis" of the observations available at time  $k-1$ . The analysis vector is assumed to be unbiased, i.e.,

$$E(\underline{w}_{k-1}^a - \underline{w}_{k-1}^t) = 0. \quad (2.4)$$

Like the state vector, the analysis vector has dimension  $n$ .

The purpose of a data assimilation scheme is to combine the estimate  $\underline{w}_{k-1}^a$  with new observations  $\underline{w}_k^o$  which become available at time  $k$ , to produce a new estimate  $\underline{w}_k^a$ . We consider only unbiased, linear assimilation methods: a new unbiased estimate is sought as a linear combination of the old estimate and the new observations, i.e.,

$$E(\underline{w}_k^a - \underline{w}_k^t) = 0, \quad (2.5)$$

$$\underline{w}_k^a = L_{k-1}\underline{w}_{k-1}^a + K_k\underline{w}_k^o. \quad (2.6)$$

The matrices  $L_{k-1}$  and  $K_k$  are nonrandom and have dimensions  $n \times n$  and  $n \times p$ , respectively.

The assumptions inherent in the stochastic-dynamic models actually determine  $L_{k-1}$ , and allow Eq. (2.6) to be written in a more intuitively appealing way. Substituting Eq. (2.6) into Eq. (2.5), and using Eqs. (2.2a,b), (2.3a,b) and (2.4), one finds that

$$0 = E(\underline{w}_k^a - \underline{w}_k^t) = [L_{k-1} - (I - K_k H_k) \Psi_{k-1}] E \underline{w}_{k-1}^t.$$

Since  $E \underline{w}_{k-1}^t \neq 0$  generally, it must be that

$$L_{k-1} = (I - K_k H_k) \Psi_{k-1},$$

so that Eq. (2.6) becomes

$$\underline{w}_k^a = \Psi_{k-1} \underline{w}_{k-1}^a + K_k (\underline{w}_k^o - H_k \Psi_{k-1} \underline{w}_{k-1}^a).$$

Now  $\Psi_{k-1} \underline{w}_{k-1}^a$  is just a one-step prediction from time  $k-1$  to time  $k$ , cf. Eq. (2.1). Defining the forecast vector  $\underline{w}_k^f$ ,

$$\underline{w}_k^f = \Psi_{k-1} \underline{w}_{k-1}^a, \quad (2.7a)$$

we therefore have

$$\underline{w}_k^a = \underline{w}_k^f + K_k (\underline{w}_k^o - H_k \underline{w}_k^f); \quad (2.7b)$$

cf. Eq. (1.1). The forecast and analysis vectors, given by Eqs. (2.7a,b), are both estimates of the atmospheric state. The forecast is

a first guess; the analysis is presumably a better estimate since it incorporates the new observational information.

Eqs. (2.7) represent the general form of all linear, unbiased data assimilation schemes. With Eq.(2.7a) replaced by a fully nonlinear NWP model, all statistical assimilation schemes used at NWP centers can be written in the form (2.7); see, for example, Gustavsson (1981).

The general form of the scheme (2.7) states that the analysis vector is the sum of the forecast vector and a linear combination of the elements of the observed-minus-forecast residual  $\underline{w}_k^o - H_k \underline{w}_k^f$ . The gain matrix  $K_k$  specifies the linear combination, and therefore characterizes the assimilation method. We take the dynamics matrix  $\Psi_k$  and the observing pattern  $H_k$  to be given, and focus attention on how to specify the gain matrix.

If there are no observations available at some time  $k$ , then the second term on the right-hand side of Eq. (2.6) is not present; equivalently,  $K_k = 0$ . In this case, Eqs. (2.7) become

$$\underline{w}_k^f = \Psi_{k-1} \underline{w}_{k-1}^a, \quad (2.8a)$$

$$\underline{w}_k^a = \underline{w}_k^f; \quad (2.8b)$$

i.e., the forecast simply proceeds when there are no data to be assimilated.

In particular, Eqs. (2.8) hold for all  $k > N$ , where  $N$  is the most recent time at which observations are available. The assimilation scheme is provided an unbiased initial estimate  $\underline{w}_0^a$ , data are

assimilated at times  $k = 1, \dots, N$ , and then a forecast is issued, using  $\underline{w}_N^a$  as initial data. We are concerned primarily with the case  $k \leq N$ .

### 2.3. Assessing the Performance of Data Assimilation Methods

One of the main advantages of assuming the stochastic-dynamic models (2.2) and (2.3) is that they lead to a method for assessing the performance of data assimilation methods of the form (2.7). That is, for any choice of gain matrix sequence  $\{K_k: k = 1, 2, 3, \dots\}$ , it can be determined how well the corresponding estimates  $\{\underline{w}_k^f, \underline{w}_k^a: k = 1, 2, 3, \dots\}$  represent the true states  $\{\underline{w}_k^t: k = 1, 2, 3, \dots\}$ .

To show how this is so, we introduce the estimation error covariance matrices. These are the forecast error covariance matrices, defined by

$$P_k^f = E(\underline{w}_k^f - \underline{w}_k^t)(\underline{w}_k^f - \underline{w}_k^t)^T, \quad (2.9a)$$

and the analysis error covariance matrices, defined by

$$P_k^a = E(\underline{w}_k^a - \underline{w}_k^t)(\underline{w}_k^a - \underline{w}_k^t)^T. \quad (2.9b)$$

The forecast and analysis error variances, which are the primary measures of an assimilation scheme's performance, are located along the main diagonals of  $P_k^f$  and  $P_k^a$ , respectively.

From Eqs. (2.2) and (2.7a), it follows that  $P_{k-1}^a$  is advanced by one time step to  $P_k^f$  according to

$$P_k^f = \Psi_{k-1} P_{k-1}^a \Psi_{k-1}^T + Q_{k-1}, \quad (2.10a)$$

while Eqs. (2.3) and (2.7b) imply that  $P_k^a$  is found from  $P_k^f$  by the formula

$$P_k^a = (I - K_k H_k) P_k^f (I - K_k H_k)^T + K_k R_k K_k^T. \quad (2.10b)$$

The estimation error variances and covariances can therefore actually be computed, provided that  $P_0^a$  is known. Eqs. (2.10) will be used repeatedly in our numerical experiments, to compare the performance of data assimilation schemes based on a variety of choices of the gain matrix sequence.

The terms in Eqs. (2.10) have a simple intuitive interpretation. The first term on the right-hand side of Eq. (2.10a) determines how estimation errors are advected between data-dense and data-sparse regions from one time step to the next. The numerical experiments reported in Chapters 6 and 7 indicate that the effect of advection of information is important in data assimilation. The second term in Eq. (2.10a) is due to the presence of system noise, and results in a tendency of linear growth of estimation error variance.

The first term on the right-hand side of Eq. (2.10b) determines the extent to which new observational information improves the forecast, and the second term indicates the deterioration due to observational error. For a data assimilation scheme to perform properly, its gain matrices  $K_k$  must be such that the error reduction given by the first term dominates the error growth given by the second term.



The simple form of Eqs. (2.10) is due primarily to the assumed linearity of the stochastic-dynamic models. For nonlinear models, equations like (2.10) still hold but are more complicated (Jazwinski, 1970, Sec. 6.4): the right-hand sides depend on higher-order moments of the estimation errors.

Still, the computational task involved in advancing Eqs. (2.10) exactly is laborious: matrix-matrix operations must be performed at every time step, regardless of how often observations are assimilated. For this reason, our numerical experiments will be performed with a simple model involving only  $n = 48$  state variables.

#### 2.4. Derivation of the Kalman-Bucy Filter

Eqs. (2.10) give the estimation error variances corresponding to any choice of the sequence of gain matrices. Hence, a sequence which minimizes the variances can be determined. The assimilation method based on the minimizing sequence is called the Kalman or Kalman-Bucy (KB) filter, after Kalman (1960) and Kalman and Bucy (1961), who first formulated it for processes governed by linear systems of ordinary differential equations.

Before deriving the KB filter, we review some facts from linear algebra. All vectors and matrices in the following discussion are real.

A square matrix  $A$  is symmetric if  $A^T = A$ . An  $m \times m$  matrix  $A$  is positive definite if it is symmetric and if  $\underline{x}^T A \underline{x} > 0$  for all nonzero  $m$ -vectors  $\underline{x}$ . If  $A$  is positive definite, then  $A$  is nonsingular, i.e.,  $A^{-1}$  exists. Every positive definite matrix  $A$  can be factored (nonuniquely) as  $A = A_1^T A_1$ , where  $A_1$  is nonsingular.

An  $m \times m$  matrix  $A$  is positive semidefinite if it is symmetric and if  $\underline{x}^T A \underline{x} \geq 0$  for all  $m$ -vectors  $\underline{x}$ . Every positive semidefinite matrix  $A$  can be factored (nonuniquely) as  $A = A_1^T A_1$ , where  $A_1$  may be singular.

A covariance matrix  $A$  is a matrix of the form  $A = E \underline{y} \underline{y}^T$ , where  $\underline{y}$  is a random  $m$ -vector with  $E \underline{y} = 0$ . All covariance matrices are symmetric and positive semidefinite. If every nontrivial linear combination of the elements of  $\underline{y}$  has positive variance, i.e., if  $E(\sum_{i=1}^m x_i y_i)^2 > 0$  for all nonzero  $m$ -vectors  $\underline{x}$ , then  $A = E \underline{y} \underline{y}^T$  is actually positive definite.

The trace of a square matrix  $A$  is the sum of its diagonal elements. The trace operator has the properties

$$\text{trace } A^T = \text{trace } A, \quad (2.11a)$$

$$\text{trace } (A+B) = \text{trace } A + \text{trace } B, \quad (2.11b)$$

$$\text{trace } AB = \text{trace } BA, \quad (2.11c)$$

$$\text{trace } \underline{x} \underline{y}^T = \underline{y}^T \underline{x}, \quad (2.11d)$$

$$\text{trace } BB^T \geq 0, \quad (2.11e)$$

$$\text{trace } BB^T = 0 \text{ if and only if } B = 0, \quad (2.11f)$$

for all  $m \times m$  matrices  $A, B$ , and for all  $m$ -vectors  $\underline{x}, \underline{y}$ .

We now give an elementary derivation of the KB filter, based on minimizing a quadratic functional of the analysis error. Let  $A$  be an arbitrary nonrandom positive semidefinite  $n \times n$  matrix, and let

$$\eta_k = E[(\underline{w}_k^a - \underline{w}_k^t)^T A (\underline{w}_k^a - \underline{w}_k^t)]. \quad (2.12)$$

The functional  $\eta_k$  is a general measure of the analysis error. The

functional could represent the total expected kinetic energy of the analysis error, for example, in which case A would be a diagonal matrix with appropriate weights for the mass and wind fields along its diagonal. Weighting matrices of interest are usually positive definite, but we allow A to be positive semidefinite to include the possibility that one might not be concerned with the error in one or more meteorological fields at one or more grid points.

Eq. (2.12) will now be rewritten to make the dependence of  $\eta_k$  upon  $K_k$  explicit, and then  $\eta_k$  will be minimized with respect to  $K_k$ . First, notice that

$$\eta = E\{\text{trace}[A(\underline{w}^a - \underline{w}^t)(\underline{w}^a - \underline{w}^t)^T]\} \quad (2.13a)$$

$$= \text{trace } AP^a ; \quad (2.13b)$$

the first equality follows from property (2.11d), while the second follows from the fact that the expectation and trace operators commute, from the nonrandomness of A, and from the definition of  $P^a$ . The subscript k has been dropped in Eqs. (2.13), and will be omitted throughout the derivation. It is implicit that k is a time at which observations are available, for otherwise  $K_k = 0$ ; cf. Eqs. (2.8).

To find a suitable expression for  $P^a$  to be inserted into Eq. (2.13b), we expand the products in Eq. (2.10b), to get

$$P^a = KCK^T - KHP^f - P^fH^TK^T + P^f, \quad (2.14a)$$

where

$$C = HP^fHT + R. \quad (2.14b)$$

The matrix  $C$  is symmetric, since  $P^f$  and  $R$  are covariance matrices.

We assume that all nontrivial linear combinations of the elements of the observational noise  $b^0$  have nonzero variance, i.e., no linear combination of the measurements is "exact". The observational error covariance matrix  $R$  is therefore positive definite; it follows that  $C$  is also positive definite, and hence nonsingular. Consequently, one can complete the square in  $K$  in Eq. (2.14a), to get

$$p^a = (K - p^fHTC^{-1})C(K - p^fHTC^{-1})^T + Z, \quad (2.15a)$$

where

$$Z = p^f - p^fHTC^{-1}HP^f. \quad (2.15b)$$

Notice that  $Z$  is independent of  $K$ .

Finally, substituting Eq. (2.15a) into Eq. (2.13b), we have

$$\eta = \text{trace} [A(K - p^fHTC^{-1})C(K - p^fHTC^{-1})^T + AZ]. \quad (2.16)$$

Factoring  $A$  and  $C$  as  $A = A_1^TA_1$ ,  $C = C_1C_1^T$ , and using properties (2.11b,c), Eq. (2.16) becomes

$$\eta = \text{trace } BB^T + \text{trace } AZ, \quad (2.17a)$$

where

$$B = A_1(K - P^f H^T C^{-1}) C_1. \quad (2.17b)$$

Since  $AZ$  does not depend on  $K$ , and due to properties (2.11e,f), it follows from the representation (2.17) that  $\eta$  is minimized with respect to  $K$  if and only if  $B = 0$ , i.e., iff

$$A_1(K - P^f H^T C^{-1}) C_1 = 0. \quad (2.18)$$

Therefore, a gain matrix which minimizes  $\eta$  is given by

$$K = P^f H^T C^{-1}. \quad (2.19)$$

Moreover, the minimizing gain matrix is unique if the weighting matrix  $A$ , which was assumed to be only positive semidefinite, is actually positive definite. If  $A = A_1^T A_1$  is positive definite, then  $A_1$  is nonsingular;  $C = C_1 C_1^T$  is already known to be positive definite, so  $C_1$  is nonsingular. Premultiplying Eq. (2.18) by  $A_1^{-1}$  and postmultiplying by  $C_1^{-1}$  yields Eq. (2.19); i.e., the minimizing gain matrix is unique.

The gain matrix given by Eq. (2.19) is the Kalman or Kalman-Bucy (KB) gain matrix, which we denote by  $K^{KB}$ . Using Eq. (2.14b) in Eq. (2.19), the KB gain matrix is given for each observation time  $k$  by

$$K_k^{KB} = P_k^f H_k^T (H_k P_k^f H_k^T + R_k)^{-1}. \quad (2.20a)$$

We have simply

$$K_k^{KB} = 0 \quad (2.20b)$$

if there are no observations at time  $k$ .

Requiring  $\eta_k$  to be minimized successively, at each time  $k = 1, 2, 3, \dots$ , results in the KB gain matrix sequence  $\{K_k^{KB}: k = 1, 2, 3, \dots\}$ ; the Kalman or Kalman-Bucy filter is the corresponding data assimilation method. Since  $K_k^{KB}$  depends upon  $P_k^f$ , the estimation error covariance matrices (2.10) must be computed during the assimilation. When  $K_k = K_k^{KB}$ , however, it follows readily from Eqs. (2.15, 2.19) that the general formula (2.10b) simplifies to

$$P_k^a = (I - K_k^{KB} H_k) P_k^f. \quad (2.21)$$

Eqs. (2.7, 2.10a, 2.20, 2.21) constitute the Kalman filtering algorithm for discrete-time, linear systems. We recapitulate the equations here for convenience:

$$\underline{w}_k^f = \Psi_{k-1} \underline{w}_{k-1}^a, \quad (2.22a)$$

$$P_k^f = \Psi_{k-1} P_{k-1}^a \Psi_{k-1}^T + Q_{k-1}, \quad (2.22b)$$

$$K_k^{KB} = P_k^f H_k^T (H_k P_k^f H_k^T + R_k)^{-1}, \quad (2.22c)$$

$$P_k^a = (I - K_k^{KB} H_k) P_k^f, \quad (2.22d)$$

$$\underline{w}_k^a = \underline{w}_k^f + K_k^{KB} (\underline{w}_k^o - H_k \underline{w}_k^f), \quad (2.22e)$$

for  $k = 1, 2, 3, \dots$ , given  $\underline{w}_0^a$  and  $P_0^a$ . In the absence of observations at time  $k$ , Eq. (2.22c) is replaced by  $K_k^{KB} = 0$ , and Eqs. (2.22d,e) simplify accordingly.

Notice that Eqs. (2.22b,c,d) do not depend on the estimates provided by Eqs. (2.22a,e). This is a consequence of the linearity of the stochastic-dynamic models. Given  $P_0^a$  and the dynamics  $\Psi_k$ , the gain

matrix sequence depends only on the observing patterns and noise covariance matrices. If these are known in advance, then the gain matrix sequence can be computed before the assimilation begins.

## 2.5. Optimality Properties of the Kalman-Bucy Filter

We now discuss some of the optimality properties of the KB filter. Notice, first of all, that  $K^{KB}$  is actually independent of the weighting matrix  $A$  which defines  $\eta$ :  $A$  does not appear, explicitly or implicitly, in Eq. (2.20a). In other words,  $K^{KB}$  simultaneously minimizes all positive semidefinite quadratic functionals of the analysis error, and uniquely minimizes all positive definite quadratic functionals of the analysis error.

Suppose in particular that  $A = e_j e_j^T$ , where  $e_j$  is the  $j^{\text{th}}$  column of the  $n \times n$  identity matrix. Then, according to definition (2.12),  $\eta$  is just the variance of the  $j^{\text{th}}$  component of the analysis error. Consequently, since  $j$  is arbitrary,  $K^{KB}$  minimizes the analysis error variance of each meteorological variable at each grid point. The KB filter is a minimum-variance estimator.

Suppose we fix a time  $k = \ell$ . It was shown in Sec. 2.4 that requiring  $\eta_k$  to be minimized, in turn, for each time  $k = 1, 2, \dots, \ell$ , results in the KB gain matrix sequence  $\{K_k^{KB}: k = 1, 2, \dots, \ell\}$ . Suppose that instead we wish to minimize only  $\eta_\ell$ , without regard for the values of  $\eta_k$  at the previous times  $k = 1, 2, \dots, \ell-1$ . In other words,  $\eta_\ell$  is to be minimized with respect to the entire sequence  $K_1, K_1, \dots, K_\ell$ . The result is still  $K_k = K_k^{KB}$ ,  $k = 1, 2, \dots, \ell$ . That is, the KB filter is time-optimal: the minimum value of  $\eta_\ell$ , for each fixed  $\ell$ , is attained by using the KB gain matrix sequence.

A slightly more general statement of this fact is the following. Assimilation schemes of the form (2.7) are sequential, or recursive: the only observations upon which the current analysis vector  $\underline{w}_k^a$  explicitly depends are the current observations  $\underline{w}_k^o$ , so that observations may be discarded as soon as they are processed. Suppose that we consider a more general class of assimilation schemes, in which each analysis vector is explicitly a linear combination of all available data:

$$\underline{w}_k^a = L_{k,0} \underline{w}_0^a + \sum_{j=1}^k L_{k,j} \underline{w}_j^o, \quad k = 1, 2, 3, \dots \quad (2.23)$$

It can be shown (e.g., Jazwinski, 1970, Sec. 7.3), that in fact the KB filter is optimal among assimilation schemes of this more general class: with  $\underline{w}_k^a$  given by Eq. (2.23), minimizing  $\eta_k$  either for all  $k$  or for a fixed  $k$  still results in the KB filtering algorithm.

This wider optimality is due to assumptions (2.2c, 2.3c,d) that the system noise and observational noise are uncorrelated in time. If the system noise and observational noise are also assumed to be Gaussian, it is known (e.g., Jazwinski, 1970, Sec. 5.2) that the optimal nonlinear assimilation scheme, i.e., one in which  $\underline{w}_k^a$  might depend nonlinearly on all past and present observational data, is still the KB filter.

## 2.6. Further Remarks on Estimation Theory

By applying the theory outlined in Secs. 2.1-2.4 to a simple model  $\Psi$  based on the linearized shallow-water equations, we will see in Chapters 6 and 7 that much can be learned about the properties of data



assimilation schemes in a meteorologically familiar, but somewhat idealized setting. The method of Sec. 2.3 provides a way to determine how well any scheme of the form (2.7) performs, and for comparison we have an "optimal" scheme, namely the KB filter. For completeness, we now discuss some extensions of the rudimentary theory we have outlined, which might lead to practical assimilation schemes for global NWP.

First, notice that the sequential nature of the Kalman-Bucy filter is made possible by the fact that the forecast error covariance matrix  $P_k^f$  is known at each time  $k$ . All observational information available prior to time  $k$  is embodied in the forecast vector  $w_k^f$  and the covariance matrix  $P_k^f$ , so that the only additional information needed at time  $k$  is the current observational information  $(w_k^o, H_k, R_k)$ , cf. Eqs. (2.22c,e). That  $P_k^f$  is known is a consequence of the fact that the system noise covariance matrix  $Q_k$  was assumed to be known, cf. Eqs. (2.2c, 2.22b). A priori knowledge of  $Q_k$  is, however, not essential:  $Q_k$  can be determined adaptively, i.e., during the assimilation process itself (Bélanger, 1974; Chap and Stubberud, 1976; Chin, 1979; Maine and Iliff, 1981). The observational noise covariance matrix  $R_k$ , as well as the means of the observational and system noise, can also be determined adaptively.

For a realistic NWP model, the corresponding stochastic-dynamic model (2.2a) would be nonlinear. Estimation theory still leads to an optimal assimilation method in this case (e.g., Jazwinski, 1970, Ch. 6). However, as the right-hand sides of the equations corresponding to (2.10) would depend on all the higher-order moments of the estimation error, approximations would be required to make the algorithm finite.

Many approximate nonlinear filters have been formulated (Jazwinski, 1970, Ch. 9, and references therein). A particularly simple nonlinear filter, often used in engineering applications, is the extended Kalman filter (EKF: Jazwinski, 1970, Sec. 8.3; Gelb, 1974, Ch. 6). The EKF is essentially the usual linear KB filter, with the nonlinear dynamics being linearized about each successive state estimate. Discussion of the applicability of the EKF to numerical weather prediction appears in Ghil et al. (1981, Sec. 5).

Even for linear stochastic-dynamic models, the KB filter presents a formidable computational task. The matrix-matrix operations in Eq. (2.22b) must be performed at every time step; Eqs. (2.22c,d) are needed only when observations are available. Assimilation schemes in current use require only matrix-vector operations (2.8) in between observation times. There are, however, a variety of ways to reformulate Eqs. (2.22) for computational efficiency (Bierman, 1977; Paige and Saunders, 1977). In particular, the matrix inversion in Eq. (2.22c) can be avoided.

Still, for global NWP, it would probably be necessary to calculate Eq. (2.22b) in an efficient approximate form. Many approximate forms are possible. In fact, the "optimal interpolation" (OI) methods in operational use at NWP centers can be regarded as being based on such an approximation. In Chapter 7, we describe the approximate version of Eq. (2.22b) upon which OI is based, and we implement OI for our dynamical model  $\Psi$ . The method of Sec. 2.3 is used to determine the effect of the approximations involved in OI.

In summary, the framework of estimation theory is well-suited to study the problems of meteorological data assimilation, and we have indicated how the theory outlined in Secs. 2.1-2.4 might lead to practical assimilation algorithms for global NWP.

Our purpose here is to develop the theory in a different direction, i.e., to account for the initialization aspect of data assimilation. We show in Chapter 5 that for dynamical models having two time scales, requiring the state estimates to evolve slowly leads to a modified version of the KB filter. First, in Chapter 3, we describe the linearized shallow-water equations and their slow solutions, and then in Chapter 4 we describe the slow solutions of a corresponding discrete model  $\Psi$ .

### CHAPTER THREE

#### SLOW SOLUTIONS OF THE LINEAR SHALLOW-WATER EQUATIONS

The shallow-water equations govern the motion of a thin layer of incompressible, inviscid fluid over a given surface. The shallow-water equations over a rotating sphere give a simplified description of the dynamics of the earth's atmosphere, and solutions of the equations exhibit many important properties of large-scale atmospheric flow (e.g., Pedlosky, 1979, Ch. 3). In particular, the equations possess both slowly evolving solutions and rapidly evolving solutions.

In this chapter we describe the slow-wave subspace of a linear, spatially one-dimensional version of the shallow-water equations. The slow-wave subspace is the set of all initial data which lead only to slowly evolving solutions of the linearized equations.

#### 3.1. The Equations

The linear, spatially one-dimensional shallow-water equations, written in cartesian coordinates for a plane tangent to the earth at latitude  $\theta_0$ , are given by

$$u_t + Uu_x + \phi_x - fv = 0, \quad (3.1a)$$

$$v_t + Uv_x + fu = 0, \quad (3.1b)$$

$$\phi_t + U\phi_x + \phi u_x - fUv = 0. \quad (3.1c)$$

The coordinate  $x$  points eastward, in the zonal direction, along the circle of latitude  $\theta = \theta_0$ , while  $y$  points northward, in the meridional direction;  $u$  and  $v$  are velocity components in the  $x$  and  $y$  directions,

respectively. The geopotential  $\phi = gh$  measures the deviation of the height  $H+h$  of the free surface from its equilibrium value  $H$ ;  $\phi = gH$  is constant and  $g$  is the acceleration due to gravity. The constant  $U$  is the mean zonal velocity and  $f = 2\Omega \sin \theta_0$  is the Coriolis parameter, with  $\Omega$  the angular velocity of the earth. The subscripts  $x$  and  $t$  denote differentiation with respect to  $x$  and the time  $t$ ; all quantities are independent of  $y$ .

These equations are derived from the full, nonlinear shallow-water equations on a tangent plane,

$$u_t + uu_x + vu_y + \phi_x - fv = 0, \quad (3.2a)$$

$$v_t + uv_x + vv_y + \phi_y + fu = 0, \quad (3.2b)$$

$$\phi_t + u\phi_x + v\phi_y + \phi(u_x + v_y) = 0, \quad (3.2c)$$

by linearization around the solution  $u = U$ ,  $v = 0$ ,  $\phi = \phi(y)$  satisfying  $fU = -\phi_y = \text{const.}$  The quantities  $(u, v, \phi)$  in Eqs. (3.1) are perturbation quantities, or departures from the equilibrium values  $(U, 0, \phi)$ , while in Eqs. (3.2) they denote the total amplitudes. The derivation of Eqs. (3.1) from Eqs. (3.2) is based on the assumption that the perturbation quantities do not depend on  $y$ .

The parameters  $f$ ,  $U$  and  $\phi$  in Eqs. (3.1) will be chosen to correspond to midlatitude flow,  $\theta_0 \approx 45^\circ\text{N}$ . An important feature of large-scale midlatitude atmospheric dynamics is the approximate balance which exists between the pressure-gradient force and the Coriolis force (e.g., Holton, 1972, Sec. 2.4). Atmospheric states in which these two forces are exactly balanced are called geostrophic. In the nonlinear system (3.2), the pressure-gradient terms are  $\phi_x$  and  $\phi_y$ , and the

Coriolis terms are  $-fv$  and  $fu$ ; geostrophic states of this system are those for which  $u = -\phi_y/f$  and  $v = \phi_x/f$ . Notice that the solution about which Eqs. (3.2) were linearized is geostrophic.

Since  $x$  is the coordinate along a circle of latitude, the appropriate boundary conditions for Eqs. (3.1) are periodic:  $u(x+2L, t) = u(x, t)$ , and similarly for  $v$  and  $\phi$ , where  $2L$  is the earth's circumference at latitude  $\theta_0$ . For reasons described in Sec. 6.1, we seek only two-periodic solutions of the equations. We therefore impose the boundary condition

$$\underline{w}(-\frac{L}{2}, t) = \underline{w}(\frac{L}{2}, t), \quad (3.3)$$

where  $\underline{w}(x, t) = [u(x, t), v(x, t), \phi(x, t)]^T$ , and we solve the system (3.1, 3.3) in the spatial domain  $-L/2 \leq x \leq L/2$ .

Corresponding to latitude  $\theta_0 \approx 45^\circ\text{N}$ , we take  $f = 10^{-4} \text{ sec}^{-1}$  and  $L = 14000 \text{ km}$  for our system (3.1, 3.3). The mean zonal current is taken to be  $U = 20 \text{ ms}^{-1}$ , which is typical for mid-tropospheric flow at this latitude, while  $\phi = 3 \times 10^4 \text{ m}^2 \text{ s}^{-2}$ , which corresponds to an equivalent depth of  $H \approx 3 \text{ km}$  for a homogeneous atmosphere.

The initial-value problem for the hyperbolic system (3.1), with boundary condition (3.3), is well-posed (e.g., Courant and Hilbert, 1962, Sec. 5.6). That is, for arbitrary initial data  $\underline{w}(x, 0)$  which satisfy the boundary condition and have continuous first derivatives, there exists a unique solution  $\underline{w}(x, t)$  of Eqs. (3.1, 3.3) and the solution depends continuously on the initial data. If the initial data are  $j$  times differentiable, then all  $j^{\text{th}}$  order partial derivatives of the solution exist.

Since the equations are linear and have constant coefficients, the solution corresponding to any legitimate choice of initial data can be expressed as a Fourier series. We shall do so, and then use the result to determine the slow-wave subspace. Slowly evolving atmospheric states are approximately geostrophic, or quasigeostrophic (e.g., Leith, 1980). We will see that slowly evolving solutions of our linear system are also quasigeostrophic.

### 3.2. Fourier Series

First, we review some of the properties of Fourier series; for further reference see, e.g., Churchill (1969). Let  $g(x)$  be a vector or scalar function defined for  $x \in [-\frac{L}{2}, \frac{L}{2}]$ , which is continuous there, and which satisfies  $g(-L/2) = g(L/2)$ . The Fourier coefficients  $\hat{g}(\xi)$  of  $g(x)$  exist and are defined by

$$\hat{g}(\xi) = \frac{1}{L} \int_{-L/2}^{L/2} e^{-i\xi x} g(x) dx, \quad (3.4a)$$

for  $\xi$  ranging over the discrete values

$$\xi = \xi(\omega) = \frac{2\pi}{L} \omega, \quad \omega = 0, \pm 1, \pm 2, \dots; \quad (3.4b)$$

$\xi$  is the spatial frequency and  $\omega$  is the wave number. Henceforth it is understood that the variable  $\xi$  takes on only the discrete values defined in Eq. (3.4b).

If  $g(x)$  is real, it follows immediately from Eq. (3.4a) that

$$\hat{g}(-\xi) = \overline{\hat{g}(\xi)}, \quad (3.5a)$$

for all  $\xi$ , where the overbar denotes complex conjugation. In particular,

$$\hat{g}(0) \text{ is real ;} \quad (3.5b)$$

$\hat{g}(0)$  is just the average value of  $g(x)$ .

If  $g(x)$  is also differentiable on  $[-L/2, L/2]$ , then the Fourier series representation of  $g$  converges pointwise to  $g$  on  $[-L/2, L/2]$ . That is,

$$g(x) = \sum_{\xi} e^{i\xi x} \hat{g}(\xi), \quad (3.6)$$

for all  $x \in [-L/2, L/2]$ , where  $\hat{g}(\xi)$  is given by Eq. (3.4a). The symbol  $\sum_{\xi}$  indicates summation over the discrete values of  $\xi$  given by Eq. (3.4b).

If, in addition, the second derivative  $g_{xx}$  exists on  $[-\frac{L}{2}, \frac{L}{2}]$ , and if  $g_x(-L/2) = g_x(L/2)$ , then the series obtained by termwise differentiation of the series in Eq. (3.6) converges pointwise on  $[-L/2, L/2]$  to  $g_x$ . That is,

$$g_x(x) = \sum_{\xi} e^{i\xi x} \hat{g}_x(\xi), \quad (3.7a)$$

for all  $x \in [-\frac{L}{2}, \frac{L}{2}]$ , where

$$\hat{g}_x(\xi) = i\xi \hat{g}(\xi). \quad (3.7b)$$



### 3.3. Solution of the Initial-Value Problem

Let  $L$  be the set of real 3-vectors  $g(x)$  which are twice-differentiable on  $[-L/2, L/2]$  and which satisfy  $g(-\frac{L}{2}) = g(\frac{L}{2})$  and  $g_x(-\frac{L}{2}) = g_x(\frac{L}{2})$ . We consider for Eqs. (3.1) only those initial data which lie in  $L$ .

Suppose initial data  $\underline{w}(x, 0) \in L$  are given. According to the well-posedness discussion in Sec. 3.1, a corresponding unique solution  $\underline{w}(x, t)$  exists, and  $\underline{w}(x, t) \in L$  for each  $t > 0$ . Eqs.(3.4-3.7) therefore apply to  $\underline{w}(x, t)$ , from which it follows that

$$\underline{w}(x, t) = \sum_{\xi} e^{i\xi x} \hat{\underline{w}}(\xi, t), \quad (3.8)$$

for all  $x \in [-\frac{L}{2}, \frac{L}{2}]$ , where, corresponding to Eqs. (3.1), the Fourier coefficients  $\hat{\underline{w}}(\xi, t)$  satisfy the ordinary differential equation

$$\frac{\partial}{\partial t} \hat{\underline{w}}(\xi, t) = iG(\xi) \hat{\underline{w}}(\xi, t), \quad (3.9a)$$

for all  $\xi$ , and  $G(\xi)$  is given by

$$G(\xi) = - \begin{bmatrix} \xi U & if & \xi \\ -if & \xi U & 0 \\ \xi \phi & ifU & \xi U \end{bmatrix}. \quad (3.9b)$$

To express the solution  $\underline{w}(x, t)$  in terms of the Fourier coefficients  $\hat{\underline{w}}(\xi, 0)$  of the initial data, it remains to solve Eqs.(3.9) and substitute the result into Eq. (3.8). The solution of Eqs. (3.9) is simply

$$\hat{\underline{w}}(\xi, t) = e^{iG(\xi)t} \hat{\underline{w}}(\xi, 0); \quad (3.10)$$

see, for example, Coddington and Levinson (1955, Sec. 3.4).

Equation (3.10) can be expressed more conveniently by expanding  $\hat{\underline{w}}(\xi, 0)$  in terms of the eigenvectors of  $G(\xi)$ . Let  $\lambda_l(\xi)$ ,  $l = -1, 0, 1$ , be the eigenvalues of  $G(\xi)$ , with corresponding eigenvectors  $\underline{q}_l(\xi)$ :

$$G(\xi)\underline{q}_l(\xi) = \lambda_l(\xi) \underline{q}_l(\xi), \quad (3.11a)$$

for  $l = 0, \pm 1$ , and for all  $\xi$ . The matrix  $e^{iG(\xi)t}$  has the same eigenvectors, but with eigenvalues  $e^{i\lambda_l(\xi)t}$ :

$$e^{iG(\xi)t} \underline{q}_l(\xi) = e^{i\lambda_l(\xi)t} \underline{q}_l(\xi), \quad (3.11b)$$

for  $l = 0, \pm 1$ , for all  $\xi$ , and for all  $t \geq 0$ .

It will be shown in Sec. 3.5 that the three eigenvalues  $\lambda_l(\xi)$  corresponding to each  $\xi$  are real and distinct. Given that the eigenvalues are distinct, it follows that each triplet of eigenvectors is a linearly independent set. Each Fourier coefficient  $\hat{\underline{w}}(\xi, 0)$  therefore has a unique expansion in terms of the eigenvectors:

$$\hat{\underline{w}}(\xi, 0) = \sum_l \alpha_l(\xi) \underline{q}_l(\xi), \quad (3.12a)$$

for some scalars  $\alpha_l(\xi)$ , where the summation runs over the values  $l = -1, 0, 1$ .

It follows from Eqs. (3.11b, 3.12a) that Eq. (3.10) can be written

$$\hat{w}(\xi, t) = \sum_l \alpha_l(\xi) q_l(\xi) e^{i\lambda_l(\xi)t}. \quad (3.12b)$$

Substituting this result into Eq. (3.8) yields the Fourier series solution of the initial-value problem for the system (3.1, 3.3):

$$w(x, t) = \sum_{\xi} \sum_l \alpha_l(\xi) q_l(\xi) e^{i(\xi x + \lambda_l(\xi)t)}. \quad (3.13)$$

The solution is a superposition of plane waves (e.g., John, 1978, Sec. 5.2d).

### 3.4. The Slow-Wave Subspace

From Eq. (3.13) it is clear that the eigenvalues  $\lambda_l(\xi)$  are also the eigenfrequencies of the solutions of Eqs. (3.1, 3.3); i.e., they are the rates at which waves of spatial frequency  $\xi$  can evolve. For given  $l$  and  $\xi$ , eigenfrequency  $\lambda_l(\xi)$  is present in the solution if, and only if, the coefficient  $\alpha_l(\xi) \neq 0$  in Eq. (3.13). The quantities  $\alpha_l(\xi)$  are the defining coefficients in expansion (3.12a): frequency  $\lambda_l(\xi)$  is present in the solution if, and only if, the Fourier coefficient  $\hat{w}(\xi, 0)$  of the initial data has a component along the eigenvector  $q_l(\xi)$ .

As previously noted, it will be shown that, for each  $\xi$ , the eigenfrequencies  $\lambda_l(\xi)$  are real and distinct. It will also be shown that one eigenfrequency, say  $\lambda_0(\xi)$ , in fact has magnitude much smaller than the magnitudes of the other two:

$$|\lambda_0(\xi)| \ll |\lambda_{\pm 1}(\xi)|, \quad (3.14)$$

for each  $\xi$ . Actually, because of the reality condition (3.5a), this need be verified only for  $\xi \geq 0$ : according to Eq. (3.9b),  $G(-\xi) = -\bar{G}(\xi)$ , which implies that  $\lambda_{\pm}(-\xi) = -\bar{\lambda}_{\pm}(\xi)$ , so that  $|\lambda_{\pm}(-\xi)| = |\lambda_{\pm}(\xi)|$ .

Slow solutions of system (3.1,3.3) are those in which only the low frequencies  $\lambda_0(\xi)$  are present. The preceding discussion makes it clear that for a solution to evolve slowly, it is necessary and sufficient that the initial data  $\underline{w}(x,0)$  lie in the slow-wave subspace  $R_c$ , which is given by

$$R_c = \{ \underline{w}(x) \in L : \hat{\underline{w}}(\xi) = \alpha_0(\xi) q_0(\xi) \text{ for all } \xi, \\ \text{for some scalars } \alpha_0(\xi) \}. \quad (3.15)$$

The slow-wave subspace is the set of all initial data in  $L$  which lead to slowly evolving, Rossby wave solutions of the continuous, or differential, equations.

It follows from the linearity of Eqs. (3.4a,3.6) that all linear combinations of vectors from  $R_c$  lie in  $R_c$ , so  $R_c$  is in fact a subspace of  $L$ . Furthermore,  $R_c$  is an invariant subspace of the solution operator of the system (3.1,3.3): it follows from Eq. (3.13) that  $\underline{w}(x,t) \in R_c$  for all  $t > 0$  if  $\underline{w}(x,0) \in R_c$ .

### 3.5. The Eigenfrequencies and Phase Speeds

Exact and approximate formulas for the eigenfrequencies  $\lambda_{\pm}(\xi)$  will now be determined, in order to show that the eigenfrequencies are real and distinct, and in order to verify their relationship (3.14). The

slow-wave eigenvectors  $q_0(\xi)$  will be determined afterwards, to make the definition (3.15) of the slow-wave subspace more explicit.

The eigenfrequencies are the eigenvalues of  $G(\xi)$ , which is given by Eq. (3.9b). Setting the determinant of  $\lambda I - G$  equal to zero gives

$$(\lambda + \xi U)^3 - (\xi^2 + f^2)(\lambda + \xi U) + f^2 \xi U = 0. \quad (3.16)$$

Equation (3.16) is the dispersion relation for the system (3.1,3.3), relating the temporal frequencies  $\lambda$  to the spatial frequencies  $\xi$ .

For  $\xi = 0$ , the roots of Eq. (3.16) are

$$\lambda_0(0) = 0, \quad \lambda_{\pm 1}(0) = \pm f. \quad (3.17a)$$

Oscillations with frequency  $f = 2\Omega \sin \theta$ , known as inertial oscillations, are quite rapid outside the tropics. The period of inertial oscillations at  $\theta = \theta_0$ , i.e., for  $f = 10^{-4} \text{sec}^{-1}$ , is  $2\pi/f \approx 17.5$  hr. Pure inertial oscillations are rare in the atmosphere (Dutton, 1976, Sec. 9.3). The root  $\lambda_0 = 0$  is the slow-wave eigenfrequency for  $\xi = 0$ .

The eigenvectors corresponding to the eigenvalues  $\lambda_l(0)$  are

$$q_0(0) = (0, 0, 1)^T, \quad q_{\pm 1}(0) = (1, \pm i, U)^T. \quad (3.17b)$$

Since  $\hat{w}(0, t)$  is the average value of  $w(x, t)$ , the expression for  $q_0(0)$  means that all slow solutions of the system (3.1,3.3), as well as the corresponding initial data  $\underline{w}(x, 0) \in R_c$ , must have  $u$  and  $v$  components with average value zero. Equations (3.17) correspond to the spatially-independent solutions

$$u(t) = u_0 \cos ft + v_0 \sin ft, \quad (3.18a)$$

$$v(t) = v_0 \cos ft - u_0 \sin ft, \quad (3.18b)$$

$$\phi(t) = \phi_0 + U(-u_0 + u_0 \cos ft + v_0 \sin ft), \quad (3.18c)$$

which arise from constant initial data  $(u_0, v_0, \phi_0)$ .

For  $\xi > 0$ , it is natural to express the roots of Eq. (3.16) as phase speeds. Referring to Eq. (3.13), the phase speeds  $c_l(\xi)$  are related to the eigenfrequencies by

$$c_l(\xi) = -\frac{1}{\xi} \lambda_l(\xi); \quad (3.19)$$

relationship (3.14) will be demonstrated in the equivalent form

$$|c_0(\xi)| \ll |c_{\pm 1}(\xi)|. \quad (3.20)$$

The roots of the cubic equation

$$y^3 - ay + b = 0 \quad (3.21a)$$

are given by

$$y_l = \frac{2}{\sqrt{3}} \sqrt{a} \cos \left[ (l+1) \frac{2\pi}{3} - \frac{1}{3} \cos^{-1} \left( -\frac{\sqrt{3}}{2} \frac{b}{a^{3/2}} \right) \right]. \quad (3.21b)$$

The roots of Eq. (3.16), expressed as phase speeds, are therefore given by

$$c_l(\xi) = U - \gamma(\xi) \cos \left[ (l+1) \frac{2\pi}{3} - \frac{1}{3} \cos^{-1}(-\epsilon(\xi)) \right], \quad (3.22a)$$

where

$$\gamma(\xi) = \frac{2}{\sqrt{3}} \frac{1}{\xi} (\xi^2 \phi + f^2)^{1/2}, \quad (3.22b)$$

$$\epsilon(\xi) = \frac{3\sqrt{3}}{2} f^2 \xi U (\xi^2 \phi + f^2)^{-3/2}. \quad (3.22c)$$

The eigenfrequencies are real since  $\xi^2 \phi + f^2 > 0$ .

Equation (3.22a) can be approximated in such a way as to make the magnitudes of the phase speeds more transparent. The dimensionless quantity  $\epsilon(\xi)$  is small, and approaches zero quadratically as  $\xi \rightarrow \pm\infty$ . For the choice of parameters  $f$ ,  $U$ ,  $\phi$  and  $L$  given in Sec. 3.1,  $\epsilon(\xi(\omega)) = 0.115$  for wave number  $\omega = 1$ ,  $\epsilon = 0.074$  for  $\omega = 2$ ,  $\epsilon = 0.043$  for  $\omega = 3$ , and  $\epsilon = 0.007$  for  $\omega = 8$ . Since

$$\cos^{-1}(-\epsilon) = \frac{\pi}{2} + \epsilon + O(\epsilon^3),$$

a good approximation to  $c_l$  is given by

$$c_l(\xi) \approx U - \gamma(\xi) \cos \left[ (l+1) \frac{2\pi}{3} - \frac{\pi}{6} - \frac{1}{3} \epsilon(\xi) \right]. \quad (3.23)$$

Expanding the cosine to first order in a Taylor series about  $(l+1) \frac{2\pi}{3} - \frac{\pi}{6}$  gives

$$c_0(\xi) \approx U - \frac{1}{3} \gamma(\xi) \epsilon(\xi), \quad (3.24a)$$

$$c_{\pm 1}(\xi) \approx U \pm \frac{\sqrt{3}}{2} \gamma(\xi) + \frac{1}{6} \gamma(\xi) \epsilon(\xi); \quad (3.24b)$$

substituting Eqs. (3.22b,c) into Eqs. (3.24) gives

$$c_0(\xi) \approx U - \frac{f^2 U}{\xi^2 \phi + f^2}, \quad (3.25a)$$

$$c_{\pm 1}(\xi) \approx U \pm \frac{1}{\xi} \sqrt{\xi^2 \phi + f^2} + \frac{1}{2} \frac{f^2 U}{\xi^2 \phi + f^2}. \quad (3.25b)$$

For the aforementioned choice of parameters  $f$ ,  $U$ ,  $\phi$ ,  $L$ , and for the first eight wave numbers, the exact values of the phase speeds, Eqs. (3.22), are presented in Table 1. The corresponding approximate phase speeds, Eqs. (3.25), are presented in Table 2. Comparison of the tables indicates excellent agreement between the approximate and exact values, and both tables verify the separation of phase speeds (3.20).

Individual wave components of slow solutions of the differential equations have the relatively small phase speeds  $c_0(\xi)$  and are called slow waves, or Rossby waves. They are an important feature of midlatitude atmospheric dynamics. The slow waves retrogress: as indicated by Eq. (3.25a), their propagation relative to the mean current  $U$  is westward. The slow wave phase speeds are comparable to  $U$ , and increase monotonically toward  $U$  as the wave number increases.



The fast waves, with the large phase speeds  $c_{\pm 1}(\xi)$ , are known as inertia-gravity waves since they are the usual gravity waves of shallow-water theory, for which  $c_{\pm 1} = U \pm \sqrt{\Phi}$ , modified by the presence of the Coriolis force. The speed of the inertia-gravity waves is dominated by the second term in Eq. (3.25b); waves with speed  $c_1$  propagate toward the east and waves with speed  $c_{-1}$  propagate toward the west. The inertia-gravity wave phase speeds decrease monotonically in magnitude, toward  $|U \pm \sqrt{\Phi}|$ , as the wave number increases.

As explained in Sec. 1.2, Rossby waves and inertia-gravity waves are both present in slow solutions of the fully nonlinear, primitive-equation models actually used in NWP: a small inertia-gravity wave component maintains the quasigeostrophic equilibrium. Slow solutions of our linear shallow-water equations model, produced by initial data in the slow-wave subspace  $R_c$ , consist entirely of Rossby waves.

### 3.6. Approximate Slow Initial Data

Having determined the slow-wave eigenvalues  $\lambda_0(\xi)$ , the slow-wave eigenvectors  $g_0(\xi)$ , upon which the definition (3.15) of the slow-wave subspace depends, are obtained by solving Eq. (3.11a) with  $\ell = 0$ . It is found that

$$g_0(\xi) = \left[ \mu(\xi), \frac{1\xi}{f}, \frac{\xi^2}{f^2} \left( -\Phi + \frac{U}{\mu(\xi)} \right) \right]^T, \quad (3.26a)$$

for each  $\xi$ , where

$$\mu(\xi) = \frac{\xi^2}{f^2} \gamma(\xi) \cos \left[ \frac{2\pi}{3} - \frac{1}{3} \cos^{-1}(-\varepsilon(\xi)) \right], \quad (3.26b)$$

and  $\gamma(\xi)$ ,  $\varepsilon(\xi)$  are given by Eqs. (3.22b,c).

Introducing the same approximations into Eq. (3.26b) as those that lead to Eqs. (3.24) results in

$$\mu(\xi) \approx \frac{\xi^2 U}{\xi^2 \phi + f^2}, \quad (3.27)$$

whence Eq. (3.26a) becomes

$$g_0(\xi) \approx \left[ \frac{\xi^2 U}{\xi^2 \phi + f^2}, \frac{1\xi}{f}, 1 \right]^T. \quad (3.28)$$

Eq. (3.28) is exact for  $\xi = 0$ : it reduces to the expression for  $g_0(0)$  in Eq. (3.17b).

If  $w(x,0) \in R_c$ , then  $u(x,0)$  and  $v(x,0)$  are determined by  $\phi(x,0)$ . Eq. (3.28), with Eqs. (3.6,3.7,3.15), implies that if  $\phi(x,0)$  is specified arbitrarily,

$$\phi(x,0) = \sum_{\xi} \alpha_0(\xi) e^{i\xi x}, \quad (3.29a)$$

then approximate formulas for  $u(x,0)$  and  $v(x,0)$  such that  $w(x,t)$  evolves slowly are

$$u(x,0) \approx \sum_{\xi} \frac{\xi^2 U}{\xi^2 \phi + f^2} \alpha_0(\xi) e^{i\xi x}, \quad (3.29b)$$

$$v(x,0) \approx \int_{\xi} \frac{i\xi}{f} \alpha_0(\xi) e^{i\xi x} = \frac{1}{f} \phi_x(x,0). \quad (3.29c)$$

Formulas (3.29b,c) are exact to first order in the small parameter  $\epsilon(\xi)$ .

Geostrophic states of our linear system (3.1) are those for which

$$u = 0, \quad v = \phi_x/f; \quad (3.30a,b)$$

the u-component of a geostrophic state is zero since there is no pressure-gradient term to balance the Coriolis term in Eq. (3.1b). Equivalently to Eqs. (3.30), the Fourier components of a geostrophic state are

$$\hat{\underline{w}}(\xi) = [0, i\xi/f, 1]^T. \quad (3.31)$$

Comparing Eq. (3.31) with Eq. (3.26a), it follows that slowly evolving states of our linear system are not geostrophic.

However, comparing Eqs. (3.30) with Eqs. (3.29b,c), we see that slowly evolving states are quasigeostrophic. For the v-components, Eqs. (3.29c, 3.30b), this is readily apparent. As for the u-components, a numerical calculation shows that  $\xi^2\phi$  is the dominant term in the denominator of Eq. (3.29b), except for wave number  $\omega = 1$ , for which  $\xi^2\phi$  and  $f^2$  are roughly equal. It follows that  $u(x,0)$  and  $\phi(x,0) - \alpha_0(0)$ , given by Eqs. (3.29b,a) respectively, are approximately proportional, with constant of proportionality  $U/\phi$ . The amplitude  $\phi_0$  of the perturbation geopotential  $\phi(x,0)$  is typically

smaller than the mean geopotential height  $\phi$  by an order of magnitude.

The amplitude  $u_0$  of  $u(x,0)$ ,

$$u_0 \approx \frac{U}{\phi} |\phi_0 - \alpha_0(0)| \leq \frac{U}{\phi} \phi_0 ,$$

is therefore smaller than the mean zonal current  $U$  by at least an order of magnitude: slowly evolving solutions have small  $u$ -components. Hence, slowly evolving solutions are quasigeostrophic.

The  $u$ -component of solutions of the linear system (3.1) is special. Its magnitude in our assimilation experiments will provide one convenient check of the proximity of state estimates to the slow-wave subspace.

# CHAPTER FOUR

## SLOW SOLUTIONS OF DISCRETE LINEAR SHALLOW-WATER EQUATIONS

We introduce now the discretization  $\Psi$  of the linear shallow-water equations which will be used later in the assimilation experiments; here we formulate the discrete model's slow-wave subspace  $R$ . The discrete slow-wave subspace is defined directly in terms of  $\Psi$ , rather than in terms of the original differential equations or their slow-wave subspace  $R_c$ . In particular,  $R$  will have the property of being an invariant subspace of  $\Psi$ , and this property will be important in our formulation of the modified KB filter.

### 4.1. The Discrete Equations

To discretize the differential equations, we use the Richtmyer two-step formulation of the Lax-Wendroff scheme (Richtmyer and Morton, 1967, Sec. 12.7 and 13.4). Reasons for the suitability of this particular scheme to discretization of the linear shallow-water equations appear in Ghil et al. (1981, Sec. 3.2). The scheme is second-order accurate in time and space, and fourth-order dissipative in the sense of Kreiss (Richtmyer and Morton, 1967, Sec. 5.4).

The finite-difference grid

$$t_k = k\Delta t, \quad k = 0, 1, 2, \dots, \quad (4.1a)$$

$$x_j = j\Delta x, \quad j = -\frac{M}{2} + 1, -\frac{M}{2} + 2, \dots, \frac{M}{2}, \quad (4.1b)$$

is introduced, where

$$\Delta x = L/M, \quad (4.1c)$$

and the number of grid points  $M$  is assumed to be even. The 3-vector

$$\underline{w}_k^j = [u_k^j, v_k^j, \phi_k^j]^T \quad (4.1d)$$

will approximate the exact solution  $w(j\Delta x, k\Delta t)$ .

Rewriting the original system (3.1) in matrix notation,

$$\underline{w}_t = C\underline{w}_x + B\underline{w}, \quad (4.2a)$$

where

$$C = - \begin{bmatrix} U & 0 & 1 \\ 0 & U & 0 \\ \phi & 0 & U \end{bmatrix}, \quad (4.2b)$$

$$B = - \begin{bmatrix} 0 & -f & 0 \\ f & 0 & 0 \\ 0 & -fU & 0 \end{bmatrix}, \quad (4.2c)$$

the difference scheme is written, for  $k = 1, 2, 3, \dots$ , as

$$\begin{aligned} \underline{w}_k^j &= \underline{w}_{k-1}^j + (\Delta t) \underline{w}_t|_{k-1/2}^j \\ &= \underline{w}_{k-1}^j + \frac{\Delta t}{\Delta x} C(\underline{w}_{k-1/2}^{j+1/2} - \underline{w}_{k-1/2}^{j-1/2}) + \frac{\Delta t}{2} B(\underline{w}_{k-1/2}^{j-1/2} + \underline{w}_{k-1/2}^{j+1/2}), \end{aligned} \quad (4.3a)$$

for  $j = -(M/2)+1, \dots, M/2$ , where the intermediate values  $w_{k-1}^{j+1/2}$  are given by

$$\begin{aligned} w_{k-1}^{j+1/2} &= w_{k-1}^{j+1/2} + \frac{\Delta t}{2} w_t|_{k-1}^{j+1/2} \\ &= \frac{1}{2} \left( I + \frac{\Delta t}{2} B \right) (w_{k-1}^j + w_{k-1}^{j+1}) + \frac{\Delta t}{2\Delta x} C (w_{k-1}^{j+1} - w_{k-1}^j), \end{aligned} \quad (4.3b)$$

for  $j = -M/2, \dots, M/2$ ; the scheme is closed by defining

$$w_{k-1}^{-M/2} = w_{k-1}^{M/2}, \quad w_{k-1}^{M/2+1} = w_{k-1}^{-M/2+1}, \quad (4.3c,d)$$

which corresponds to the periodic boundary condition (3.3).

By combining Eqs. (4.3a,b), the scheme may be rewritten as

$$w_k^j = \sum_{\ell=-1}^1 \psi_\ell w_{k-1}^{j+\ell}, \quad (4.4a)$$

for  $j = -(M/2)+1, \dots, M/2$ , and  $k = 1, 2, 3, \dots$ , where

$$w_{k-1}^{-M/2} = w_{k-1}^{M/2}, \quad w_{k-1}^{M/2+1} = w_{k-1}^{-M/2+1}, \quad (4.4b,c)$$

and the  $3 \times 3$  matrices  $\psi_\ell$  are given by

$$\psi_0 = I - \sigma^2 C^2 + \frac{\Delta t}{2} B \left( I + \frac{\Delta t}{2} B \right), \quad (4.5a)$$

$$\psi_{\pm 1} = \pm \frac{\sigma}{2} C + \frac{\sigma^2}{2} C^2 \pm \frac{\sigma \Delta t}{4} (CB + BC) + \frac{\Delta t}{4} B \left( I + \frac{\Delta t}{2} B \right), \quad (4.5b)$$

where

$$\sigma = \frac{\Delta t}{\Delta x} . \quad (4.5c)$$

Finally, to write the difference scheme in the notation of Chapter 2, we introduce the composite vector

$$\underline{w}_k = [(\underline{w}_k^{M/2+1})^T, (\underline{w}_k^{M/2+2})^T, \dots, (\underline{w}_k^{M/2})^T]^T ; \quad (4.6)$$

$\underline{w}_k$  is an  $n$ -vector, with  $n = 3M$ , which is composed of  $M$  3-vectors. Equations (4.4) can then be written as

$$\underline{w}_k = \Psi \underline{w}_{k-1} , \quad (4.7a)$$

where  $\Psi$  is the  $3M \times 3M$  block-circulant matrix with  $3 \times 3$  blocks (Davis, 1979, Sec. 5.6) denoted by

$$\Psi = \text{circ} [\Psi_0, \Psi_1, 0, \dots, 0, \Psi_{-1}] ; \quad (4.7b)$$

the individual blocks  $\Psi_0, \Psi_{\pm 1}$  are given by Eqs. (4.5).

A  $3M \times 3M$  block-circulant matrix with  $3 \times 3$  blocks is a matrix that, when partitioned regularly into  $M^2$   $3 \times 3$  blocks, has  $M$  arbitrary blocks across its first row, with each of the succeeding  $M-1$  rows obtained by circularly shifting the previous row one block to the right. It is denoted by listing the blocks which appear across the first row, as in Eq. (4.7b).

Thus, our dynamics matrix  $\Psi$  has only three nonzero blocks in each row. In fact,  $\Psi$  is almost block-tridiagonal: the only nonzero blocks away from the diagonal are in the upper right and lower left corners of



$\Psi$ , which contain the blocks  $\Psi_{-1}$  and  $\Psi_1$ , respectively, as a result of the periodic boundary conditions. The matrix is independent of the time  $k\Delta t$ , unlike the general dynamics matrix of Chapter 2.

Equations (4.7), with the submatrices  $\Psi_0$ ,  $\Psi_{\pm 1}$  given by Eqs. (4.5), constitute the discrete "forecast model" upon which the assimilation experiments of Chapters 6 and 7 will be based. The remainder of this chapter is devoted to formulation of the discrete model's slow-wave subspace. The development parallels that of Chapter 3: the discrete Fourier transform is introduced first, then  $w_k$  is written in terms of the Fourier coefficients of arbitrary initial data  $w_0$ , and finally the slow-wave subspace is defined.

#### 4.2. The Discrete Fourier Transform

An  $M$ -vector  $\underline{u}$  is now denoted by

$$\underline{u} = [u(-\frac{M}{2}+1), \dots, u(\frac{M}{2})]^T; \quad (4.8a)$$

for consistency with Sec. 3.2, spatial indices appear as arguments instead of as superscripts. The discrete Fourier transform of  $\underline{u}$  is the  $M$ -vector

$$\hat{\underline{u}} = [\hat{u}(-\frac{M}{2}+1), \dots, \hat{u}(\frac{M}{2})]^T, \quad (4.8b)$$

whose components  $\hat{u}(\omega)$  are defined by

$$\hat{u}(\omega) = \frac{1}{\sqrt{M}} \sum_j e^{-2\pi i j \omega / M} u(j), \quad (4.9a)$$

for  $\omega = -(M/2)+1, \dots, M/2$ . If  $\hat{u}(\omega)$  is given by Eq. (4.9a), then  $u(j)$  can be recovered by the inversion formula

$$u(j) = \frac{1}{\sqrt{M}} \sum_{\omega} e^{2\pi i j \omega / M} \hat{u}(\omega), \quad (4.9b)$$

for  $j = -(M/2)+1, \dots, M/2$ . In Eqs. (4.9) and in the sequel, the symbols  $\sum_j$  and  $\sum_{\omega}$  always refer to summation over the index set  $\{-\frac{M}{2}+1, \dots, \frac{M}{2}\}$ . Formulas (4.9) are discrete analogues of Eqs. (3.4, 3.6).

Equations (4.9) can be written more compactly in matrix notation. The  $M \times M$  Fourier matrix  $F_M$  (e.g., Davis, 1979, Sec. 2.5) is the matrix whose  $(l, m)^{th}$  element is

$$(F_M)_{l,m} = \frac{1}{\sqrt{M}} \exp \left[ -2\pi i \left( p - \frac{M}{2} \right) \left( q - \frac{M}{2} \right) / M \right]. \quad (4.10)$$

The Fourier matrix is symmetric and unitary, i.e.,

$$F_M^T = F_M, \quad F_M^* = F_M^{-1}, \quad (4.11a,b)$$

where the asterisk indicates the complex conjugate transpose. From definitions (4.8, 4.10), it follows directly that Eq. (4.9a) can be written as

$$\hat{\underline{u}} = F_M \underline{u}, \quad (4.12a)$$

while Eq. (4.11b) then implies that Eq. (4.9b) becomes

-63-

$$\underline{u} = F_M^* \hat{\underline{u}}. \quad (4.12b)$$

For an  $n$ -vector  $\underline{w}$ , composed of  $M$  3-vectors,

$$\underline{w} = [\underline{w}^T(-\frac{M}{2}+1), \dots, \underline{w}^T(\frac{M}{2})]^T, \quad (4.13a)$$

where

$$\underline{w}(j) = [u(j), v(j), \phi(j)]^T, \quad (4.13b)$$

the Fourier transform is defined consistently with Eqs. (4.9). That is,  $\hat{\underline{w}}$  is the  $n$ -vector

$$\hat{\underline{w}} = [\hat{\underline{w}}^T(-\frac{M}{2}+1), \dots, \hat{\underline{w}}^T(\frac{M}{2})]^T, \quad (4.14a)$$

whose component 3-vectors

$$\hat{\underline{w}}(\omega) = [\hat{u}(\omega), \hat{v}(\omega), \hat{\phi}(\omega)]^T, \quad (4.14b)$$

are given by

$$\hat{\underline{w}}(\omega) = \frac{1}{\sqrt{M}} \sum_j e^{-2\pi i j \omega / M} \underline{w}(j), \quad (4.15a)$$

for  $\omega = -(M/2)+1, \dots, M/2$ . The inversion formula is

$$\underline{w}(j) = \frac{1}{\sqrt{M}} \sum_{\omega} e^{2\pi i j \omega / M} \hat{\underline{w}}(\omega), \quad (4.15b)$$

for  $j = -(M/2)+1, \dots, M/2$ .

In order to write Eqs. (4.15) in matrix notation, we define the  $n \times n$  permutation matrix  $V$  as that matrix which reorders the elements of  $\underline{w}$ , Eqs. (4.13), according to

$$\underline{Vw} = [\underline{u}^T, \underline{v}^T, \underline{\phi}^T]^T, \quad (4.16)$$

where the  $M$ -vector  $\underline{u}$  is defined in Eq. (4.8a), and  $\underline{v}$  and  $\underline{\phi}$  are defined similarly;  $V$  is real and unitary, so that

$$\underline{V}^T = \underline{V}^* = \underline{V}^{-1}. \quad (4.17)$$

It follows from Eqs. (4.11, 4.17) that the  $n \times n$  matrix  $F$ , defined by

$$F = \underline{V}^{-1} \begin{bmatrix} F_M & 0 & 0 \\ 0 & F_M & 0 \\ 0 & 0 & F_M \end{bmatrix} \underline{V}, \quad (4.18)$$

is symmetric and unitary,

$$F^T = F, \quad F^* = F^{-1}. \quad (4.19a, b)$$

Equations (4.12a, 4.16, 4.18) imply that Eq. (4.15a) can be written as

$$\hat{\underline{w}} = F \underline{w}, \quad (4.20a)$$

which, with Eq. (4.19b), implies that Eq. (4.15b) becomes

$$\underline{w} = F^* \hat{\underline{w}} \quad (4.20b)$$

The n-vectors  $\underline{w}$  and  $\hat{\underline{w}}$  given by Eqs.(4.20) constitute a discrete Fourier transform pair.

#### 4.3. Solution of the Initial-Value Problem

The iterates  $\underline{w}_k$  of the finite-difference scheme (4.7) can now be expressed in terms of the Fourier components of arbitrary initial data  $\underline{w}_0$ . It follows from Eqs. (4.20) that Eq. (4.7a) is equivalent to

$$\hat{\underline{w}}_k = \hat{\Psi} \hat{\underline{w}}_{k-1}, \quad (4.21)$$

where the  $n \times n$  matrix  $\hat{\Psi}$  is given by

$$\hat{\Psi} = F \Psi F^* \quad (4.22)$$

Due to the block-circulant structure of  $\Psi$ , the matrix  $\hat{\Psi}$  is block-diagonal: the matrix  $F$  block-diagonalizes all  $3M \times 3M$  block-circulant matrices having  $3 \times 3$  blocks (Davis, 1979, Thm. 5.6.4).

The matrix  $\hat{\Psi}$  has  $M$   $3 \times 3$  blocks, denoted by  $\hat{\Psi}(\omega)$ , along its main diagonal, and zeros elsewhere. It is denoted by

$$\hat{\Psi} = \text{diag}[\hat{\Psi}(-\frac{M}{2}+1), \hat{\Psi}(-\frac{M}{2}+2), \dots, \hat{\Psi}(\frac{M}{2})], \quad (4.23)$$

and the individual blocks are given by

$$\hat{\Psi}(\omega) = \sum_{j=-1}^1 e^{2\pi i j \omega / M} \Psi_j, \quad (4.24)$$

for  $\omega = -(M/2)+1, \dots, M/2$ ; the matrices  $\Psi_j$  are defined by Eqs. (4.5). The matrix  $\hat{\Psi}(\omega)$  is called the symbol, or amplification matrix, of the difference scheme (e.g., Isaacson and Keller, 1966, Sec. 9.5).

Since  $\hat{\Psi}$  is block-diagonal, the  $n$ -vector equation (4.21) decouples into  $M$  3-vector equations. The decoupled equations are written, in the notation of Eqs. (4.14), as

$$\hat{w}_k(\omega) = \hat{\Psi}(\omega) \hat{w}_{k-1}(\omega), \quad (4.25)$$

for  $\omega = -\frac{M}{2}+1, \dots, \frac{M}{2}$ ; therefore, by repeated application of  $\hat{\Psi}(\omega)$ ,

$$\hat{w}_k(\omega) = \hat{\Psi}^k(\omega) \hat{w}_0(\omega). \quad (4.26)$$

Eqs. (4.25, 4.26) correspond to the fact that, for constant-coefficient linear difference (or differential) equations, waves with different wave numbers evolve separately.

Equation (4.26), like its continuous counterpart (3.10), is simplified by an appropriate eigenvector expansion. Let  $\delta_l(\omega)$  be the eigenvalues of  $\hat{\Psi}(\omega)$ , with corresponding eigenvectors  $\underline{\mathbf{x}}_l(\omega)$ :

$$\hat{\Psi}(\omega) \underline{\mathbf{x}}_l(\omega) = \delta_l(\omega) \underline{\mathbf{x}}_l(\omega), \quad (4.27)$$

for  $l = 0, \pm 1$ . The eigenvalues are generally complex, and we write them in polar form, as

$$\delta_l(\omega) = \rho_l(\omega) e^{i\nu_l(\omega)\Delta t}, \quad (4.28)$$

where  $\rho_\ell(\omega)$  and  $\nu_\ell(\omega)$  are real. The matrix  $\hat{\Psi}^k(\omega)$  in Eq. (4.26) has the same eigenvectors as  $\hat{\Psi}(\omega)$ , but with eigenvalues  $\delta_\ell^k(\omega)$ :

$$\hat{\Psi}^k(\omega) \mathbf{z}_\ell(\omega) = \delta_\ell^k(\omega) \mathbf{z}_\ell(\omega). \quad (4.29)$$

It will be shown in Sec. 4.4 that the triplet of eigenvectors corresponding to each  $\omega$  is a linearly independent set. Hence, the Fourier transform of the initial data can be expanded as

$$\hat{w}_0(\omega) = \sum_{\ell} \beta_\ell(\omega) \mathbf{z}_\ell(\omega), \quad (4.30)$$

for some scalars  $\beta_\ell(\omega)$ . From Eqs. (4.28-4.30) it follows that Eq. (4.26) can be written as

$$\hat{w}_k(\omega) = \sum_{\ell} \beta_\ell(\omega) \mathbf{z}_\ell(\omega) \rho_\ell^k(\omega) e^{i\nu_\ell(\omega)t_k}. \quad (4.31)$$

Finally, using Eq. (4.31) in the inversion formula (4.15b), it follows that  $w_k(j)$  can be written as

$$w_k(j) = \frac{1}{\sqrt{M}} \sum_{\omega} \sum_{\ell} \beta_\ell(\omega) \mathbf{z}_\ell(\omega) \rho_\ell^k(\omega) \exp\{i[\xi(\omega)x(j) + \nu_\ell(\omega)t_k]\}, \quad (4.32)$$

where  $\xi(\omega) = 2\pi\omega/M\Delta x$  and  $x(j) = j\Delta x$ .

Equation (4.32) is the Fourier series solution of the initial-value problem for the discrete system (4.7). The quantities  $(\beta_\ell, \mathbf{z}_\ell, \nu_\ell)$  in Eq. (4.32) have counterparts  $(\alpha_\ell, \mathbf{g}_\ell, \lambda_\ell)$  in the solution (3.13) of the continuous equations. The factors  $\rho_\ell(\omega)$  are due to discretization.

#### 4.4. The Eigenfrequencies and Phase Speeds

According to Eq. (4.32), the eigenfrequencies associated with the difference scheme are the quantities  $v_l(\omega)$ . We now show that they separate naturally into low and high frequencies, like the eigenfrequencies of the differential equations, and then we define the discrete slow-wave subspace.

To classify the eigenfrequencies, the eigenvalues  $\delta_l(\omega)$  were computed numerically, cf. Eqs. (4.27, 4.24, 4.5), after which the eigenfrequencies were obtained by use of Eq. (4.28). As in the assimilation experiments of Chapters 6 and 7, the values  $M = 16$ ,  $\Delta t = 30$  min., were used in the eigenvalue computation.

The eigenfrequencies corresponding to  $\omega = 0$  are

$$v_0(0) = 0, \quad v_{\pm 1}(0) = \pm 1.0053 f, \quad (4.33)$$

in close agreement with the corresponding result (3.17a) for the continuous system.

For wave numbers  $\omega = 1, 2, \dots, 8$ , the phase speeds

$$c_l(\omega) = -\frac{v_l(\omega)}{\xi(\omega)} \quad (4.34)$$

are presented in Table 3. Comparison with Tables 1 and 2 shows that the phase speeds associated with the difference scheme are good approximations to those of the differential equations only for the smallest one or two wave numbers. This behavior is typical of dissipative difference schemes, such as the Richtmyer scheme, although the discrepancy between discrete and continuous phase speeds is somewhat



exaggerated by our relatively coarse mesh:  $\Delta x = L/16 = 875$  km., which is much larger than mesh spacings typically used in NWP. The discrepancy is an indication of the difference between the discrete and continuous slow-wave subspaces.

Except for  $\omega = 8$ , the table does show that the phase speeds, and hence the eigenfrequencies, are well-separated:

$$|v_0(\omega)| \ll |v_{\pm 1}(\omega)|, \quad (4.35)$$

for  $\omega = 1, \dots, 7$ . The same is true for  $\omega = -1, \dots, -7$ , since Eq. (4.24) implies  $\hat{\Psi}(-\omega) = \overline{\hat{\Psi}(\omega)}$ , whence  $\delta_\ell(-\omega) = \overline{\delta_\ell(\omega)}$  and  $|v_\ell(-\omega)| = |v_\ell(\omega)|$ .

For  $\omega = M/2 = 8$ , all phase speeds and eigenfrequencies are zero: waves with the highest spatial frequency are stationary. All three of these waves could be associated with the discrete slow-wave subspace, but we select only one, as follows. According to Eqs. (4.5, 4.24),  $\hat{\Psi}(M/2)$  is given by

$$\hat{\Psi}\left(\frac{M}{2}\right) = \Psi_0 - \Psi_1 - \Psi_{-1} = I - 2\sigma^2 C^2, \quad (4.36)$$

where  $C$  is given by Eq. (4.2b). Since the eigenvalues of  $C$  are  $U$ ,  $U \pm \sqrt{\Phi}$ , the eigenvalues of  $\hat{\Psi}(M/2)$  are given by

$$\delta_0\left(\frac{M}{2}\right) = 1 - 2\sigma^2 U^2, \quad (4.37a)$$

$$\delta_{\pm 1}\left(\frac{M}{2}\right) = 1 - 2\sigma^2 (U \pm \sqrt{\Phi})^2; \quad (4.37b,c)$$

the eigenvalues  $\delta_{0,\pm 1}(M/2)$  are distinct, although the corresponding

frequencies  $\nu_{0,\pm 1}(M/2)$  are all zero. Due to the appearance of the factors  $U$  and  $U \pm \sqrt{\Phi}$  in Eqs. (4.37), and according to the discussion following Eqs. (3.25), it is appropriate to refer to  $\delta_0(M/2)$  as the Rossby eigenvalue for wave number  $M/2$ .

According to Eqs. (4.33,4.37) and Table 3, the eigenvalues  $\delta_\ell(\omega)$  are distinct for each  $\omega$ . The corresponding eigenvectors  $\underline{x}_\ell(\omega)$  are therefore linearly independent, and expansion (4.30) is valid.

#### 4.5. The Discrete Slow-Wave Subspace

It has been shown that the eigenfrequencies  $\nu_\ell(\omega)$ , defined in Eq. (4.28) by the eigenvalues  $\delta_\ell(\omega)$ , can be classified into Rossby frequencies  $\nu_0(\omega)$  and inertia-gravity frequencies  $\nu_{\pm 1}(\omega)$ , for each possible wave number  $\omega$ . The corresponding Rossby eigenvectors  $\underline{x}_0(\omega)$  and inertia-gravity eigenvectors  $\underline{x}_{\pm 1}(\omega)$  are defined by Eq. (4.27).

According to Eqs. (4.30,4.32), if the initial vector  $\underline{w}_0$  has Fourier components solely along the Rossby eigenvectors, then the corresponding solution  $\underline{w}_k$  of the difference scheme (4.7) evolves slowly, with frequencies  $\nu_0(\omega)$ . That is, analogously to the definition (3.15) of the continuous slow-wave subspace, the discrete slow-wave subspace is the set  $R$ , given by

$$R = \{ \underline{w} \in R^n: \hat{\underline{w}}(\omega) = \beta_0(\omega) \underline{x}_0(\omega) \text{ for some} \\ \text{scalars } \beta_0(\omega) \text{ and for all } \omega = -\frac{M}{2}+1, \dots, \frac{M}{2} \}, \quad (4.38)$$

where  $R^n$  denotes the set of real  $n$ -vectors.

We give two further definitions of  $R$ , equivalent to (4.38).

Introducing the  $n$ -vector

$$\underline{s}_\omega = [0, \dots, 0, \underline{s}_0^T(\omega), 0, \dots, 0]^T, \quad (4.39)$$

where there are  $3(\omega + \frac{M}{2} - 1)$  zeros on the left and  $3(\frac{M}{2} - \omega)$  zeros on the right, an equivalent definition is

$$R = \{ \underline{w} \in R^n : \hat{\underline{w}} = \sum_{\omega} \beta_0(\omega) \underline{s}_\omega \text{ for some scalars } \beta_0(\omega) \} ; \quad (4.40)$$

definition (4.14a) has been used. It follows from the Fourier transform pair (4.20) that another equivalent definition is

$$R = \{ \underline{w} \in R^n : \underline{w} = \sum_{\omega} \beta_0(\omega) F^* \underline{s}_\omega \text{ for some scalars } \beta_0(\omega) \} . \quad (4.41)$$

Definition (4.41) makes it clear that  $R$  is a subspace of  $R^n$ . That is,  $R$  is a nonempty subset of  $R^n$ , and

$$\alpha_1 \underline{y}_1 + \alpha_2 \underline{y}_2 \in R \text{ if } \underline{y}_1 \in R \text{ and } \underline{y}_2 \in R, \quad (4.42)$$

for all real scalars  $\alpha_1, \alpha_2$ . In fact,  $R$  is an  $M = n/3$ -dimensional subspace of  $R^n$ .

The  $n$ -vector  $F^* \underline{s}_\omega$  represents a pure wave of wave number  $\omega$ . It is also, for each  $\omega$ , an eigenvector of  $\Psi$  with eigenvalue  $\delta_0(\omega)$ :

$$\begin{aligned} \Psi F^* \underline{s}_\omega &= F^* \hat{\Psi} F F^* \underline{s}_\omega, & \text{from (4.19b, 4.22)} \\ &= F^* \hat{\Psi} \underline{s}_\omega, & \text{from (4.19b)} \\ &= \delta_0(\omega) F^* \underline{s}_\omega, & \text{from (4.23, 4.27, 4.39).} \end{aligned} \quad (4.43)$$

According to definition (4.41),  $R$  is therefore an invariant subspace of  $\Psi$ :

$$\Psi y \in R \text{ if } y \in R. \quad (4.44)$$

This fact also follows immediately from Eqs. (4.30,4.32): if the initial data  $w_0 \in R$ , then  $w_k \in R$  for all  $k$ .

Analogously to Eq. (4.38), the discrete fast-wave subspace  $G$ , consisting of inertia-gravity waves, is defined as

$$G = \{ \underline{w} \in R^n: \hat{w}(\omega) = \beta_{-1}(\omega) \underline{E}_{-1}(\omega) + \beta_1(\omega) \underline{E}_1(\omega) \}$$

$$\text{for some scalars } \beta_{\pm 1}(\omega) \text{ and for all } \omega = -\frac{M}{2} + 1, \dots, \frac{M}{2} \}; (4.45)$$

$G$  is a  $2M$ -dimensional invariant subspace of  $\Psi$ . Taken together,  $R$  and  $G$  span all of  $R^n$ .

## CHAPTER FIVE

### ESTIMATION THEORY AND INITIALIZATION

#### 5.1. Introduction

Although the Kalman-Bucy filter possesses many optimality properties, it lacks one property of primary importance in numerical weather prediction. Namely, there is no guarantee that the state estimates produced by the KB filter evolve slowly: the KB filter does not solve the initialization problem. In this chapter we introduce a filter, or data assimilation scheme, which, automatically produces slowly evolving state estimates and which retains much of the optimality of the KB filter. The filter consists of a simple modification to the usual KB gain matrices. We now summarize the results concerning the modified KB filter.

The standard KB filter was derived in Chapter 2 by solving an unconstrained minimization problem: the quadratic error functional

$$\eta_k = E[(w_k^a - w_k^t)^T A(w_k^a - w_k^t)]$$

was minimized, in turn, at each time  $k = 1, 2, 3, \dots$ . The modified KB filter is derived by solving a constrained minimization problem: again  $\eta_k$  is minimized with respect to the gain matrix  $K_k$ , but now subject to the constraint that

$$\text{Range } K_k \subset R,$$

i.e., that each column of  $K_k$  lies in the discrete slow-wave subspace. As a result of the fact that the discrete slow-wave subspace is an

invariant subspace of  $\Psi$ , and provided  $w_0^2 \in R$ , we will see that satisfaction of this constraint is necessary and sufficient for the state estimates to evolve slowly.

It was shown in Chapter 2 that the KB filter minimizes  $\eta_k$  for all choices of the positive semidefinite weighting matrix  $A$ . Constraining the state estimates to evolve slowly results in a trade-off: the modified filter depends on the choice of  $A$ . When using the modified filter, one must actually choose the error functional to be minimized.

Provided the class of weighting matrices  $A$  is suitably restricted, the constrained minimization problem has a unique solution, and the modified KB filter is uniquely determined. It is given by multiplying the usual KB gain matrices by a projection matrix  $\Pi$  which depends on  $A$ ,  $\Pi = \Pi(A)$ ;  $\Pi$  is the A-orthogonal projection matrix onto  $R$ , and will be defined below. We denote the modified filter's gain matrices by  $K_k^{\Pi KB}$ :

$$K_k^{\Pi KB} = \Pi K_k^{KB}.$$

The modified filter corresponds to following the standard KB filter with linear normal mode initialization at each observation time.

Linear normal mode initialization, in its nonvariational form, consists of setting to zero all fast components of the analysis vector, while leaving the slow components unchanged, cf. Eqs. (1.3). For the modified filter, this is accomplished by taking  $\Pi$  to be the projection onto  $R$  along the fast-wave subspace  $G$ . We refer to this projection as the parallel projection. This projection is A-orthogonal for an appropriate choice of the weighting matrix  $A$ .

Other choices of  $A$  correspond to performing variational linear

normal mode initialization: the fast components are still set to zero, but the slow components are altered also, cf. Eqs. (1.7,1.8). One such choice is  $A = I$ , in which case  $\Pi$  is the usual orthogonal projection onto  $R$ . As a result of the fact that the slow-wave subspace  $R$  is not orthogonal to the fast-wave subspace  $G$ , we will see that the orthogonal projection is not the same as the parallel projection, so that the corresponding filters produce different results. This is the general situation: it is not particular to the continuous model (3.1) or to its discretization (4.7). Cases in which  $G$  and  $R$  are orthogonal are very special.

The choice  $A = I$  is not appropriate for our model, since it corresponds to minimizing a sum of squares of dimensionally inconsistent quantities. We introduce therefore an additional projection, the minimum-energy projection, in which  $A$  is chosen as the diagonal matrix which makes  $\eta_k$  the expected energy of the analysis error.

After relevant material on projections is discussed in Sec. 5.2, the modified filter is formulated in Sec. 5.3. It is shown in Sec. 5.4 how to efficiently compute  $A$ -orthogonal projections onto  $R$ , for general classes of weighting matrices  $A$ . The parallel, orthogonal, and minimum-energy projections are discussed in Sec. 5.5.

Some of the results of this chapter are stated as lemmas and theorems. These are all proven in the Appendix.

## 5.2. Projection Matrices

Let  $S$  be a subspace of  $R^n$ . That is,  $S$  is a nonempty subset of  $R^n$  and

$$\alpha_1 \underline{x}_1 + \alpha_2 \underline{x}_2 \in S \quad \text{if } \underline{x}_1 \in S \text{ and } \underline{x}_2 \in S ,$$

for all real scalars  $\alpha_1, \alpha_2$ . Notice that  $S$  must contain at least the zero vector.

An  $n \times n$  matrix  $\Pi$  is called a projection matrix onto  $S$ , or simply a projection, if it has the properties

$$\text{Range } \Pi = S , \tag{5.1a}$$

$$\Pi^2 = \Pi ; \tag{5.1b}$$

the range of a matrix is the set of linear combinations of its columns, i.e.,

$$\text{Range } \Pi = \{ \underline{x} : \underline{x} = \Pi \underline{y} \text{ for some } \underline{y} \in \mathbb{R}^n \} .$$

If  $\Pi$  is a projection onto  $S$  and  $\underline{x} = \Pi \underline{y}$ , we refer to the vector  $\underline{x}$  as a projection of  $\underline{y}$  onto  $S$ .

A subspace has a simple characterization in terms of projections onto it. Suppose  $\Pi$  is a projection matrix onto  $S$ . If  $\underline{x}$  is a vector in  $S$ , then

$$\begin{aligned} \underline{x} &= \Pi \underline{y} , \quad \text{for some } \underline{y} \in \mathbb{R}^n , \quad \text{by Eq. (5.1a) ,} \\ &= \Pi^2 \underline{y} , \quad \text{by Eq. (5.1b) ,} \\ &= \Pi \underline{x} , \quad \text{since } \Pi \underline{y} = \underline{x} ; \end{aligned}$$

i.e.,  $\underline{x} = \Pi \underline{x}$ . On the other hand, if  $\underline{x} \in \mathbb{R}^n$  and  $\underline{x} = \Pi \underline{x}$ , then Eq.



(5.1a) implies that  $\underline{x} \in S$ . That is, if  $\Pi$  is a projection onto  $S$ , we can write

$$S = \{ \underline{x} \in R^n : \Pi \underline{x} = \underline{x} \} . \quad (5.2)$$

Equation (5.2) states that a projection matrix acts on its range like the identity matrix. To completely characterize a projection matrix, it remains to specify how it acts on the rest of  $R^n$ . One way to do so is as follows.

Let  $V$  be a fixed, but arbitrary, positive semidefinite  $n \times n$  matrix. The kernel, or null space, of  $V$  is the set of its null vectors,

$$\text{Ker } V = \{ \underline{x} \in R^n : V \underline{x} = 0 \} .$$

Since  $V$  is positive semidefinite, rather than positive definite,  $\text{Ker } V$  may contain vectors other than the zero vector.

Two vectors  $\underline{y}_1, \underline{y}_2 \in R^n$  are said to be orthogonal if  $\underline{y}_1^T \underline{y}_2 = 0$ . More generally, if  $\underline{y}_1^T V \underline{y}_2 = 0$ , then the vectors are said to be V-orthogonal. In particular,  $\underline{y}_1$  and  $\underline{y}_2$  are V-orthogonal if  $\underline{y}_1 \in \text{Ker } V$  or  $\underline{y}_2 \in \text{Ker } V$ .

Suppose one can find a projection matrix  $\Pi$  which, in addition to satisfying Eqs. (5.1), satisfies

$$(V \Pi)^T = V \Pi . \quad (5.3)$$

It follows that, if  $\underline{y}$  is any vector in  $R^n$ , then

$$\underline{x}^T V (\underline{y} - \Pi \underline{y}) = 0$$

for all  $\underline{x} \in S$ . That is, the vector  $\underline{y} - \Pi \underline{y}$ , which is the vector difference between  $\underline{y}$  and its projection onto  $S$ , is  $V$ -orthogonal to every vector  $\underline{x} \in S$ . Indeed, from Eq. (5.2) we have  $\Pi \underline{x} = \underline{x}$ , whence

$$\begin{aligned} \underline{x}^T V (\underline{y} - \Pi \underline{y}) &= (\Pi \underline{x})^T V (\underline{y} - \Pi \underline{y}) \\ &= \underline{x}^T (V \Pi)^T (\underline{y} - \Pi \underline{y}) \\ &= \underline{x}^T V \Pi (\underline{y} - \Pi \underline{y}) \\ &= 0 ; \end{aligned}$$

the last two equalities follow from Eqs. (5.3, 5.1b), respectively.

A projection matrix onto  $S$  is therefore called  $V$ -orthogonal if, in addition to satisfying Eqs. (5.1), it satisfies Eq. (5.3). In the special case in which  $V$  is actually positive definite, it is well-known that Eqs. (5.1, 5.3) define a unique matrix  $\Pi$  (e.g., Halmos, 1958, Sec. 75), i.e., Eq. (5.3) serves to characterize the projection matrix (5.1). For reasons which will soon be made clear, we allow  $V$  to be semidefinite. One can still find a  $V$ -orthogonal projection matrix onto  $S$  in this case, and there is a simple necessary and sufficient condition under which the projection matrix is determined uniquely.

Lemma 1. Let  $S$  be a subspace of  $R^n$  and let  $V$  be a positive semidefinite  $n \times n$  matrix. Then there exists a  $V$ -orthogonal projection matrix onto  $S$ .

If  $S = \{0\}$  or if  $S = R^n$ , it is clear that there exists exactly one  $V$ -orthogonal projection matrix onto  $S$ , regardless of the choice of  $V$ . In the former case it follows from Eq. (5.1a) that  $\Pi = 0$ , while in the

latter case  $\Pi = I$  since  $\Pi$  must act like the identity on its range, which in this case is all of  $R^n$ ; in both cases Eqs. (5.1, 5.3) are satisfied. We therefore state the uniqueness criterion only for proper subspaces  $S$ , i.e., for subspaces of  $R^n$  other than  $\{0\}$  and  $R^n$  itself.

Lemma 2. Let  $S$  be a proper subspace of  $R^n$  and let  $V$  be a positive semidefinite  $n \times n$  matrix. There exists a unique  $V$ -orthogonal projection matrix onto  $S$  if and only if

$$S \cap \text{Ker } V = \{0\}. \quad (5.4)$$

The symbol  $\cap$  indicates set intersection. Lemma 2 states that for exactly one matrix  $\Pi$  to exist which satisfies Eqs. (5.1, 5.3), it is necessary and sufficient that  $S$  and the kernel of  $V$  have only the zero vector in common.

The uniqueness condition (5.4) is satisfied, in particular, if  $V$  is actually positive definite, for then  $V$  is nonsingular and  $\text{Ker } V = \{0\}$ . The  $I$ -orthogonal projection matrix onto  $S$ , known simply as the orthogonal projection onto  $S$ , is therefore unique.

We have already seen that if  $\Pi$  is a  $V$ -orthogonal projection matrix onto  $S$  and if  $y \in R^n$ , then the vector  $y - \Pi y$  is  $V$ -orthogonal to every vector in  $S$ . The following lemma states that, provided the uniqueness condition (5.4) is satisfied, there is a vector in  $S$  which is "closest" to  $y$ , and in fact the "closest" vector is  $\Pi y$ .

Lemma 3. Let  $S$  be a proper subspace of  $R^n$ , let  $V$  be a positive semidefinite  $n \times n$  matrix, and let an arbitrary vector  $y \in R^n$  be given. There exists a unique solution  $\underline{x}$  of the problem

$$\text{minimize } (\underline{x} - y)^T V(\underline{x} - y), \quad (5.5a)$$

$$\text{subject to } \underline{x} \in S, \quad (5.5b)$$

if and only if  $S$  and  $V$  are such that Eq. (5.4) is satisfied, in which case the solution is

$$\underline{x} = \Pi y, \quad (5.6)$$

where  $\Pi$  is the unique  $V$ -orthogonal projection onto  $S$ .

Suppose now that  $V$  is actually positive definite. In this case, there is a simple formula for the  $V$ -orthogonal projection onto  $S$ , in terms of the (I-) orthogonal projection onto  $S$  and in terms of the square root of  $V$ .

For every positive definite matrix  $V$ , there is a unique positive definite matrix  $B$  such that  $B^2 = V$ . This matrix is called the (positive) square root of  $V$ , and we denote it by  $V^{1/2}$ . The inverse (positive) square root of  $V$ , defined by

$$V^{-1/2} \equiv (V^{1/2})^{-1},$$

is also positive definite.

The square root of  $V$  can be constructed as follows. Since  $V$  is symmetric,  $V$  can be diagonalized by an orthogonal matrix  $U$ ,

$$V = UDU^T, \quad U^T U = U U^T = I. \quad (5.7a,b)$$

Here  $U$  is an  $n \times n$  matrix whose columns are the normalized eigenvectors of  $V$ , and  $D$  is a diagonal matrix whose diagonal elements  $\lambda_i$  are the eigenvalues of  $V$ ;  $\lambda_i > 0$  since  $V$  is positive definite. The square root of  $V$  is then given by

$$V^{1/2} = U D^{1/2} U^T, \quad (5.7c)$$

where  $D^{1/2}$  is the diagonal matrix whose diagonal elements,  $+\sqrt{\lambda_i}$ , are the positive square roots of the eigenvalues of  $V$ . We have also

$$V^{-1/2} = U D^{-1/2} U^T, \quad (5.7d)$$

where  $D^{-1/2} \equiv (D^{1/2})^{-1}$ .

Lemma 4. Let  $S$  be a subspace of  $R^n$  and let  $V$  be a positive definite  $n \times n$  matrix. Denote by  $\Pi_V$  the  $V$ -orthogonal projection onto  $S$  and denote by  $\Pi_I$  the orthogonal projection onto  $S$ . Then

$$\Pi_V = V^{-1/2} \Pi_I V^{1/2}. \quad (5.8)$$

Lemma 4 has a simple generalization. Applying the lemma to another positive definite matrix  $W$ , we have

$$\Pi_W = W^{-1/2} \Pi_I W^{1/2},$$

or

$$\Pi_I = W^{1/2} \Pi_W W^{-1/2},$$

which, upon substitution into Eq. (5.8), gives

$$\Pi_V = V^{-1/2} W^{1/2} \Pi_W W^{-1/2} V^{1/2}. \quad (5.9)$$

Thus, two projections based on positive definite matrices can always be expressed in terms of one another.

In case  $V$  is positive definite, then

$$(\underline{x}, \underline{y})_V \equiv \underline{x}^T V \underline{y}, \text{ for } \underline{x}, \underline{y} \in R^n,$$

defines an inner product on  $R^n$ , with corresponding norm  $\|\underline{x}\|_V$ ,

$$\|\underline{x}\|_V^2 \equiv (\underline{x}, \underline{x})_V = \underline{x}^T V \underline{x}, \text{ for } \underline{x} \in R^n;$$

$\|\underline{x}\|_V \geq 0$  and  $\|\underline{x}\|_V = 0$  if and only if  $\underline{x} = 0$ . Equation (5.3) is equivalent to requiring a matrix  $\Pi$  to be symmetric with respect to this inner product, i.e.,

$$(\underline{x}, \Pi \underline{y})_V = (\Pi \underline{x}, \underline{y})_V \text{ for all } \underline{x}, \underline{y} \in R^n,$$

which is the usual way of defining orthogonality of projection matrices on inner product spaces (e.g., Halmos, 1958, Sec. 75).

For positive semidefinite matrices  $V$ ,  $\|\underline{x}\|_V = 0$  does not imply  $\underline{x} = 0$ , i.e.,  $\|\cdot\|_V$  is only a seminorm on  $R^n$ . However, we note that the

uniqueness condition (5.4) is necessary and sufficient for  $I \cdot I_V$  to define a norm on the subspace  $S$ ; see the proof of Lemma 1 in the Appendix.

Lemmas 1 and 2 will be important in the derivation of the modified Kalman-Bucy filter. The arbitrary subspace  $S$  of the present section will be taken to be the slow-wave subspace  $R$ , and the matrix  $V$  will be the weighting matrix  $A$  of the error functional  $\eta$ .

The uniqueness condition of Lemma 2 will turn out to be the condition for uniqueness of the modified KB filter, i.e., the class of positive semidefinite matrices  $A$  satisfying

$$R \cap \text{Ker } A = \{0\}$$

will be the appropriate class of weighting matrices. We saw in Sec. 2.4 that positive definiteness of  $A$  is the condition for uniqueness of the standard KB filter; positive definiteness of  $A$  is not necessary for uniqueness of the modified KB filter. However, the modified filter will depend on  $A$ , regardless of whether  $A$  is positive definite. Some natural weighting matrices, both semidefinite and definite, will be considered in Sec. 5.5.

Lemma 3 serves as a prototype for Theorem 1 of Sec. 5.3, from which the modified filter follows, and it gives the modified filter an interpretation in terms of normal mode initialization. Lemma 4 will be used in Sec. 5.4 to describe one way, among others, of computing the modified filter.

### 5.3. The Modified Kalman-Bucy Filter

We begin by formulating a simple necessary and sufficient condition under which an assimilation scheme for our discrete model  $\Psi$ , Eqs. (4.7), will yield slowly evolving state estimates. As usual, we consider only assimilation schemes which are linear and unbiased. According to Eqs. (2.7,2.8), these schemes are of the form

$$\underline{w}_k^f = \Psi \underline{w}_{k-1}^a, \quad (5.10a)$$

$$\underline{w}_k^a = \underline{w}_k^f + K_k \underline{w}_k^r, \quad (5.10b)$$

for times  $k$  when observations are available; when no observations are available, Eq. (5.10b) is replaced by

$$\underline{w}_k^a = \underline{w}_k^f. \quad (5.10c)$$

The notation

$$\underline{w}_k^r = \underline{w}_k^o - H_k \underline{w}_k^f, \quad (5.11)$$

for the observed-minus-forecast residual, has been introduced in Eq. (5.10b). The true states,  $\underline{w}_k^t$ , and the observations,  $\underline{w}_k^o$ , are assumed to be given by stochastic-dynamic models (2.2,2.3), with  $\Psi_k = \Psi$  given by Eq. (4.7b).

The state estimates in Eqs. (5.10) will be said to evolve slowly if they always lie in the discrete slow-wave subspace, i.e., if

$$\underline{w}_k^f \in R \text{ and } \underline{w}_k^a \in R \text{ for } k=1,2,3,\dots. \quad (5.12)$$



An immediate consequence of the fact that  $R$  is an invariant subspace of  $\Psi$ , Eqs. (4.42,4.44), is that (5.12) is satisfied if and only if

$$\underline{w}_0^a \in R \quad (5.13a)$$

and

$$K_k \underline{w}_k^r \in R \quad \text{at each observation time } k. \quad (5.13b)$$

Condition (5.13a) says that the assimilation must start from an initialized state, while (5.13b) is a condition on the "correction" vectors in Eq. (5.10b).

To see that conditions (5.13) imply (5.12), notice that if  $\underline{w}_{k-1}^a \in R$ , then  $\underline{w}_k^f \in R$  since  $R$  is invariant under  $\Psi$ ; if  $k$  is not an observation time then we have  $\underline{w}_k^a = \underline{w}_k^f \in R$ , while if  $k$  is an observation time and  $K_k \underline{w}_k^r \in R$  then we still have  $\underline{w}_k^a \in R$ , since  $R$  is a subspace. Upon continuing the cycle, the implication is clear. On the other hand, if  $\underline{w}_k^f \in R$  at some observation time  $k$  but  $K_k \underline{w}_k^r \notin R$ , then  $\underline{w}_k^a \notin R$  since  $R$  is a subspace. Thus, (5.12) and (5.13) are equivalent.

Conditions (5.13) are necessary and sufficient for the assimilation scheme to yield slowly evolving estimates for a particular realization of the state and observation processes, Eqs. (2.2a,2.3a). For the scheme to yield slowly evolving estimates for all realizations of the state and observation processes, it is necessary and sufficient that

$$\underline{w}_0^a \in R \quad (5.14a)$$

and

$$\text{Range } K_k \subset R \text{ at each observation time } k. \quad (5.14b)$$

To see that this is the case, recall from Sec. 2.2 that the gain matrices  $K_k$  are supposed to be nonrandom, i.e., they are supposed to be independent of individual realizations of the state and observation processes. The residual  $\underline{w}_k^r$  is a random vector and, unless restrictions are placed on the system noise and observational noise,  $\underline{w}_k^r$  can take on any value in  $R^n$ . Therefore condition (5.14b), which says that  $K_k \underline{x} \in R$  for all  $\underline{x} \in R^n$ , is just the statement that (5.13b) should hold for all realizations. In other words, the set of gain matrices which satisfy (5.14b) is the set of gain matrices which are independent of  $\underline{w}_k^r$  and which satisfy (5.13b).

If the initial estimate satisfies (5.14a) and if the gain matrices satisfy (5.14b), then the state estimates evolve slowly in between observation times, as well as after the final observation time  $k = N$ . That slow evolution is possible depends crucially, as we have seen, on the fact that  $R$  is an invariant subspace of  $\Psi$ . This is why we work directly with the discrete slow-wave subspace  $R$ . Any other discrete approximation to the continuous slow-wave subspace  $R_c$  will not have the property of being invariant under  $\Psi$ .

The Kalman-Bucy filter generally does not yield slowly evolving state estimates, unless it is assumed that the true state evolves slowly,

$$\underline{w}_k^t \in R, \text{ for } k = 0, 1, 2, \dots. \quad (5.15a)$$

If (5.14a) is satisfied, then (5.15a) is equivalent to requiring the initial estimation error and the system noise to lie in  $R$ ,

$$\underline{w}_0^a - \underline{w}_0^t \in R \text{ and } \underline{b}_k^t \in R \text{ for } k=0,1,2,\dots; \quad (5.15b)$$

cf. Eq. (2.2a). If (5.15b) holds, then it follows from Eqs. (2.22b,c,d) and the definitions of the initial estimation error covariance and the system noise covariance, Eqs. (2.9b,2.2c), that the KB gain matrices satisfy (5.14b): the state estimates evolve slowly. See also Petersen (1973) for a similar result.

We do not assume conditions (5.15a) or (5.15b) to hold: atmospheric states generally do have fast components. Instead, we seek an alternative to the KB filter, by imposing condition (5.14b) as an explicit constraint on the minimization of the usual error functional  $\eta_k$ ,

$$\eta_k = E[(\underline{w}_k^a - \underline{w}_k^t)^T A(\underline{w}_k^a - \underline{w}_k^t)]; \quad (5.16)$$

$A$  is a fixed, but arbitrary, nonrandom positive semidefinite  $n \times n$  matrix. That is, we seek gain matrices  $K_k$  which

$$\text{minimize } \eta_k \text{ with respect to } K_k, \quad (5.17a)$$

$$\text{subject to } \text{Range } K_k \subset R, \quad (5.17b)$$

at each successive observation time  $k$ ; we already know that  $K_k = 0$  if there are no observations at time  $k$ . Notice the similarity between problem (5.17) and problem (5.5) of Lemma 3. The solutions, and conditions for their uniqueness, are also similar.

Theorem 1. All solutions of problem (5.17) are given by

$$K_k = \Pi_k K_k^{KB} + L_k, \quad (5.18)$$

where  $\Pi_k$  is any  $A$ -orthogonal projection matrix onto  $R$ , i.e., any matrix such that

$$\text{Range } \Pi = R, \quad (5.19a)$$

$$\Pi^2 = \Pi, \quad (5.19b)$$

$$(A\Pi)^T = A\Pi, \quad (5.19c)$$

and where  $L_k$  is any  $n \times p$  matrix such that

$$\text{Range } L_k \subset R \cap \text{Ker } A; \quad (5.20)$$

$K_k^{KB}$  is the usual Kalman-Bucy gain matrix, Eq. (2.20a). There exists a unique solution of problem (5.17) if and only if the weighting matrix  $A$  is such that

$$R \cap \text{Ker } A = \{0\}; \quad (5.21)$$

in case Eq. (5.21) holds, there exists exactly one  $A$ -orthogonal projection matrix onto  $R$ , denoted by  $\Pi$ , and the unique solution of problem (5.17) is

$$K_k = K_k^{\Pi KB} \equiv \Pi K_k^{KB}. \quad (5.22)$$

The proof of Theorem 1, which appears in the Appendix, follows easily from Lemmas 1 and 2 and from our derivation of the KB filter in Sec. 2.4.

Theorem 1 states that the constrained minimization problem (5.17) uniquely determines a gain matrix sequence if and only if the error functional is based on a weighting matrix  $A$  which satisfies  $R \cap \text{Ker } A = \{0\}$ , in which case the gain matrices are obtained by multiplying the usual KB gain matrices by the  $A$ -orthogonal projection onto  $R$ . The uniqueness condition is not very restrictive. For example, weighting matrices of interest are usually positive definite, rather than merely positive semidefinite; if  $A$  is positive definite, then it is nonsingular and  $\text{Ker } A = \{0\}$ , so that  $R \cap \text{Ker } A = \{0\}$  automatically. Essentially, weighting matrices satisfying the uniqueness condition are the appropriate ones for consideration. We discuss some of them, including some singular ones, in Sec. 5.5.

Suppose, therefore, that  $A$  satisfies the uniqueness condition, Eq. (5.21). According to Eqs. (5.22, 2.20), the resulting gain matrices are given by

$$K_k^{\Pi KB} = \Pi P_k^f H_k^T (H_k P_k^f H_k^T + R_k)^{-1} \quad (5.23a)$$

at observation times  $k$ , where  $\Pi$  is the unique  $A$ -orthogonal projection onto  $R$ , and

$$K_k^{\Pi KB} = 0 \quad (5.23b)$$

in the absence of observations at time  $k$ . We refer to the corresponding

data assimilation scheme as the modified Kalman-Bucy filter. To summarize, it is given in full by

$$\underline{w}_k^f = \Psi \underline{w}_{k-1}^a, \quad (5.24a)$$

$$\underline{P}_k^f = \Psi \underline{P}_{k-1}^a \Psi^T + \underline{Q}_{k-1}, \quad (5.24b)$$

$$\underline{K}_k = \underline{K}_k^{KB}, \quad (5.24c)$$

$$\underline{P}_k^a = (\underline{I} - \underline{K}_k \underline{H}_k) \underline{P}_k^f (\underline{I} - \underline{K}_k \underline{H}_k)^T + \underline{K}_k \underline{R}_k \underline{K}_k^T, \quad (5.24d)$$

$$\underline{w}_k^a = \underline{w}_k^f + \underline{K}_k (\underline{w}_k^o - \underline{H}_k \underline{w}_k^f), \quad (5.24e)$$

for  $k = 1, 2, 3, \dots$ ; cf. the standard KB filter, Eqs. (2.22). Note that the general formula (2.10b) is used for the analysis error covariance matrix  $\underline{P}_k^a$ .

The modified KB filter results in slowly evolving state estimates provided initialization is performed at the start of the assimilation, Eq. (5.14a). The filter is optimal in the sense that slow evolution is achieved simultaneously with the successive minimization of the error functionals  $\eta_k$ . Unlike the standard KB filter, however, the modified filter depends on the error functional's weighting matrix  $\underline{A}$ , cf. Eqs. (5.19c, 5.8). One must therefore choose the error functional to be minimized.

Lemma 3 offers a simple interpretation of the modified filter. Equation (5.24e) can be written

$$\underline{w}_k^a = \underline{w}_k^f + \Pi \underline{K}_k^{KB} (\underline{w}_k^o - \underline{H}_k \underline{w}_k^f).$$

If  $\underline{w}_0^a \in \mathbb{R}$  and the modified filter has been used up to time  $k$ , then  $\underline{w}_k^f \in \mathbb{R}$ . Therefore  $\underline{w}_k^f = \Pi \underline{w}_k^f$ , cf. Eq. (5.2), and we have

$$\underline{w}_k^a = \Pi [\underline{w}_k^f + K_k^{KB}(\underline{w}_k^o - H_k \underline{w}_k^f)] = \Pi \underline{y}_k^a ; \quad (5.25)$$

here  $\underline{y}_k^a$  is the analysis vector that would be produced by using the KB filter at time  $k$ , cf. Eq. (2.22e). Thus,  $\underline{w}_k^a$  is the  $A$ -orthogonal projection of  $\underline{y}_k^a$  onto  $R$ .

In fact, according to Lemma 3 and Eq. (5.25),  $\underline{w}_k^a$  is that vector in  $R$  which is closest to the KB analysis vector  $\underline{y}_k^a$ , in the sense that

$$(\underline{w}_k^a - \underline{y}_k^a)^T A (\underline{w}_k^a - \underline{y}_k^a) \quad (5.26)$$

is minimized. In other words, the modified KB filter is equivalent to following computation of the KB analysis vector with variational normal mode initialization;  $\underline{y}_k^a$  is an "objective analysis" and  $\underline{w}_k^a$  is the "initialized" version of  $\underline{y}_k^a$ , as  $\underline{w}_k^a \in R$  and (5.26) is minimum. Equation (5.24d), as compared with Eq. (2.22d), determines the effect on the analysis error of combining initialization and assimilation.

Theorem 1 shows that (5.26) is not the only functional being minimized by use of the modified KB filter. The functional  $\eta_k$  of the difference between the analysis vector  $\underline{w}_k^a$  and the true state  $\underline{w}_k^t$  is also being minimized. This stronger result obtains, in essence, because the assimilation part of our initialization-assimilation scheme is the standard KB filter.

To conclude this section, we point out that although Theorem 1 is stated for our discrete model  $\Psi$  and its slow-wave subspace  $R$ , the theorem is actually quite general. The proof of Theorem 1, and the discussion leading to the statement of the theorem, depends only on the fact that  $R$  is a proper invariant subspace of  $\Psi$ ; the actual definition

of  $R$  is immaterial. In particular, the theorem holds for other discrete models  $\Psi$  and their slow-wave subspaces. In general, the theorem shows how to estimate the state of a stochastic-dynamic system, given noisy observations, in case the state estimates are confined to an invariant subspace of the system's dynamics.

In the trivial case  $R = R^n$ , Eq. (5.17b) presents no constraint and, as one would expect, the modified filter reduces to the standard KB filter. To see this we can still use the first part of Theorem 1, since only the uniqueness part of the proof depends on the fact that  $R$  is a proper subspace of  $R^n$ .

If  $R = R^n$  then, regardless of the choice of  $A$ , there is exactly one  $A$ -orthogonal projection onto  $R$ , namely  $\Pi = I$ ; see the discussion following Lemma 1. Equations (5.18, 5.20) therefore become

$$K_k = K_k^{KB} + L_k, \quad (5.27a)$$

$$\text{Range } L_k \subset \text{Ker } A. \quad (5.27b)$$

This gives the unique formula  $K_k = K_k^{KB}$ , the KB gain matrix, if and only if  $\text{Ker } A = \{0\}$ , i.e., iff  $A$  is positive definite. Positive definiteness of  $A$  was the condition already found to be necessary and sufficient for uniqueness of the KB filter; see the discussion following Eq. (2.19). In fact, the general solution of Eq. (2.18) is given by Eqs. (5.27).

#### 5.4. Computation of Projections onto the Slow-Wave Subspace

In order to actually carry out computation of the modified KB filter, one must be able to calculate the  $A$ -orthogonal projection



matrix  $\Pi$ , or at least to compute  $\Pi \underline{w}$  for arbitrary vectors  $\underline{w} \in R^n$ . The main result of this section, Theorem 2, gives a formula for efficient computation of  $\Pi$  in case the weighting matrix  $A$  is block circulant. We show that in this case, the fast Fourier transform (FFT) can be used to compute  $\Pi \underline{w}$  in only  $O(n \log n)$  arithmetic operations. After discussing this case, we apply Lemma 4 to the more general case, in which  $A$  is not necessarily block circulant.

Suppose that in the error functional

$$\eta = E[(\underline{w}^a - \underline{w}^t)^T A (\underline{w}^a - \underline{w}^t)] ,$$

the weights are homogeneous in space, i.e., the weights applied to variables situated around a given grid point are the same as the weights applied to the variables identically situated around each of the remaining grid points. Since our domain is periodic, and due to the ordering (4.6) of the components of the vectors  $\underline{w}^a$  and  $\underline{w}^t$ , this means that the weighting matrix  $A$  is block circulant with  $3 \times 3$  blocks,

$$A = \text{circ}[A_0, A_1, \dots, A_{M/2}, A_{-M/2+1}, \dots, A_{-1}] ; \quad (5.28)$$

cf. Eq. (4.7b). That is, with  $A$  partitioned regularly into  $M^2$   $3 \times 3$  blocks, the  $3 \times 3$  submatrices  $A_0, A_1, \dots, A_{M/2}, A_{-M/2+1}, \dots, A_{-1}$  appear in order across the first row of  $A$ , and each of the remaining  $M-1$  rows is obtained by circularly shifting the previous row one block to the right.

The submatrix  $A_j$  ( $A_{-j}$ ) gives the weights applied to the variables  $u, v, \phi$  at the grid point located  $j$  intervals to the right (left) of a given grid point. In case one applies only local weights, which is

typical in practice, one has  $A_j = 0$  for  $j \neq 0$  and  $A$  would be block-diagonal, with the matrix  $A_0$  repeated along the main diagonal of  $A$ .

In the sequel, whenever we refer to a matrix as being block circulant, it is implicit that the blocks are  $3 \times 3$  and that the matrix is  $n \times n = 3M \times 3M$ , since these are the only block circulant matrices with which we will be concerned.

Our results are based on the fact that if  $A$  is block circulant, then the Fourier matrix  $F$  defined in Eq. (4.18) block-diagonalizes  $A$ , and vice-versa. That is, if  $A$  is of the form (5.28) then, defining

$$\hat{A} = FAF^*, \quad (5.29)$$

we have

$$\hat{A} = \text{diag} \left[ \hat{A}(-\frac{M}{2}+1), \hat{A}(-\frac{M}{2}+2), \dots, \hat{A}(\frac{M}{2}) \right], \quad (5.30)$$

where the  $3 \times 3$  matrices  $\hat{A}(\omega)$  are given by

$$\hat{A}(\omega) = \sum_{j=-\frac{M}{2}+1}^{\frac{M}{2}} e^{2\pi i j \omega / M} A_j, \quad \omega = -\frac{M}{2}+1, \dots, \frac{M}{2}. \quad (5.31)$$

On the other hand, given any  $3 \times 3$  matrices  $\hat{A}(\omega)$ , and defining

$$A = F^* \hat{A} F, \quad (5.32)$$

where  $\hat{A}$  is given by Eq. (5.30), then  $A$  is block circulant. For proof, see Davis (1979, Theorem 5.6.4).

The  $n \times n$  matrix  $A$  therefore defines  $3 \times 3$  matrices  $\hat{A}(\omega)$ , and vice-versa; it will be most convenient to work with the  $3 \times 3$  matrices. Recall that  $A$  is supposed to be real, symmetric, and positive

semidefinite. We first translate these conditions into restrictions on  $\hat{A}(\omega)$ .

Lemma 5. If the block circulant matrix  $A$  in Eq. (5.28) is real, symmetric, and positive semidefinite, then the matrices  $\hat{A}(\omega)$  in Eq. (5.31) satisfy

$$\hat{A}(-\omega) = \overline{\hat{A}(\omega)}, \quad \text{for } \omega = 0, 1, \dots, \frac{M}{2} - 1, \quad (5.33a)$$

$$\hat{A}\left(\frac{M}{2}\right) = \overline{\hat{A}\left(\frac{M}{2}\right)}, \quad (5.33b)$$

$$\hat{A}^*(\omega) = \hat{A}(\omega), \quad \text{for } \omega = -\frac{M}{2} + 1, \dots, \frac{M}{2}, \quad (5.33c)$$

$$\underline{y}^* \hat{A}(\omega) \underline{y} \geq 0, \quad \text{for } \omega = -\frac{M}{2} + 1, \dots, \frac{M}{2} \quad (5.33d)$$

and for all complex 3-vectors  $\underline{y}$ .

Conversely, given any  $3 \times 3$  matrices  $\hat{A}(\omega)$  which satisfy Eqs. (5.33), the block circulant matrix thereby defined in Eqs. (5.30, 5.32) is real, symmetric and positive semidefinite.

Equations (5.33a, b) express the condition that  $A$  is real; they are similar to Eqs. (3.5). The conditions that  $A$  is symmetric and positive semidefinite are expressed by Eqs. (5.33c, d); these equations state that  $\hat{A}(\omega)$  must be Hermitian positive semidefinite.

We would now like to translate the condition for uniqueness of the modified KB filter,

$$R \cap \text{Ker } A = \{0\},$$

into an equivalent condition on the matrices  $\hat{A}(\omega)$ . To do so, we will have to be somewhat more specific about the vectors  $\underline{e}_0(\omega)$  which define the slow-wave subspace in Eq. (4.38).

Recall that the vectors  $\underline{e}_0(\omega)$  are eigenvectors of  $\hat{\Psi}(\omega)$ , Eq. (4.27). Since the submatrices  $\Psi_j$  which define  $\hat{\Psi}(\omega)$  in Eq. (4.24) are real, it follows that

$$\hat{\Psi}(-\omega) = \overline{\hat{\Psi}(\omega)}, \quad \text{for } \omega = 0, 1, \dots, \frac{M}{2} - 1, \quad (5.34a)$$

$$\hat{\Psi}\left(\frac{M}{2}\right) = \overline{\hat{\Psi}\left(\frac{M}{2}\right)}. \quad (5.34b)$$

Since the eigenvalues  $\delta_0(0)$  and  $\delta_0\left(\frac{M}{2}\right)$  are real, Eqs. (4.28, 4.33, 4.37), it follows from Eqs. (5.34) that the eigenvectors can be chosen in such a way that

$$\underline{e}_0(-\omega) = \overline{\underline{e}_0(\omega)}, \quad \text{for } \omega = 0, 1, \dots, \frac{M}{2} - 1, \quad (5.35a)$$

$$\underline{e}_0\left(\frac{M}{2}\right) = \overline{\underline{e}_0\left(\frac{M}{2}\right)}. \quad (5.35b)$$

That is, we can assume that  $\underline{e}_0(0)$  and  $\underline{e}_0\left(\frac{M}{2}\right)$  are real and that, for the remaining eigenvectors,  $\underline{e}_0(-\omega)$  is the complex conjugate of  $\underline{e}_0(\omega)$ . We do not assume, however, that the eigenvectors are scaled in any particular way.

Definition (4.38) of the slow-wave subspace can now be replaced by

$$R = \{ \underline{w} \in C^n: \hat{\underline{w}}(\omega) = \beta_0(\omega) \underline{e}_0(\omega) \text{ for all } \omega = -\frac{M}{2}+1, \dots, \frac{M}{2},$$

where  $\beta_0(\omega)$  are any scalars such that  $\beta_0(-\omega) = \overline{\beta_0(\omega)}$

$$\text{and } \beta_0\left(\frac{M}{2}\right) = \overline{\beta_0\left(\frac{M}{2}\right)}, \quad (5.36)$$

where  $C^n$  denotes the set of complex  $n$ -vectors; Eqs. (4.15) imply that a complex  $n$ -vector  $\underline{w}$  is real if and only if

$$\hat{\underline{w}}(-\omega) = \overline{\hat{\underline{w}}(\omega)}, \text{ for } \omega = 0, 1, \dots, \frac{M}{2} - 1, \quad (5.37a)$$

$$\hat{\underline{w}}\left(\frac{M}{2}\right) = \overline{\hat{\underline{w}}\left(\frac{M}{2}\right)}, \quad (5.37b)$$

whence, by Eqs. (5.35), a vector  $\underline{w}$  defined by

$$\hat{\underline{w}}(\omega) = \beta_0(\omega) \underline{e}_0(\omega) \quad (5.38)$$

is real iff the scalars  $\beta_0(\omega)$  satisfy the conditions in Eq. (5.36).

Lemma 6. Suppose the block circulant matrix  $A$  in Eq. (5.28) is real, symmetric, and positive semidefinite, and define matrices  $\hat{A}(\omega)$  by Eq. (5.31). Then the following three statements are equivalent:

$$R \cap \text{Ker } A = \{0\}, \quad (5.39a)$$

$$\hat{A}(\omega) \underline{e}_0(\omega) \neq 0, \text{ for } \omega = -\frac{M}{2}+1, \dots, \frac{M}{2}, \quad (5.39b)$$

$$\underline{e}_0^*(\omega) \hat{A}(\omega) \underline{e}_0(\omega) > 0, \text{ for } \omega = -\frac{M}{2}+1, \dots, \frac{M}{2}. \quad (5.39c)$$

Condition (5.39c) simply states that in addition to being Hermitian positive semidefinite, Eqs. (5.33c,d),  $\hat{A}(\omega)$  must be positive definite on the space spanned by the slow-wave eigenvectors  $\underline{e}_0(\omega)$ . We are now ready to state the main result concerning computation of  $\Pi$ .

Theorem 2. Suppose the block circulant matrix  $A$  in Eq. (5.28) is real, symmetric, and positive semidefinite, and define matrices  $\hat{A}(\omega)$  by Eq. (5.31). Suppose further that

$$R \cap \text{Ker } A = \{0\}, \quad (5.40)$$

so that there exists a unique  $A$ -orthogonal projection matrix onto  $R$ , denoted by  $\Pi$ . Then  $\Pi$  is block circulant and is given by

$$\Pi = F^* \hat{\Pi} F, \quad (5.41a)$$

where

$$\hat{\Pi} = \text{diag} \left[ \hat{\Pi}(-\frac{M}{2}+1), \hat{\Pi}(-\frac{M}{2}+2), \dots, \hat{\Pi}(\frac{M}{2}) \right], \quad (5.41b)$$

$$\hat{\Pi}(\omega) = \alpha_\omega \underline{e}_0(\omega) \underline{e}_0^*(\omega) \hat{A}(\omega), \quad (5.41c)$$

$$\alpha_\omega = [\underline{e}_0^*(\omega) \hat{A}(\omega) \underline{e}_0(\omega)]^{-1}. \quad (5.41d)$$

Notice that, according to Lemmas 5 and 6, the hypotheses of Theorem 2 can be replaced by Eqs. (5.33) and either of Eqs. (5.39b,c). This will be important in the next section, where we define projections directly in terms of prescribed matrices  $\hat{A}(\omega)$ , rather than in terms of the corresponding matrix  $A$ . Notice also that Lemma 6 guarantees that the scaling constants  $\alpha_\omega$  in Eq. (5.41d) are well-defined.

Theorem 2 gives an efficient method for computing  $\Pi \underline{w}$  for any  $\underline{w} \in \mathbb{R}^n$ . First, one finds  $\underline{Fw}$ , i.e., the discrete Fourier transform of each of the three  $M$ -vectors of which  $\underline{w}$  is composed. This can be done in only  $O(n \log n)$  arithmetic operations, by use of the FFT algorithm (e.g., Brigham, 1974). Next, one multiplies the resulting 3-vector Fourier components  $\hat{\underline{w}}(\omega)$  by  $\hat{\Pi}(\omega)$ , to find  $\hat{\Pi} \underline{Fw}$ ; this takes only  $O(n)$  operations. Finally, one finds  $\Pi \underline{w} = F^{*} \hat{\Pi} \underline{Fw}$  by performing three inverse FFTs, taking an additional  $O(n \log n)$  operations. To carry out the second step, of course, one must have already computed the slow-wave eigenvectors  $\underline{x}_0(\omega)$  and the matrices  $\hat{A}(\omega)$ ; this computation need only be done once and for all.

In our discussion of variational normal mode initialization in Sec. 1.2, we saw that different weights are usually specified over regions of different data densities. In this case  $A$  is not block circulant, but we still have recourse to Lemma 4. To compute  $\Pi \underline{w}$  in this case, according to Eq. (5.8), one computes  $A^{1/2} \underline{w}$ , then  $\Pi_I A^{1/2} \underline{w}$ , then  $A^{-1/2} \Pi_I A^{1/2} \underline{w} = \Pi \underline{w}$ . The second step is carried out according to Theorem 2:  $\Pi_I$  is the projection matrix corresponding to the trivially block circulant matrix  $I$ . Computation of  $A^{1/2}$  and  $A^{-1/2}$  is usually simple also, because one is usually interested in local weighting, in which

case A is block-diagonal with  $3 \times 3$  blocks, or even diagonal, as in the case of functionals (1.7, 1.8). At worst, therefore, one would have to compute square roots of  $3 \times 3$  matrices. In the usual case, in which A is diagonal, only scalar square roots are required.

### 5.5. Choice of the Weighting Matrix

We have seen that the modified KB filter depends, through the A-orthogonal projection matrix  $\Pi$ , upon the weighting matrix A chosen for the error functional. We now describe several choices of A and discuss the projections to which they lead, namely, the parallel projection, the orthogonal projection and the minimum-energy projection. The latter projection is the one chosen for the numerical experiments described in the following two chapters.

First we introduce some assumptions and notation. Recall that the slow-wave subspace R is defined in Eq. (5.36) in terms of the eigenvectors  $\underline{x}_0(\omega)$  of  $\hat{\Psi}(\omega)$ , Eq. (4.27), and that the fast-wave subspace G is defined in Eq. (4.45) in terms of the remaining eigenvectors  $\underline{x}_{\pm 1}(\omega)$ . We assume that the eigenvectors have been chosen in such a way that

$$\underline{x}_j(-\omega) = \overline{\underline{x}_j(\omega)}, \quad \omega = 0, 1, \dots, \frac{M}{2} - 1, \quad (5.42a)$$

$$\underline{x}_j\left(\frac{M}{2}\right) = \overline{\underline{x}_j\left(\frac{M}{2}\right)}, \quad (5.42b)$$

for  $j = 0, \pm 1$ ; we already saw that this is possible for  $j = 0$  and, for the same reasons, such a choice is possible for  $j = \pm 1$ . For simplicity we now assume that also



-101-

$$\underline{x}_j^*(\omega) \underline{x}_j(\omega) = 1, \quad \omega = -\frac{M}{2} + 1, \dots, \frac{M}{2}, \quad j = 0, \pm 1, \quad (5.43)$$

i.e., that all the eigenvectors have been normalized.

Equation (4.27) can be written as

$$\hat{\Psi}(\omega) = R(\omega) D(\omega) R^{-1}(\omega), \quad (5.44a)$$

where  $R(\omega)$  is the  $3 \times 3$  matrix whose columns are the eigenvectors,

$$R(\omega) = [\underline{x}_{-1}(\omega), \underline{x}_0(\omega), \underline{x}_1(\omega)], \quad (5.44b)$$

and where  $D(\omega)$  is the diagonal matrix of eigenvalues,

$$D(\omega) = \text{diag} [\delta_{-1}(\omega), \delta_0(\omega), \delta_1(\omega)]. \quad (5.44c)$$

We denote by  $\underline{x}_j^*(\omega)$  the rows of  $R^{-1}(\omega)$ :

$$R^{-1}(\omega) = \begin{bmatrix} \underline{x}_{-1}^*(\omega) \\ \underline{x}_0^*(\omega) \\ \underline{x}_1^*(\omega) \end{bmatrix}. \quad (5.45)$$

Clearly we have

$$\underline{x}_j(-\omega) = \overline{\underline{x}_j(\omega)}, \quad \omega = 0, 1, \dots, \frac{M}{2} - 1, \quad (5.46a)$$

$$\underline{x}_j\left(\frac{M}{2}\right) = \overline{\underline{x}_j\left(\frac{M}{2}\right)}, \quad (5.46b)$$

for  $j = 0, \pm 1$ , since, for example, Eq. (5.42a) is equivalent to  $R(-\omega) = \overline{R(\omega)}$ , and therefore  $R^{-1}(-\omega) = \overline{R^{-1}(\omega)}$ .

The  $\underline{x}_j^*(\omega)$  are left eigenvectors of  $\hat{\Psi}(\omega)$ , i.e.,

$$\underline{x}_j^*(\omega) \hat{\Psi}(\omega) = \delta_j(\omega) \underline{x}_j^*(\omega), \quad (5.47)$$

which follows upon premultiplying Eq. (5.44a) by  $R^{-1}(\omega)$ . Notice also that the equation  $R(\omega)R^{-1}(\omega) = I$  can be written as

$$\underline{x}_{-1}(\omega) \underline{x}_{-1}^*(\omega) + \underline{x}_0(\omega) \underline{x}_0^*(\omega) + \underline{x}_1(\omega) \underline{x}_1^*(\omega) = I, \quad (5.48a)$$

and that

$$\underline{x}_1^*(\omega) \underline{x}_j(\omega) = \delta_{1j}, \quad (5.48b)$$

which follows from  $R^{-1}(\omega)R(\omega) = I$ .

Before discussing the projections mentioned at the beginning of this section, we point out that the correspondence between "legitimate" weighting matrices  $A$ , i.e., those satisfying  $R \cap \text{Ker } A = \{0\}$ , and  $A$ -orthogonal projections onto  $R$  is not one-to-one; rather, it is many-to-one. For example, if  $\Pi$  is the unique  $A$ -orthogonal projection onto  $R$  for some block circulant matrix  $A$  satisfying  $R \cap \text{Ker } A = \{0\}$ , then  $\Pi$  is also the unique  $A'$ -orthogonal projection, where

$$\hat{A}'(\omega) = \hat{A}(\omega) + \gamma_{-1}(\omega) \underline{x}_{-1}(\omega) \underline{x}_{-1}^*(\omega) + \gamma_1(\omega) \underline{x}_1(\omega) \underline{x}_1^*(\omega), \quad (5.49)$$

for any real scalars  $\gamma_{\pm 1}(\omega)$ . It is clear from Eqs. (5.46, 5.48b) that if  $\hat{A}(\omega)$  satisfies conditions (5.33, 5.39c) of Lemmas 5 and 6, then so does  $\hat{A}'(\omega)$ , while from Eq. (5.48b) we also have

$$\underline{E}_0^H(\omega) \hat{A}'(\omega) = \underline{E}_0^* \hat{A}(\omega),$$

from which Theorem 2 implies that the projections corresponding to  $\hat{A}(\omega)$  and  $\hat{A}'(\omega)$  are identical.

It is similarly verified that another such equivalent weighting matrix is  $A''$ , where

$$\hat{A}''(\omega) = \hat{A}(\omega) + I - \underline{E}_0(\omega) \underline{E}_0^*(\omega) / \underline{E}_0^*(\omega) \underline{E}_0(\omega), \quad (5.50a)$$

or simply

$$\hat{A}''(\omega) = \hat{A}(\omega) + I - \underline{E}_0(\omega) \underline{E}_0^*(\omega), \quad (5.50b)$$

in light of the scaling assumption (5.43). Although the modified KB filter is chosen to minimize a certain functional  $\eta(A)$  of the analysis error, it will also minimize, for example,  $\eta(A')$  and  $\eta(A'')$ .

The parallel projection. For the parallel projection it is most natural to define the projection matrix first, and then to determine a weighting matrix  $A$  from which it can be obtained.

By the parallel projection we mean the projection onto  $R$  along the fast-wave subspace  $G$ . That is, the parallel projection matrix is that matrix  $\Pi$ , such that for each  $\underline{x} \in R^n$ ,  $\underline{w} = \Pi \underline{x}$  has the same slow components as  $\underline{x}$ , and no fast components: the projection is parallel to the  $G$  -"axis". In other words, the parallel projection is the one which corresponds to the nonvariational formulation of normal mode initialization. A two-dimensional interpretation of the parallel projection is given in Fig. 2.

A precise definition of the parallel projection is as follows. Since  $R$  and  $G$  together span all of  $R^n$ , it is clear from Eqs. (4.45, 5.36, 5.42) that the Fourier components of every  $\underline{x} \in R^n$  can be written in the form

$$\hat{\underline{x}}(\omega) = \sum_{j=-1}^1 \beta_j(\omega) \underline{e}_j(\omega), \quad (5.51a)$$

for some scalars  $\beta_j(\omega)$  satisfying

$$\beta_j(-\omega) = \overline{\beta_j(\omega)}, \quad \omega = 0, 1, \dots, \frac{M}{2} - 1, \quad (5.51b)$$

$$\beta_j\left(\frac{M}{2}\right) = \overline{\beta_j\left(\frac{M}{2}\right)}, \quad (5.51c)$$

for  $j = 0, \pm 1$ . The parallel projection matrix is that matrix  $\Pi_1$  for which the Fourier components of  $\underline{w} = \Pi_1 \underline{x}$  are given by

$$\hat{\underline{w}}(\omega) = \beta_0(\omega) \underline{e}_0(\omega); \quad (5.52)$$

the slow components of  $\underline{x}$  are unaltered and the fast components are set to zero.

The parallel projection matrix is defined implicitly by Eqs. (5.51, 5.52). Clearly there is at most one such matrix, for we have defined how it acts on all of  $R^n$ . It is also clear that  $\text{Range } \Pi_1 = R$  and that  $\Pi_1(\Pi_1 \underline{x}) = \Pi_1 \underline{x}$  for every  $\underline{x} \in R^n$ , so that such a matrix must indeed be a projection matrix onto  $R$ .

Now define  $3 \times 3$  matrices  $\hat{A}(\omega)$  by

$$\hat{A}(\omega) = \underline{e}_0(\omega) \underline{e}_0^*(\omega), \quad (5.53a)$$

and define the corresponding block circulant matrix

$$A = F \hat{A} F^* \quad (5.53b)$$

where

$$\hat{A} = \text{diag} [\hat{A}(-\frac{M}{2}+1), \hat{A}(-\frac{M}{2}+2), \dots, \hat{A}(\frac{M}{2})]. \quad (5.53c)$$

It is clear from Eqs. (5.46) that  $\hat{A}(\omega)$  satisfies conditions (5.33a,b) of Lemma 5; satisfaction of conditions (5.33c,d) is obvious. The block circulant matrix  $A$  is therefore real, symmetric and positive semidefinite. Notice that  $A$  is not positive definite; it has rank  $M = n/3$  since, for each  $\omega$ , the rank of  $\hat{A}(\omega)$  is one. However, it follows from Eq. (5.48b) that

$$\underline{E}_0^*(\omega) \hat{A}(\omega) \underline{E}_0(\omega) = 1 > 0,$$

whereby Lemma 6 implies that  $R \cap \text{Ker } A = \{0\}$ . There exists, therefore, a unique  $A$ -orthogonal projection matrix onto  $R$ ; we show that it is in fact the parallel projection matrix.

With  $\hat{A}(\omega)$  given by Eq. (5.53a), and using Eq. (5.48b), it follows from Theorem 2 that the  $A$ -orthogonal projection matrix is that block circulant matrix  $\Pi_A$  for which

$$\hat{\Pi}_A(\omega) = \underline{E}_0(\omega) \underline{E}_0^*(\omega). \quad (5.53d)$$

Letting  $\underline{w} = \Pi_A \underline{x}$  with  $\underline{x} \in R^n$ , we have

$$\underline{\hat{w}} = F \Pi_A \underline{x} = (F \Pi_A F^*) (F \underline{x}) = \hat{\Pi}_A \hat{\underline{x}},$$

so that, with  $\hat{x}(\omega)$  given by Eqs. (5.51), we have

$$\begin{aligned}\hat{w}(\omega) &= \hat{\Pi}_A(\omega) \hat{x}(\omega) \\ &= \sum_{j=-1}^1 \beta_j(\omega) \underline{x}_0(\omega) \underline{x}_0^*(\omega) \underline{x}_j(\omega) \\ &= \beta_0(\omega) \underline{x}_0(\omega); \end{aligned}$$

the last equality follows from Eq. (5.48b). Comparing this result with Eq. (5.52), it is clear that Eq. (5.53d) does give the parallel projection matrix, i.e.,  $\Pi_A = \Pi_{\parallel}$ .

To summarize, the parallel projection matrix  $\Pi_{\parallel}$  is a block circulant matrix; it is defined by setting

$$\hat{\Pi}_{\parallel}(\omega) = \underline{x}_0(\omega) \underline{x}_0^*(\omega). \quad (5.54)$$

The parallel projection matrix is A-orthogonal for A given by Eqs. (5.53a-c).

The orthogonal projection. The orthogonal projection matrix is the one corresponding to the choice  $A = I$ . In Sec. 5.2, the orthogonal projection matrix was denoted by  $\Pi_I$ ; we now denote it by  $\Pi_{\perp}$ , in contradistinction with the parallel projection matrix  $\Pi_{\parallel}$ .

If  $A = I$ , then we can write

$$A = \text{circ} [I, 0, \dots, 0],$$

whence, by Eqs. (5.28, 5.31),  $\hat{A}(\omega) = I$  for all  $\omega$ . According to Theorem 2, the orthogonal projection matrix  $\Pi_{\perp}$  is therefore block circulant, and is defined by setting

$$\hat{\Pi}_1(\omega) = \underline{\varepsilon}_0(\omega) \underline{\varepsilon}_0^*(\omega), \quad (5.55)$$

as the scale factor  $\alpha_\omega = 1$  by assumption (5.43).

It was shown in Sec. 5.2 that for every  $\underline{x} \in \mathbb{R}^n$ , the vector  $\underline{x} - \Pi_1 \underline{x}$ , which is the vector between  $\underline{x}$  and its orthogonal projection onto  $R$ , is orthogonal to every  $\underline{w} \in R$ , i.e.,

$$\underline{w}^T (\underline{x} - \Pi_1 \underline{x}) = 0 \text{ for all } \underline{w} \in R, \underline{x} \in \mathbb{R}^n.$$

Equivalently, for all  $\omega$  and for  $j = 0, \pm 1$ , we have

$$\underline{\varepsilon}_0^*(\omega) [\underline{\varepsilon}_j(\omega) - \Pi_1(\omega) \underline{\varepsilon}_j(\omega)] = 0,$$

which follows from Eqs. (5.43, 5.55). The orthogonal projection in two dimensions is illustrated in Fig. 2.

The orthogonal projection is not appropriate for our discrete system (4.7). With  $A = I$  in the error functional (5.16), we see that the modified filter based on the orthogonal projection would minimize a dimensionally inconsistent sum of squares, i.e., squares of the velocity components (m/s) and of the geopotential (m<sup>2</sup>/s<sup>2</sup>).

Comparison of the parallel and orthogonal projections. Having defined the parallel and orthogonal projections, we wish to make it clear that these two projections are not the same,  $\Pi_{||} \neq \Pi_{\perp}$ , and to clarify why this is the case.

Since the Fourier matrix  $F$  is nonsingular, it is clear that  $\Pi_{||} = \Pi_{\perp}$  if and only if  $\hat{\Pi}_{||}(\omega) = \hat{\Pi}_{\perp}(\omega)$  for all  $\omega$ . According to definitions (5.54, 5.55), the latter equality holds if and only if

$$\underline{z}_0(\omega) = \underline{z}_0(\omega) \text{ for all } \omega. \quad (5.56a)$$

Notice that if Eq. (5.56a) is satisfied, then there is no conflict between the matrix  $\hat{A}(\omega) = \underline{z}_0(\omega)\underline{z}_0^*(\omega)$  which we used to obtain the parallel projection and the matrix  $\hat{A}(\omega) = I$  which generates the orthogonal projection. From Eq. (5.50b) it follows that the parallel projection is also  $A''$ -orthogonal, where

$$\hat{A}''(\omega) = \underline{z}_0(\omega)\underline{z}_0^*(\omega) + I - \underline{z}_0(\omega)\underline{z}_0^*(\omega),$$

and if Eq. (5.56a) is satisfied, then  $\hat{A}''(\omega) = I$ .

Now, from Eq. (5.45), we have

$$\underline{z}_0(\omega) = [R^{-1}(\omega)]^* \underline{e}_0,$$

where  $\underline{e}_0$  is the vector  $(0,1,0)^T$ ; therefore Eq. (5.56a) is equivalent to

$$\underline{z}_0(\omega) = [R^{-1}(\omega)]^* \underline{e}_0, \text{ for all } \omega,$$

or

$$R^*(\omega)\underline{z}_0(\omega) = \underline{e}_0, \text{ for all } \omega,$$

or

$$\underline{z}_{\pm 1}^*(\omega)\underline{z}_0(\omega) = 0, \text{ for all } \omega, \quad (5.56b)$$

since we already assumed  $\underline{z}_0^*(\omega)\underline{z}_0(\omega) = 1$ , Eq. (5.43). By definition of the fast-wave and slow-wave subspaces, Eq. (5.56b) is equivalent to



$$\underline{x}^T \underline{y} = 0 \text{ for all } \underline{x} \in G, \underline{y} \in R. \quad (5.56c)$$

Thus, the parallel and orthogonal projections are identical if and only if the fast-wave subspace is orthogonal to the slow-wave subspace. This statement should also be clear from the geometrical interpretation of the parallel and orthogonal projections indicated in Fig. 2.

The axes in Figure 2 are drawn obliquely because the eigenvectors of our discrete model do not satisfy Eq. (5.56b): the fast-wave and slow-wave subspaces are not orthogonal. Primitive-equation models linearized about a state with nonzero mean flow also have nonorthogonal fast-wave and slow-wave subspaces (Kasahara, 1981).

This nonorthogonality is not an artifact of discretization. Rather, it is a property of the differential equations. Nonorthogonality of the fast-wave and slow-wave subspaces of the shallow-water equations (3.1) is due to the asymmetric form of the equations and to the appearance of the term  $(-fUv)$  in Eq. (3.1c). This term arises because the solution about which Eqs. (3.2) were linearized has  $\phi_y \neq 0$ , i.e., a free surface with nonzero slope in the meridional direction.

With the term  $(-fUv)$  removed from Eq. (3.1c), the change of variables

$$u \rightarrow \sqrt{\phi} u, \quad v \rightarrow \sqrt{\phi} v, \quad \phi \rightarrow \phi \quad (5.57)$$

in Eqs. (3.1) results in the symmetrized shallow-water equations,

$$u_t + Uu_x + \sqrt{\phi} \phi_x - fv = 0, \quad (5.58a)$$

$$v_t + Uv_x + fu = 0, \quad (5.58b)$$

$$\phi_t + U\phi_x + \sqrt{\phi} u_x = 0; \quad (5.58c)$$

cf. Kreiss and Oliger (1973, Ch. 7). For this system, corresponding to Eq. (3.9b) we have

$$G_S(\xi) = - \begin{bmatrix} \xi U & if & \xi \sqrt{\phi} \\ -if & \xi U & 0 \\ \xi \sqrt{\phi} & 0 & \xi U \end{bmatrix}.$$

Since  $G_S(\xi)$  is Hermitian, i.e.,

$$G_S^*(\xi) = G_S(\xi),$$

its eigenvectors are orthogonal, and therefore the slow-wave and fast-wave subspaces of the continuous system (5.58) are orthogonal.

Since  $G_S(\xi)$  is Hermitian, it is also normal, i.e.,

$$G_S^*(\xi)G_S(\xi) = G_S(\xi)G_S^*(\xi).$$

A matrix has a complete set of orthogonal eigenvectors if and only if it is normal. The matrix  $G(\xi)$  given by Eq. (3.9b) is not normal, and the slow-wave and fast-wave subspaces of the original system (3.1) are not orthogonal.

As a consequence, the slow-wave and fast-wave subspaces of the discrete model (4.7) are not orthogonal: the symbol  $\hat{\psi}(\omega)$  given by Eq.

(4.24) is not a normal matrix and its eigenvectors do not satisfy Eq. (5.56b). The Richtmyer two-step scheme for the modified system (5.58) does have a normal symbol, and therefore has orthogonal slow-wave and fast-wave subspaces.

We hope to have illustrated by means of this example that continuous models having orthogonal fast-wave and slow-wave subspaces are special: the equations must be written in symmetric form and must have been linearized about a specially chosen state. Orthogonality may or may not carry over to a corresponding discrete version of the model; one must still check to see if the discrete model's symbol is normal.

The minimum-energy projection. For the numerical experiments, we choose the modified filter to minimize a physical quantity, namely, the expected energy of the analysis error. The energy of solutions of Eqs. (3.1) is proportional to

$$\int_{-L/2}^{L/2} (u^2 + v^2 + \phi^2/\delta) dx .$$

We choose A to be the diagonal matrix with the elements  $(1,1,1/\delta)$  repeated along its diagonal; the corresponding error functional  $\eta$  represents the expected energy of the analysis error, and we refer to the corresponding projection as the minimum-energy projection. The minimum-energy projection, denoted by  $\Pi_E$ , is distinct from the parallel and orthogonal projections, and is depicted in Fig. 2.

The minimum-energy projection was computed by the method of Theorem 2. The weighting matrix A is block circulant,

$$A = \text{circ} [A_0, 0, \dots, 0] , \quad (5.59a)$$

where

$$\Lambda_0 = \text{diag} (1, 1, 1/\phi) , \quad (5.59b)$$

whence, from Eq. (5.31),

$$\hat{\Lambda}(\omega) = \text{diag} (1, 1, 1/\phi) . \quad (5.59c)$$

According to Theorem 2, therefore, the minimum-energy projection matrix is the block circulant matrix  $\Pi_E$  for which

$$\hat{\Pi}_E(\omega) = \alpha_\omega \underline{x}_0(\omega) \underline{x}_0^*(\omega) \text{diag}(1, 1, 1/\phi) , \quad (5.60a)$$

where

$$\alpha_\omega = [\underline{x}_0^*(\omega) \text{diag}(1, 1, 1/\phi) \underline{x}_0(\omega)]^{-1} . \quad (5.60b)$$

## CHAPTER SIX

### EXPERIMENTS WITH THE STANDARD AND MODIFIED KALMAN-BUCY FILTERS

Numerical experiments with the standard and modified KB filters will now be described. The results show that the modified filter produces slowly evolving state estimates, at the expense of estimation errors only slightly larger than those resulting from use of the standard KB filter. Results show also how each filter utilizes the information advected between data-dense and data-sparse regions. The importance of proper use of advected information will be further demonstrated in Chapter 7.

#### 6.1. Observing Pattern, Noise Covariances and Initial Data

We complete the description of our implementation of the standard and modified KB filters, Eqs. (2.22, 5.24), by choosing an observational pattern  $H_k$ , noise covariances  $R_k$  and  $Q_k$ , and initial data  $w_0^a$  and  $P_0^a$ ; the dynamics matrix  $\Psi$  and projection matrix  $\Pi = \Pi_E$  have already been described.

To recapitulate, the projection matrix is given by Eqs. (5.60): by the symbol  $\Pi$  we now always mean the minimum-energy projection  $\Pi_E$ . The dynamics matrix  $\Psi$  is given by Eq. (4.7b); the parameters  $f$ ,  $U$ ,  $\phi$  and  $L$  are given following Eq. (3.3), and the mesh parameters are  $M = 16$  grid points and  $\Delta t = 30$  min., as mentioned in Section 4.4. Discretization with 16 grid points leaves a computational problem of easily manageable size. The corresponding choice of  $\Delta t = 30$  min. is near the stability limit of the difference scheme, and results in  $r = 24$  time steps per synoptic period. An experiment using 32 grid points,

for a spatial resolution closer to that of operational NWP models, gave results quite similar to the comparable experiment with 16 points.

We study an observing pattern corresponding to the conventional meteorological upper-air network: all quantities  $(u, v, \phi)$  are observed over "land", at synoptic times, and there are no observations over the "ocean". The distribution of land and ocean at latitude  $\theta = \theta_0$ , where the earth's circumference is  $2L$ , is simplified to be 2-periodic, so that half of each interval of length  $L$  is covered by ocean (Pacific or Atlantic), and half by land (North America or Eurasia). For this reason we consider only 2-periodic solutions of Eqs. (3.1), and our computational domain is of length  $L$ ; cf. Eq. (3.3).

We consider the left half of the computational domain to be covered by land, and the right half to be covered by ocean. For simplicity we take the observing stations to be located precisely at grid points. The observation matrix is therefore

$$H_k = (I \ 0) \quad (6.1a)$$

when  $k$  is a multiple of  $r = 24$  time steps, and

$$H_k = 0 \quad (6.1b)$$

otherwise; observations are available at synoptic times only, i.e., every twelve hours.

For a single wave number  $\omega$ , initial data for the continuous system (3.1) which lead only to slow waves are given approximately, according to Eqs. (3.29), by

$$\phi(x,0) = \phi_0 \sin \xi x, \quad (6.2a)$$

$$u(x,0) = \frac{\xi^2 u_0 \phi_0}{\xi^2 \phi_0 + f^2} \sin \xi x, \quad (6.2b)$$

$$v(x,0) = \frac{\xi \phi_0}{f} \cos \xi x, \quad (6.2c)$$

where  $\xi = 2\pi\omega/L$ . We choose initial data  $w_0$  corresponding to a single Rossby wave with wave number  $\omega = 2$ , i.e.,  $\xi = 4\pi/L$ , and amplitude  $\phi_0 = 2.5 \times 10^3 \text{ m}^2/\text{s}^2$ . The latter is in accordance with a typical ridge-to-trough difference of 500 m in the height of the 500 millibar pressure surface (Palmén and Newton, 1969, Sec. 6.6). It follows that  $\phi_0/\phi = 1/12$ , which partially justifies the linearization of Eqs. (3.2).

It follows also that the amplitude of  $v(x,0)$ ,

$$v_0 = \frac{\xi \phi_0}{f} \approx 1.122 U, \quad (6.3)$$

is roughly equal to  $U$ , a realistic value. Note, however, that the amplitude of  $u(x,0)$ ,

$$u_0 = \frac{\xi^2 u_0 \phi_0}{\xi^2 \phi_0 + f^2} \approx 0.059 U, \quad (6.4)$$

is relatively small. This is in agreement with the results of Section 3.6: due to the absence in Eq. (3.1b) of a pressure-gradient term to balance the Coriolis term, the continuous and discrete slow-wave

subspaces have rather small  $u$ -components. The  $u$ -component is special, and its behavior during an assimilation will provide one convenient check of the departure of estimates from the slow-wave subspace.

Initial data for experiments with both the standard and modified filters were obtained by evaluating  $\underline{w}(x + (M/2 - 1)\Delta x, 0)$ , given by Eqs. (6.2), at the grid points  $x^j = j\Delta x$ ,  $j = -M/2+1, \dots, M/2$ . Denoting the result by  $\underline{w}_0^f$ , we then set

$$\underline{w}_0^a = \Pi \underline{w}_0^f, \quad (6.5)$$

in accordance with Eq. (5.14a). The difference between  $\underline{w}_0^a$  and  $\underline{w}_0^f$  is indicative of the difference between the discrete and continuous slow-wave subspaces, and of the degree of approximation in Eq. (3.28). We found a small but significant difference between  $\underline{w}_0^a$  and  $\underline{w}_0^f$ . In particular, the amplitudes of the  $u$ -,  $v$ -, and  $\phi$ -components of  $\underline{w}_0^a$  are  $0.993 u_0$ ,  $1.016 v_0$  and  $0.960 \phi_0$ .

As we have already pointed out following Eqs. (2.22, 5.14), the gain matrices of the standard and modified KB filters are independent of the state estimates. In particular, the gain matrices are independent of  $\underline{w}_0^a$ . Thus the choice of  $\underline{w}_0^a$  is made primarily for orientation purposes, and similar results will obtain for any initial estimate satisfying Eq. (5.14a).

The observations, made twice per day over the eight grid points located on "land",  $x^j \leq 0$ , are assumed to have errors uncorrelated in space, as well as in time. That is, we take the observation error covariance matrix  $R_k$  to be diagonal. The observation error variances, or diagonal elements of  $R_k$ , are taken to be constant in time:  $R_k = R =$



const. when  $k$  is a multiple of 24 time steps. The variances are also constant in space, and their values are based on data from McPherson et al. (1979, Table 2).

The standard deviation of conventional temperature observations used there is  $1^{\circ}\text{C}$ . This can be converted, based on the customary hydrostatic assumption, to a 500 millibar level geopotential error of approximately  $200 \text{ m}^2/\text{s}^2$ . This value corresponds to an error of about  $0.1 \phi_0$ . A corresponding 10 % error in the wind components, relative to  $v_0$ , is roughly 2 m/s ; this is slightly larger than the value of 1.5 m/s used by McPherson et al. (1979). We take the standard deviation in observations of  $\phi$  to be  $200 \text{ m}^2/\text{s}^2$ , and that in observations of  $u$  and  $v$  to be 2 m/s. Relative errors in all observations are thus about 10%.

The initial error covariance matrix  $P_0^a$  is taken to have the form

$$P_0^a = \Pi D_1^2 \Pi^T + (I - \Pi) D_2^2 (I - \Pi)^T, \quad (6.6)$$

which results from the assumption that the slow-wave and fast-wave components of the initial error are uncorrelated:

$$\underline{w}_0^a - \underline{w}_0^f = \Pi \underline{y}_1 + (I - \Pi) \underline{y}_2, \quad (6.7a)$$

where

$$E \underline{y}_i \underline{y}_j^T = D_i^2 \delta_{ij}. \quad (6.7b)$$

This assumption is made for convenience, and because of lack of information on the cross-correlations of the two types of errors; it can, of course, be easily removed.

Denoting by  $D$  the diagonal matrix with the elements  $(v_0, v_0, \phi_0)$  repeated on the diagonal, we take

$$D_1 = 0.4 D, \quad D_2 = 0.1 D. \quad (6.8)$$

Thus the initial error covariances are uniform over the entire domain and the initial error variances are much larger than the observational error variances. Most of the initial error lies in the discrete slow-wave subspace; the true initial state  $\underline{w}_0^t$  has only a small fast component,  $(\Pi - I)\underline{y}_2$ . This uniform distribution of initial error will make it easy to visualize the reduction of error resulting from the first synoptic observation.

The form chosen for the system noise covariance matrix  $Q_k$  is similar to that of  $P_0^a$ . We take  $Q_k$  to be constant,  $Q_k = Q$ , with

$$Q = \Pi D_3^2 \Pi^T + (I - \Pi) D_4^2 (I - \Pi)^T, \quad (6.9a)$$

where

$$D_3 = \gamma D, \quad D_4 = 0.25 \gamma D. \quad (6.9b)$$

The parameter  $\gamma$  is chosen on the basis of atmospheric predictability studies, cf. Sec. 1.2 and the discussion following Eq. (2.2a), as follows.

Suppose that  $\{\underline{w}_k^s\}$  and  $\{\underline{w}_k^t\}$  are two realizations of our stochastic-dynamic model, Eqs. (2.2, 4.7b, 6.9), starting from identical initial states,  $\underline{w}_0^s = \underline{w}_0^t$ . The covariance matrix

$$X_k = E(\underline{w}_k^s - \underline{w}_k^t)(\underline{w}_k^s - \underline{w}_k^t)^T \quad (6.10)$$

evolves according to

$$X_k = \Psi X_{k-1} \Psi^T + 2 Q, \quad (6.11a)$$

$$X_0 = 0; \quad (6.11b)$$

cf. Eq. (2.10a). The expected energy of the difference between the two realizations is  $E_k^2$ ,

$$E_k^2 = E(\underline{w}_k^s - \underline{w}_k^t)^T A (\underline{w}_k^s - \underline{w}_k^t), \quad (6.12)$$

where  $A$  is the energy-weighting matrix given by Eqs. (5.59a,b). We have

$$E_k^2 = \text{trace } A X_k \quad (6.13a)$$

$$E_0^2 = 0; \quad (6.13b)$$

cf. Eqs. (2.12, 2.13).

The correlation matrix of the two realizations is given by

$$C_k = E(\underline{w}_k^s)(\underline{w}_k^t)^T, \quad (6.14a)$$

and evolves according to

$$C_k = \Psi C_{k-1} \Psi^T. \quad (6.14b)$$

The correlation matrix starts from a nonzero value and tends to zero as  $k \rightarrow \infty$ , as a result of the dissipation of the dynamics matrix  $\Psi$ .

For our stochastic-dynamic model to have the same predictability as the atmosphere, we would like the two realizations, perfectly correlated at the initial time, to become nearly uncorrelated,

$$C_p \approx 0,$$

after a finite predictability time  $p$  of about two to three weeks. If  $C_p = 0$  exactly, then we would have

$$X_p = E(\underline{w}_p^s)(\underline{w}_p^s)^T + E(\underline{w}_p^t)(\underline{w}_p^t)^T$$

and

$$E_p^2 = E(\underline{w}_p^s)^T A(\underline{w}_p^s) + E(\underline{w}_p^t)^T A(\underline{w}_p^t).$$

That is,  $E_k^2$  would grow from zero at time zero to an amount at time  $p$  equal to twice the expected energy  $E_\star^2$  of either  $\underline{w}_p^s$  or  $\underline{w}_p^t$ ,

$$E_p^2 = 2 E_\star^2. \quad (6.15)$$

Of course Eq. (6.15) would be true of functionals other than the energy. For simplicity we base the choice of  $Q$  on only one free parameter,  $Q = Q(\gamma)$ , so that the growth of only one functional can be prescribed.

We regard the energy  $E_\star^2$  as a "typical" energy, as system (2.2a) is not conservative. We take the typical energy to be that of  $\underline{w}_0^a$ ,

$$E_\star^2 = \text{trace } A(\underline{w}_0^a)(\underline{w}_0^a)^T, \quad (6.16a)$$

with  $\underline{w}_0^a$  given by Eq. (6.5). Our assimilation experiments are run for 10 days, i.e., for  $N = 480$  time steps. We determine  $\gamma$ , and hence  $Q(\gamma)$ , by specifying a parameter  $\alpha$  close to one and requiring

$$E_N^2 = 2\alpha^2 E_k^2 . \quad (6.16b)$$

Thus, for convenience we specify the amount of loss of predictability over the length of an assimilation run.

We set  $\alpha = 0.7$ , and found  $\gamma = 0.028$ . This was easily done by trial and error: according to Eqs. (2.10a, 6.11, 6.13),

$$E_N^2 = 2 \text{ trace } AP_N , \quad (6.16c)$$

where  $P_N$  is the estimation error covariance at the end of a run with zero initial error and no observations. Thus, we computed  $E_N^2$  in Eq. (6.16c) for various choices of  $\gamma$ , until Eq. (6.16b) was satisfied.

The choice of  $\alpha = 0.7$  corresponds to a 70% rms loss of predictability at time  $k = N$ . This value of  $\alpha$ , rather than a value closer to one, was chosen because  $N < p$ :  $E_k^2$  continues to grow after time  $N$  and  $C_k$  continues to decay. The leveling-off time of  $E_k$ , and the decay time of  $C_k$ , is much longer than  $N$  and is a function only of the amount of dissipation in the dynamics matrix  $\Psi$ ; cf. Eq. (6.14b).

To complete the description of our assimilation experiments, we note that the observations  $\underline{w}_k^0$  in Eqs. (2.22e, 5.24e) were obtained from an actual realization of the stochastic-dynamic system (2.2, 2.3). That is, we generated independent random vectors  $\{\underline{w}_0^t, \underline{b}_k^t, \underline{b}_k^0\}$  having the prescribed covariances,  $P_0^a$  for  $\underline{w}_0^t - \underline{w}_0^a$ ,  $Q$  for  $\underline{b}_k^t$ , and  $R$  for  $\underline{b}_k^0$ , and accordingly obtained random vectors  $\underline{w}_k^0$  from Eq. (2.3a).

## 6.2. Numerical Results

In Figure 3 we show at selected grid points the time histories of the estimates  $\{\underline{w}_k^f, \underline{w}_k^a: k = 0, 1, 2, \dots, N\}$  produced by the KB filter; u-components of the estimates are shown in Fig. 3a, v-components in Fig. 3b, and  $\phi$ -components in Fig. 3c. We show a point on the West coast of the continent, labeled SF (for San Francisco), one on the East coast, labeled NY (for New York), and one in the middle of the ocean, labeled HA (for Hawaii). Note that "Tokyo" = "New York" by periodicity. The ordinates in Figs. 3a,b are scaled by  $v_0$ , Eq. (6.2), and the ordinate in Fig. 3c is scaled by  $\phi_0$ .

On each curve, small-amplitude fast oscillations are superimposed on a smooth, slowly varying wave pattern. The fast oscillations are caused by the introduction of noisy observations of the true state; the true state has a fast component due to that of the system noise and that of the initial state  $\underline{w}_0^f$ . The fast oscillations are especially apparent in the u-components, Fig. 3a; recall from Sec. 3.6 and from the discussion following Eq. (6.4) that u-components are very sensitive to departures from the slow-wave subspace. Notice in Figs. 3b,c the underlying periodicity of about 6 days. This is in agreement with the phase speed  $c_0(2)$  shown in Table 3,

$$c_0(2) = 13.12 \text{ m/s} \approx \frac{L}{12.35 \text{ days}};$$

one-half of the 2-wave we are estimating passes through the L-domain in just over 6 days.

For the assimilation run with the modified filter, the results corresponding to Fig. 3 are shown in Fig. 4. The time histories of

the estimates in this case are perfectly smooth, apart from the jumps due to observational insertions: the estimates evolve entirely in the slow-wave subspace. The 6-day periodicity is now evident even in the u-components, Fig. 4a. The u-components change very little at observation times: the corrections added to the forecast at observation times lie in the slow-wave subspace, and therefore have small u-components. By contrast, the corrections to  $v$  and  $\phi$  at observation times, Figs. 4b,c, are often quite large at SF and NY. The corrections at HA are much smaller because no observations are made there. Corrections at HA are due only to, and are made to a degree consistent with, the correlation of the forecast error at HA with the forecast error at observation stations inland.

To study the behavior of the estimation error for the KB filter experiment, we show in Fig. 5 components of the expected rms estimation error resulting from use of the KB filter. Figure 5a shows the expected rms error over land, Fig. 5b over the ocean, and Fig. 5c over the entire domain. The individual curves are labeled U, V, P and E, for the expected error in  $u$ ,  $v$ ,  $\phi$  and the total energy, averaged over the indicated region. Thus, the U-curve in Fig. 5a gives the square root of the average of the first eight u-components along the diagonal of  $P_k^{f,a}$ . The ordinate in each panel is scaled by  $v_0$  for the U- and V-curves, by  $\phi_0$  for the P-curve, and by  $2v_0^2 + \phi_0^2/\phi$  for the E-curve. Thus, the observational error level in each panel is 0.089 for the U- and V-curves, 0.080 for the P-curve, and 0.088 for the E-curve.

The errors over land, Fig. 5a, drop below the observational error level immediately, at the first synoptic time. In fact, the error

reduction over land at each synoptic time is dramatic, and results in errors below the level of observational noise. The error reduction over ocean at each synoptic time, Fig. 5b, is less pronounced but is still significant: the KB filter is able to spread out the new information from observations over land to adjacent ocean areas.

Also striking is the difference between Figs. 5a and 5b in the error growth between synoptic times. The large increase of error over land in between synoptic times, shown in Fig. 5a, is due to the combined effect of system noise and advection of error from over the data-sparse ocean. The much milder increase of error over the ocean in between synoptic times, shown in Fig. 5b, is due to partial cancellation of these two effects: the effect of system noise is still the same, but relatively error-free information is being advected from over the data-dense land.

Notice also that the curves shown in each of Figs. 5a,b,c quickly settle into an asymptotically periodic pattern, with the synoptic interval of 12 hours as the period. This behavior is typical of time-independent models  $(\Psi, Q)$  with periodic observations  $(H_k, R)$ . The convergence occurs within about one day over land, and in about 5 days over the ocean. In fact, the KB gain matrices used at observation times tend rapidly to a constant gain matrix,  $K_k^{KB} \rightarrow K_\infty^{KB}$ .

Expected rms errors for the experiment with the modified filter are shown in Fig. 6. The errors in  $v$  and  $\phi$ , over both land and ocean, are nearly indistinguishable from those of the standard KB filter: slowly evolving estimates are obtained at the expense of only a very slight increase in estimation error. Errors in the  $u$ -component, however, are significantly larger than in the case of the standard



filter. The u-component errors resulting from use of the modified filter grow in time and, after 10 days, are about twice the size of those resulting from the KB filter. The larger u-component errors are due to the fact that the modified filter allows almost no observational correction to be performed on the u-components: the u-components must remain small for the analysis vector to lie in the slow-wave subspace. The u-components of the true state, on the other hand, are growing because of the continual input of the fast component of the system noise.

To visualize better the behavior of  $K_k^{KB}$  in time and to study the structure of  $K_\infty^{KB}$ , we plotted the influence functions of selected observation stations. The influence functions of an observation station show the weight given to an observation of  $u$ ,  $v$ , or  $\phi$  at that station when updating points throughout the domain. The influence functions at time  $k$  are obtained from appropriate columns of  $K_k^{KB}$ .

The chosen observation stations were SF, SL (for Saint Louis) and NY. There are no influence functions for mid-ocean points, like HA, since no observations are made there. Influence functions were plotted at every synoptic time, i.e., every 24 time steps. It was clear that convergence to  $K_\infty^{KB}$  occurred within about 5 days.

Figure 7 shows the influence functions for the selected observation stations at the end of day 10. Figure 7a, marked (u-u), gives the influence of a u observation at the selected stations on u corrections at every grid point in the domain. Figure 7b, marked (u-v), gives the weight of a v observation at a station on the u corrections at every grid point, and so on. The variables have been scaled in the usual way, u and v by  $v_0$ , and  $\phi$  by  $\phi_0$ .

All the weighting coefficients involving  $u$  are rather small (Figs. 7a,b,c,d,g). Our choice of system noise covariance matrix  $Q$ , with the 4-to-1 ratio of  $D_3$  to  $D_4$ , entails relatively good predictions of  $u$ , which have to be corrected only to a small extent by the observations. The  $(u-u)$  coefficients (Fig. 7a) are the largest of the coefficients involving  $u$ ; they still do not exceed 0.125. The  $(u-u)$  influence functions are approximately equal for SF, SL and NY; they are positive and symmetric about the observation station. They are the only ones to have both of the latter properties.

The  $(\phi-\phi)$  influence function centered at SL is the smallest one shown in Fig. 7i. It is positive over land, becoming nearly zero at SF and NY, and slightly negative out into the ocean. The symmetry and relatively small peak of this function is due to its station, SL, being located in the middle of a data-dense region: neighboring points also have observation stations and advection plays but a small role.

The peaks of the  $(\phi-\phi)$  influence functions centered at NY and at SF are considerably higher than the SL peak. This is due to the absence of observations on the ocean side of these stations. In fact, the peak of the SF function is slightly higher than the NY peak. Moreover, the former is located one grid point west of SF, rather than at SF itself, while the NY peak is at NY. Both data density and advection thus play a role.

It makes sense for the point upstream of SF to give even more weight to SF information than SF itself: SF is closer to inland points and their information is also weighted heavily. Due to the advection of error, the forecast error at synoptic times for this ocean point is considerably larger than that for the point downstream from NY,

although they are equidistant from land. Hence, more weight is given to adjacent land observations for the Pacific point than for the Atlantic point.

As in Fig. 7i, the  $(v-v)$ ,  $(v-\phi)$  and  $(\phi-v)$  influence functions (Figs. 7e,f,h) all show strong inhomogeneity differences between the SF, SL and NY functions, as well as anisotropy differences to the west and east of each station. The SL influence function is nearly symmetric for  $(v-v)$ , and it is nearly antisymmetric for  $(v-\phi)$  and  $(\phi-v)$ ; the corresponding SF and NY influence functions do not have these symmetry properties. We will see in the following chapter that this differential treatment of observations located in the middle of a data-dense region (SL) and observations on the border between data-dense and data-sparse regions (SF and NY) is important for the proper performance of data assimilation schemes.

The SL influence functions at the first synoptic time (Fig. 8) are either perfectly symmetric ( $u-u$ ,  $u-v$ ,  $v-u$ ,  $v-v$ , and  $\phi-\phi$ ), or perfectly antisymmetric ( $u-\phi$ ,  $v-\phi$ ,  $\phi-u$ , and  $\phi-v$ ). Similarly, in each panel of Fig. 8, the NY influence function is either the mirror image or the inverted mirror image of the SF function.

Comparison of Fig. 8 with Fig. 7 allows us to distinguish between the effect of inhomogeneous data density and the effect of advection. Figure 8 shows the effect of data distribution only, since at the first synoptic time no information has been advected yet from previous data insertions. Figure 7 shows the combination of the two effects.

Different data densities result in different influence functions according to station location (Fig. 8): stations located in sharp

gradients of observation availability, such as SF and NY, have more influence than inland stations (SL), and their influence out to sea is also greater than their influence inland. It is advection, however, which leads to the difference between the influence functions of stations on the West coast (SF) and East coast (NY). The latter difference was discussed in connection with Fig. 7i, and is also clear in Figs. 7e,f,h.

The corresponding results for the modified KB filter (not shown) are very similar to those for the standard KB filter shown in Figs. 7 and 8. The main difference is that the  $(u-u)$ ,  $(u-v)$  and  $(u-\phi)$  influence functions are almost perfectly flat. The modified filter allows even less correction to the  $u$ -components than does the standard filter: the estimates are forced to remain in the slow-wave subspace.

The KB gain matrix at day 10, a good approximation to the asymptotic gain matrix  $K_{\infty}^{KB}$ , was used as a constant, time-independent gain matrix in another assimilation experiment. Estimation errors after 1-2 days were practically indistinguishable from those obtained when using the KB filter. Similarly, a run using the final gain matrix of the modified filter gave results almost identical to those of the modified filter itself. There is therefore no need, in our time-independent model  $(Y,Q,R)$ , to compute a new gain matrix at every synoptic time: approximate computation of the asymptotic gain matrix once and for all is sufficient for practical purposes. The asymptotic KB filter, known as the Wiener filter, is analyzed more fully in Ghil et al. (1981, Secs. 4.2, 4.3).

## CHAPTER SEVEN

### COMPARISON WITH OPTIMAL INTERPOLATION

#### 7.1. The Optimal Interpolation Filter

We have already pointed out that the difference between optimal interpolation (OI) and the KB filter is that OI is based on an assumed, prescribed forecast error covariance matrix, rather than on the covariance matrix  $P_k^f$  which results from assumption of a stochastic-dynamic model (2.2). We denote the prescribed covariance matrix by  $S_k^f$ , and base our formulation of  $S_k^f$  upon the OI schemes used at NMC (Bergman, 1979; McPherson et al., 1979) and at ECMWF (Lorenc, 1981).

We implement OI for our usual forecast model (4.7),

$$\underline{w}_k^f = \Psi \underline{w}_{k-1}^a ; \quad (7.1a)$$

as OI is an unbiased linear data assimilation scheme, the OI update equation can be written as

$$\underline{w}_k^a = \underline{w}_k^f + K_k (\underline{w}_k^o - H_k \underline{w}_k^f) , \quad (7.1b)$$

cf. Eqs. (2.7). Optimal interpolation schemes are derived by minimizing the analysis error variance at every grid point, assuming an observational error covariance matrix  $R_k$  and a forecast error covariance matrix  $S_k^f$ . The OI gain matrix,  $K_k = K_k^{OI}$ , is therefore identical to the KB gain matrix, with  $P_k^f$  replaced by  $S_k^f$ :

$$K_k^{OI} = S_k^f H_k^T (H_k S_k^f H_k^T + R_k)^{-1} ; \quad (7.2)$$

cf. Eq. (2.20a).

With  $S_k^f$  as the forecast error covariance matrix and with  $K_k = K_k^{OI}$ , it follows that the OI analysis error covariance matrix  $S_k^a$  is given by

$$S_k^a = (I - K_k^{OI} H_k) S_k^f ; \quad (7.3a)$$

cf. Eq. (2.21). We also define the diagonal matrix

$$D_k^a = \text{diag } S_k^a \quad (7.3b)$$

of analysis error variances. Equations (7.1b, 7.2, 7.3b) are identical, respectively, to Eqs. (2.5, 2.12, 2.13) in Bergman (1979), although we use a more compact notation.

It remains to describe how the forecast error covariance matrix  $S_k^f$  is formulated in OI. Every covariance matrix  $S$  can be decomposed in the form  $S = B^{1/2} C B^{1/2}$  where  $B = \text{diag } S$  is a diagonal matrix of variances and where  $C = B^{-1/2} S B^{-1/2}$  is a correlation matrix. In OI it is assumed that the forecast error correlations are time-independent,

$$S_k^f = (D_k^f)^{1/2} C (D_k^f)^{1/2} ; \quad (7.4a)$$

the correlation matrix  $C$  is constant and is a prescribed matrix in OI.

The forecast error variances,

$$D_k^f = \text{diag } S_k^f , \quad (7.4b)$$

are assumed to grow linearly in time, i.e.,

$$D_k^f = D_{k-r}^a + D, \quad (7.5)$$

where  $r$  is the length of the assimilation cycle,  $r = 24$  time steps in our case. The time-independent diagonal matrix  $D$  is a prescribed forecast error growth rate matrix; cf. McPherson *et al.* (1979, Sec. 2c.4). Equations (7.4,7.5) describe the evolution of  $S_k^f$ ; they can be regarded as an approximate version of Eq. (2.22b).

Except for choice of the matrices  $C$  and  $D$ , Eqs. (7.1-7.5) define the implementation of OI for our shallow-water model  $(\psi, H_k, R_k, w_k^o, w_k^a)$ ; we take  $S_0^a = P_0^a$ . We refer to Eqs. (7.1-7.5) as the OI filter. For experiments with the OI filter we also compute the true forecast and analysis error covariance matrices,

$$P_k^f = \Psi P_{k-1}^a \Psi^T + Q, \quad (7.6a)$$

$$P_k^a = (I - K_k H_k) P_k^f (I - K_k H_k)^T + K_k R_k K_k^T, \quad (7.6b)$$

with  $K_k = K_k^{OI}$ ; cf. Eqs. (2.10).

We define also an initialized OI filter, having gain matrix

$$K_k^{\Pi OI} = \Pi K_k^{OI}, \quad (7.7)$$

where  $\Pi$  is the usual minimum-energy projection. In this case, Eq. (7.3) is replaced by the general formula

$$S_k^a = (I - K_k H_k) S_k^f (I - K_k H_k)^T + K_k R_k K_k^T, \quad (7.8)$$

with  $K_k = K_k^{\Pi OI}$ . For experiments with the initialized OI filter we also compute the true error covariances (7.6), with  $K_k = K_k^{\Pi OI}$ .

The standard assumption by which the correlation matrix  $C$  is determined is that mass field (geopotential or temperature) correlations are homogeneous, isotropic and Gaussian, with the remaining correlations derived by assuming that forecast errors are geostrophically related (Bergman, 1979, Sec. 3; Lorenc, 1981, Sec. 4b). For our model (3.1), the geostrophic relation is

$$u = 0, \quad v = \phi_x / f, \quad (7.9a,b)$$

and therefore the assumed forecast error correlations, which define the elements of  $C$ , are given by

$$C_{ij}^{\phi\phi} = \exp [-(x_i - x_j)^2 / s_0^2], \quad (7.10a)$$

$$C_{ij}^{vv} = [1 - 2(x_i - x_j)^2 / s_0^2] C_{ij}^{\phi\phi}, \quad (7.10b)$$

$$C_{ij}^{\phi v} = \sqrt{2} [(x_i - x_j) / s_0] C_{ij}^{\phi\phi}, \quad (7.10c)$$

$$C_{ij}^{v\phi} = -C_{ij}^{\phi v}, \quad (7.10d)$$

for  $|x_i - x_j| \leq L/2$  on our periodic domain; we take for the correlation distance  $s_0 = 1000$  km, in agreement with the value used at NMC.

The five correlation functions not specified in Eqs. (7.10), i.e., those involving  $u$ , are all zero due to the geostrophic assumption (7.9a). In our version of OI, therefore, forecasts of  $u$  are not changed at analysis times, nor are the  $v$  and  $\phi$  analyses affected by observations of  $u$ . This is not unreasonable for our model; we have already seen that the same is approximately true of the standard and modified KB filters, as a result of the 4-to-1 ratio of  $D_3$  to  $D_4$  in Eq. (6.9b) and since the slow-wave subspace is quasigeostrophic.



In our first set of experiments, the diagonal forecast error growth rate matrix  $D$  was chosen in the following way. We have already seen that the KB gain matrix tends to a constant matrix, and that the corresponding error covariance matrices  $P_k^{f,a}$  tend to an  $r$ -periodic sequence,  $P_k^{f,a} = P_{k-r}^{f,a}$ . At the end of the KB filter run,  $k = 480$  time steps, we averaged the diagonal elements of  $P_k^f - P_{k-r}^a$  over the entire spatial domain. Thus, we found for the KB filter the average 12-hour growth rate for the variance of each of the three variables  $u$ ,  $v$ ,  $\phi$ . These averaged rates were then used as the diagonal elements of  $D$  for a preliminary run with the OI filter. The assumed growth rates for this first OI run, and for the runs we describe next, are therefore independent of the longitude  $x$ , as is the case with the OI scheme described by McPherson et al. (1979, Sec. 2c.4).

Using Eqs. (7.6), we computed next the true growth rates  $\{\text{diag}(P_k^f - P_{k-r}^a) : k \text{ is a multiple of } r\}$  produced by the preliminary OI run, and we averaged them over the spatial domain. These averaged rates, although relatively constant after about 5 days, were somewhat different from the originally assumed growth rates. In order to produce a control run for OI, we made the following succession of 10-day OI runs: the space-averaged true growth rates for each run, starting with the first run described already, were averaged in time over the last  $2 \frac{1}{2}$  days and used as the assumed growth rates for the next run. This procedure converged rapidly to our control OI run, which we call run  $A_1$ .

Thus the true growth rates for run  $A_1$ , averaged over days  $7 \frac{1}{2} - 10$ , agree with the prescribed growth rates  $D$ . This corresponds to the

assumed rates being specified by an "optimal verification" scheme. We denote these growth rates by  $d_u^2$ ,  $d_v^2$  and  $d_\phi^2$ .

Having determined the control run  $A_1$ , we performed next a series of OI runs  $A_\alpha$ , to study how the true error covariances  $P_k^f$  depend on the assumed growth rates. Run  $A_\alpha$  uses the elements  $((\alpha d_u)^2, (\alpha d_v)^2, (\alpha d_\phi)^2)$  repeated along the diagonal of  $D$ . We used values of  $\alpha$  ranging from 0 to 2 in increments of  $1/4$ .

In an analogous fashion, we determined an initialized OI filter control run  $B_1$  ( $K = K^{IOI}$ ), using the initialized KB run ( $K = K^{IKB}$ ) as the starting point. We then performed the corresponding series of runs  $B_\alpha$ .

## 7.2. Numerical Results

In Table 4 we summarize the results of the OI runs  $A_\alpha$  and  $B_\alpha$ . For comparison, we also include the corresponding results of the run with the KB filter, which we refer to as run  $A_{KB}$ , and of the run with the modified KB filter, which we refer to as run  $B_{KB}$ ; these are the two runs described in Chapter 6.

The table entries are the true expected rms analysis errors at selected grid points after 10 days, i.e., they are the square roots of selected diagonal elements of the analysis error covariance matrix  $P_{480}^a$  produced by each run. The selected grid points are at Saint Louis (SL,  $x = -3\Delta x$ ), Hawaii (HA,  $x = 5\Delta x$ ) and London (LN,  $x = 8\Delta x$ ); LN is an ocean location adjacent to the continent. The entries are scaled in the usual way,  $u$  and  $v$  by  $v_0$ , and  $\phi$  by  $\phi_0$ ; recall that with this scaling the observational error levels are 0.089 for  $u$  and  $v$ , and 0.080 for  $\phi$ . The  $u_{HA}$  and  $u_{LN}$  entries are omitted because the  $u$ -errors are

nearly constant over the spatial domain; the OI runs leave  $\underline{u}$  unchanged at analysis times, and the KB runs change  $\underline{u}$  only slightly.

The minimum value in each column occurs for run  $A_{KB}$ , as expected: the KB filter is optimal. The errors for run  $B_{KB}$  are only slightly larger than those for run  $A_{KB}$ , as we saw already in Chapter 6. Notice that for runs  $A_{KB}$  and  $B_{KB}$ ,  $v_{SL} < v_{LN} < v_{HA}$  and  $\phi_{SL} < \phi_{LN} < \phi_{HA}$ , as a result of our conventional observing pattern.

In contrast to the relative performance of runs  $A_{KB}$  and  $B_{KB}$ , the  $B_{\alpha}$  runs perform better than the  $A_{\alpha}$  runs. This is evident especially at SL and LN; there is little difference at HA since there are no nearby observations.

The effect of initialization is most dramatic for  $u_{SL}$ . The 4-to-1 ratio of  $D_3$  to  $D_4$  in our definition of  $Q$ , Eqs. (6.9), forces the true state  $\underline{w}_k^t$  to always lie near the slow-wave subspace, and the analysis vector in all B-runs always lies in the slow-wave subspace. Since the slow-wave subspace has small  $u$ -components, the rms errors in  $\underline{u}$  must therefore always be small in the B-runs.

In contrast, for runs  $A_{\alpha}$ ,  $u_{SL}$  is large and increases with  $\alpha$ . As  $\alpha$  increases, so do the assumed forecast error variances  $D_k^f$ . Therefore observational data are given more weight and the analyses drift further and further from the slow-wave subspace.

For  $v_{HA}$  and  $\phi_{HA}$ , there is little difference between the  $A_{\alpha}$  and  $B_{\alpha}$  runs, and these errors are relatively insensitive to the size of  $\alpha$ . There are no nearby observations to correct forecasts at HA, so the forecast error variances near HA are immaterial. However, the  $v_{HA}$  and  $\phi_{HA}$  errors are significantly larger for the  $A_{\alpha}$  and  $B_{\alpha}$  runs than for the  $A_{KB}$  and  $B_{KB}$  runs. This is due to advection of error from grid points

which have been updated by the observational data, to which slightly incorrect weights have been assigned in the OI runs.

For  $\phi_{SL}$ , notice that runs  $A_\alpha$  and  $B_\alpha$ ,  $\alpha \geq \frac{1}{2}$ , give results quite comparable to runs  $A_{KB}$  and  $B_{KB}$ . On the other hand, the  $v_{SL}$  errors are much larger for the  $A_\alpha$  runs than for the  $A_{KB}$  run, while the  $v_{SL}$  errors are quite comparable for the  $B_\alpha$  and  $B_{KB}$  runs. Figure 9 helps explain why this is so.

Figures 9a,b show the assumed  $\phi-\phi$  and  $v-v$  forecast error correlation functions, Eqs. (7.10a,b), used in the OI runs. Figures 9c,d show the true forecast error correlation functions, deduced from  $P_K^f$  at 10 days, for run  $A_1$ . Figures 9e,f show the true forecast error correlation functions at 10 days for run  $B_1$ . The short-dashed lines indicate the correlation functions at SL, the long-dashed lines correspond to HA, and the solid lines correspond to LN. The true correlations are not homogeneous: the curves in Figs. 9c-e do not superimpose.

The  $\phi-\phi$  correlations at SL are quite similar in Figs. 9c and 9e, and not altogether different from the  $\phi-\phi$  correlation in Fig. 9a. Thus the  $A_\alpha$  and  $B_\alpha$  runs are able to produce reasonably good analyses of  $\phi$  at SL, provided sufficient weight,  $\alpha \geq \frac{1}{2}$ , is given to the wealth of observations available nearby. The  $v-v$  correlation at SL in Fig. 9d is far from that in Fig. 9b, which was based on the geostrophic assumption. Consequently, OI does not make adequate use of data available nearby and, as seen in Table 4, the  $v_{SL}$  errors for the  $A_\alpha$  runs are large. The  $v-v$  correlation at SL in Fig. 9f is much closer to that in Fig. 9b; the corresponding  $v_{SL}$  errors for the  $B_\alpha$  runs are much improved.

The situation is similar at LN. The portion of the solid curve just to the right of center in Figs. 9d,f show that  $\underline{v}$  at LN is in truth positively correlated with  $\underline{v}$  at nearby land locations, with a large correlation coefficient. The curve in Fig. 9b shows that the OI runs use instead a negative correlation coefficient. As a result, the  $v_{LN}$  errors (Table 4), for large values of  $\alpha$ , are actually larger than the  $v_{HA}$  errors. In fact, the  $\underline{v}$  analyses at LN turn out to be worse than the  $\underline{v}$  forecasts at LN, in all  $A_\alpha$  and  $B_\alpha$  runs.

As the curve in Fig. 9b poorly approximates the LN curves in both Figs. 9d and 9f, we must ask why the  $v_{LN}$  results in Table 4 are better for the  $B_\alpha$  runs than for the  $A_\alpha$  runs. The answer lies in what happens between analysis times.

The analysis errors in the  $B_\alpha$  runs propagate at Rossby wave phase speeds only. The maximum Rossby speed for our model  $\Psi$ , according to Table 3, is

$$c_0(3) = 13.73 \text{ m/s} = 0.68 \Delta x / 12 \text{ hr.}$$

Errors in the  $B_\alpha$  runs are therefore localized: new observational information is inserted before error from the previous insertion can travel one grid point.

Errors in the  $A_\alpha$  runs, on the other hand, can propagate also by inertia-gravity waves, which according to Table 3 travel as fast as

$$c_1(1) = 301.31 \text{ m/s} = 14.9 \Delta x / 12 \text{ hr.}$$

Error from the poor  $v_{LN}$  analysis in the  $A_\alpha$  runs therefore quickly contaminates the forecasts over land. At the next analysis time, the

$A_\alpha$  runs then use the now large observed-minus-forecast residuals over land to produce a degraded  $v_{LN}$  analysis. This effect also explains a portion of the large  $v_{SL}$  errors for the  $A_\alpha$  runs.

Notice also that the curves in Figs. 9e,f drop to zero while those in Figs. 9c,d do not: initialization localizes errors and therefore "tightens" the correlation functions. The same is true of the cross-correlations  $v-\psi$  and  $\phi-v$  (not shown). Phillips (1981) points out that initialization has the somewhat paradoxical effect of forcing all grid variables to be changed by the insertion of observational data at only one grid point. Our results show that there might be no need to worry: initialization changes the mean fields in such a way that the errors become more localized.

Our experimental results make it clear that using improper correlation functions near boundaries separating data-dense and data-sparse regions can lead to unduly large errors near those boundaries, and that initialization is a partial cure for this boundary effect. Another way to compensate for this effect is to use forecast error growth rates which depend on data density. We saw already in Chapter 6 that for an optimal filter, growth rates over data-sparse regions are naturally much smaller than growth rates over data-dense regions (Figs. 5,6), due to advection of information.

Accordingly, we conducted two more series of experiments,  $A_{\beta,\gamma}$  and  $B_{\beta,\gamma}$ . Runs  $A_{\beta,\gamma}$  are identical to run  $A_1$  except that the growth rate  $\beta d_v$  is used over land and  $\gamma d_v$  is used over the ocean. In the same way, runs  $B_{\beta,\gamma}$  are similar to run  $B_1$ . We let  $\gamma$  vary from 0 to 1, while we let  $\beta$  vary from 1 to 2, both in increments of  $\frac{1}{4}$ .

The runs  $A_{\beta,\gamma}$  and  $B_{\beta,\gamma}$  all gave remarkably better results than the

$A_\alpha$  and  $B_\alpha$  runs. Results of the best runs,  $A_{2,0}$  and  $B_{5/4,1/4}$ , are summarized in Table 5. The  $v_{LN}$  analysis is greatly improved in both runs; run  $A_{2,0}$  also gives a substantial improvement for  $u_{SL}$  and  $v_{SL}$ . The results of both runs compare favorably with those of the  $B_{KB}$  run. We conclude that use of proper forecast error variance growth rates is essential to the performance of OI.

The tuning procedure we have described for determining proper growth rates is a manual one: analysis error variances for different runs were examined a posteriori, after which it was decided which growth rates produce the best results. For the purposes of operational NWP, a more systematic way of tuning the growth rates would be to do so adaptively; adaptive estimation was discussed, and references given, in Sec. 2.6. Correlation functions, especially those near boundaries separating data-dense and data-sparse regions, could also be determined adaptively. Still, it might be better to approximate Eq. (2.22b) in a more direct fashion than is currently done in OI, and to do so adaptively.

REFERENCES

- Baer, F., 1977. Adjustments of initial conditions required to suppress gravity oscillations in non-linear flows. Beitrage zur Physik der Atmosphäre, 50, 350-366.
- Baer, F., and J. J. Tribbia, 1977. On complete filtering of gravity modes through non-linear initialization. Mon. Wea. Rev., 105, 1536-1539.
- Bélanger, P. R., 1974. Estimation of noise covariance matrices for a linear time-varying stochastic process. Automatica, 10, 267-275.
- Bengtsson, L., 1975. Four-Dimensional Assimilation of Meteorological Observations. GARP Publications Series, No. 15, World Meteorological Organization - International Council of Scientific Unions, CH-1211, Geneva 20, Switzerland, 76 pp.
- Bengtsson, L., M. Ghil, and E. Källén (eds.), 1981. Dynamic Meteorology: Data Assimilation Methods. Applied Mathematical Sciences Series, Vol. 36, Springer-Verlag, New York, 330 pp.
- Bergman, K. H., 1979. Multivariate analysis of temperatures and winds using optimum interpolation. Mon. Wea. Rev., 107, 1423-1444.
- Bergthorsson, P., and B. R. DØss, 1955. Numerical weather map analysis. Tellus, 7, 329-340.
- Bierman, G. J., 1977. Factorization Methods for Discrete Sequential Estimation. Academic Press, New York, 241 pp.
- Brigham, E. O., 1974. The Fast Fourier Transform. Prentice-Hall, Englewood Cliffs, NJ, 252 pp.
- Bube, K. P., 1978. The construction of initial data for hyperbolic systems from nonstandard data. Ph.D. Dissertation, Department of Mathematics, Stanford University, Stanford, CA 94305, 114 pp.
- Bube, K. P., 1981. Determining solutions of hyperbolic systems from incomplete data. Comm. Pure Appl. Math., 34, 799-830.
- Charney, J., et al., 1966. The feasibility of a global observation and analysis experiment. Bull. Amer. Meteor. Soc., 47, 200-220.
- Chin, L., 1979. Advances in adaptive filtering. In: C. T. Leondes (ed.), Control and Dynamic Systems, Vol. 15, Academic Press, New York, pp. 278-356.
- Churchill, R. V., 1969. Fourier Series and Boundary Value Problems, 2nd ed. McGraw-Hill, New York, 248 pp.



- Coddington, E. A., and N. Levinson, 1955. Theory of Ordinary Differential Equations. McGraw-Hill, New York, 429 pp.
- Cohn, S., M. Ghil, and E. Isaacson, 1981. Optimal interpolation and the Kalman filter. Proc. 5th Conf. Numer. Weather Prediction, Monterey, CA, 2-6 Nov. 1981, Amer. Meteor. Soc., Boston, MA 02108, pp. 36-42.
- Courant, R., and D. Hilbert, 1962. Methods of Mathematical Physics, Vol. 2. Wiley-Interscience, New York, 830 pp.
- Cressman, G. P., 1959. An operational objective analysis system. Mon. Wea. Rev., 87, 367-374.
- Daley, R., 1978. Variational non-linear normal mode initialization. Tellus, 30, 201-218.
- Daley, R., 1981. The normal mode approach to the initialization problem. In: Bengtsson et al. (1981), pp. 77-109.
- Davis, M. H. A., 1977. Linear Estimation and Stochastic Control. Halsted Press, John Wiley and Sons, New York, 224 pp.
- Davis, P. J., 1979. Circulant Matrices. Wiley-Interscience, New York, 250 pp.
- Dickinson, R. E., and D. L. Williamson, 1972. Free oscillations of a discrete stratified fluid with applications to numerical weather prediction. J. Atmos. Sci., 29, 623-640.
- Dutton, J. A., 1976. The Ceaseless Wind. McGraw-Hill, New York, 579 pp.
- Eliassen, A., 1954. Provisional report on calculation of spatial covariance and autocorrelation of the pressure field. Videnskaps-Akademiets Institutt for Vaer-Og Klimaforskning, Oslo, Norway, Report No. 5. Reprinted in: Bengtsson et al. (1981), pp. 319-330.
- Fleming, R. J., T. M. Kaneshige, and W. E. McGovern, 1979a. The global weather experiment I. The observational phase through the first special observing period. Bull. Amer. Meteor. Soc., 60, 649-659.
- Fleming, R. J., T. M. Kaneshige, W. E. McGovern, and T. E. Bryan, 1979b. The global weather experiment II. The second special observing period. Bull. Amer. Meteor. Soc., 60, 1316-1322.
- Gandin, L. S., 1963. Objective Analysis of Meteorological Fields. Gidrometeor. Izdat., Leningrad. English translation by: Israel Program for Scientific Translations, Jerusalem, 1965, 242 pp. [NTIS N6618047, Library of Congress QC996. G3313.]

- Gelb, A. (ed.), 1974. Applied Optimal Estimation. The M.I.T. Press, Cambridge, MA, 374 pp.
- Ghil, M., S. Cohn, J. Tavantzis, K. Bube, and E. Isaacson, 1981. Applications of estimation theory to numerical weather prediction. In: Bengtsson et al. (1981), pp. 139-224.
- Gustavsson, N., 1981. A review of methods for objective analysis. In: Bengtsson et al. (1981), pp. 17-76.
- Halmos, P. R., 1958. Finite-Dimensional Vector Spaces, 2nd ed. D. Van Nostrand Company, Princeton, NJ, 200 pp.
- Haltiner, G. J., and R. T. Williams, 1980. Numerical Prediction and Dynamic Meteorology. Wiley, New York, 477 pp.
- Holton, J. R., 1972. An Introduction to Dynamic Meteorology. Academic Press, New York, 319 pp.
- Isaacson, E., and H. B. Keller, 1966. Analysis of Numerical Methods. Wiley, New York, 541 pp.
- Jazwinski, A. H., 1970. Stochastic Processes and Filtering Theory. Academic Press, New York, 376 pp.
- John, F., 1978. Partial Differential Equations, 3rd ed. Applied Mathematical Sciences Series, Vol. 1, Springer-Verlag, New York, 198 pp.
- Kalman, R. E., 1960. A new approach to linear filtering and prediction problems. Trans. ASME, Ser. D, J. Basic Eng., 82, 35-45.
- Kalman, R. E., and R. S. Bucy, 1961. New results in linear filtering and prediction theory. Trans. ASME, Ser. D, J. Basic Eng., 83, 95-108.
- Kasahara, A., 1981. Corrigendum. J. Atmos. Sci., 38, 2284-2285.
- Kreiss, H., and J. Oliger, 1973. Methods for the Approximate Solution of Time Dependent Problems. GARP Publications Series, No. 10, World Meteorological Organization - International Council of Scientific Unions, Geneva 20, Switzerland, 107 pp.
- Leith, C. E., 1980. Nonlinear normal mode initialization and quasi-geostrophic theory. J. Atmos. Sci., 37, 958-968.
- Leith, C. E., and R. H. Kraichnan, 1972. Predictability of turbulent flows. J. Atmos. Sci., 29, 1041-1058.
- Lorenc, A., 1981. A global three-dimensional multivariate statistical interpolation scheme. Mon. Wea. Rev., 109, 701-721.

- Lorenz, E. N., 1969a. Atmospheric predictability as revealed by naturally occurring analogues. J. Atmos. Sci., 26, 636-646.
- Lorenz, E. N., 1969b. The predictability of a flow which possesses many scales of motion. Tellus, 21, 289-307.
- Machenhauer, B., 1977. On the dynamics of gravity oscillations in a shallow water model, with applications to non-linear normal mode initialization. Beitrage zur Physik der Atmosphere, 50, 253-271.
- Maine, R. E., and K. W. Iliff, 1981. Formulation and implementation of a practical algorithm for parameter estimation with process and measurement noise. SIAM J. Appl. Math., 41, 558-579.
- McPherson, R. D., K. H. Bergman, R. E. Kistler, G. E. Rasch, and D. S. Cordon, 1979. The NMC operational global data assimilation system. Mon. Wea. Rev., 107, 1445-1461.
- Nering, E. D., 1970. Linear Algebra and Matrix Theory, 2nd ed. Wiley, New York, 352 pp.
- Ohap, R. F., and A. R. Stubberud, 1976. Adaptive minimum variance estimation in discrete-time linear systems. In: C. T. Leondes (ed.), Control and Dynamic Systems, Vol. 12, Academic Press, New York, pp. 583-624.
- Paige, C. C., and M. A. Saunders, 1977. Least squares estimation of discrete linear dynamic systems using orthogonal transformations. SIAM J. Numer. Anal., 14, 180-193.
- Palmén, E., and C. W. Newton, 1969. Atmospheric Circulation Systems. Academic Press, New York, 603 pp.
- Pedlosky, J., 1979. Geophysical Fluid Dynamics. Springer-Verlag, New York, 624 pp.
- Petersen, D. P., 1973. Transient suppression in optimal sequential analysis. J. Appl. Meteor., 12, 437-440.
- Phillips, N. A., 1981. Variational analysis and the slow manifold. Mon. Wea. Rev., 109, 2415-2426.
- Richtmyer, R. D., and K. W. Morton, 1967. Difference Methods for Initial-Value Problems, 2nd ed. Wiley-Interscience, New York, 405 pp.
- Rutherford, I. D., 1973. Experiments on the updating of PE forecasts with real wind and geopotential data. Preprints Third Conf. Probability and Statistics in Atmospheric Sciences, Boulder, CO, Amer. Meteor. Soc., Boston, MA 02108, pp. 198-201.
- Rutherford, I. D., 1976. An operational three-dimensional multivariate statistical objective analysis scheme. GARP Rep. No. 11, Proc. JOC Study Group Conf. Four-Dimensional Data Assimilation, Paris, 17-21 November 1975, pp. 98-121.

- Schlatter, T. W., 1975. Some experiments with a multivariate statistical objective analysis scheme. Mon. Wea. Rev., 103, 246-257.
- Schlatter, T. W., G. W. Branstator, and L. G. Thiel, 1976. Testing a global multivariate statistical objective analysis scheme with observed data. Mon. Wea. Rev., 104, 765-783.
- Talagrand, O., 1977. Contribution à l'assimilation quadri-dimensionnelle d'observations météorologiques. Doctoral Thesis, Université Pierre-et-Marie Curie, Paris.
- Talagrand, O., 1981. A study of the dynamics of four-dimensional data assimilation. Tellus, 33, 43-60.
- Williamson, D. L., 1976. Normal mode initialization procedure applied to forecasts with the global shallow water equations. Mon. Wea. Rev., 104, 195-206.
- Williamson, D. L., and R. E. Dickinson, 1976. Free oscillations of the NCAR global circulation model. Mon. Wea. Rev., 104, 1372-1391.
- Williamson, D. L., and A. Kasahara, 1971. Adaptation of meteorological variables forced by updating. J. Atmos. Sci., 28, 1313-1324.

APPENDIX

PROOFS OF RESULTS IN CHAPTER 5

Before proving the lemmas of Section 5.2, we review some elementary notions concerning subspaces. The span of a set of vectors  $\{\underline{x}_1, \underline{x}_2, \dots, \underline{x}_r\}$ , denoted by  $\langle \underline{x}_1, \underline{x}_2, \dots, \underline{x}_r \rangle$ , is the set of all linear combinations of the vectors. Let  $S \neq \{0\}$  be a subspace of  $R^n$ . There exists a set of linearly independent vectors  $\{\underline{x}_1, \underline{x}_2, \dots, \underline{x}_s\}$  such that

$$S = \langle \underline{x}_1, \underline{x}_2, \dots, \underline{x}_s \rangle ;$$

any such set is called a basis for  $S$ , and every such set consists of the same number of vectors. That number is called the dimension of  $S$ ,  $\dim S = s > 0$ ;  $\dim S \equiv 0$  if  $S = \{0\}$ .

If  $V$  is a symmetric  $n \times n$  matrix which is positive definite on  $S$ ,  $\underline{x}^T V \underline{x} > 0$  for all nonzero  $\underline{x} \in S$ , then there exists a V-orthonormal basis for  $S$ , i.e., a basis  $\{\underline{y}_1, \underline{y}_2, \dots, \underline{y}_s\}$  consisting of vectors which satisfy

$$\underline{y}_i^T V \underline{y}_j = \delta_{ij} , \text{ for } i, j = 1, \dots, s.$$

If  $\{\underline{x}_1, \underline{x}_2, \dots, \underline{x}_s\}$  is any basis for  $S$ , then the Gram-Schmidt process,

$$\underline{y}_1 = \underline{x}_1 / \sqrt{\underline{x}_1^T V \underline{x}_1}, \quad (\text{A.1a})$$

$$\underline{y}_j = \underline{w}_j / \sqrt{\underline{w}_j^T V \underline{w}_j}, \quad j=2, \dots, s, \quad (\text{A.1b})$$

where

$$\underline{w}_j = \underline{x}_j - \sum_{i=1}^{j-1} (\underline{y}_i^T V \underline{x}_j) \underline{y}_i , \quad (\text{A.1c})$$

produces a V-orthonormal basis  $\{y_1, y_2, \dots, y_s\}$  for  $S$ . An I-orthonormal basis is referred to simply as an orthonormal basis.

If  $S_1$  is a subspace of  $S$ , we denote by  $S_1^\perp$  the orthogonal complement of  $S_1$  in  $S$ , i.e., the set of all vectors in  $S$  which are orthogonal to every vector in  $S_1$ :

$$S_1^\perp = \{y \in S: y^T z = 0 \text{ for all } z \in S_1\}. \quad (\text{A.2})$$

It is a fact that  $S_1^\perp$  is a subspace of  $S$  and that

$$S_1 \cap S_1^\perp = \{0\}, \quad S_1 + S_1^\perp = S; \quad (\text{A.3a,b})$$

by the sum of two subspaces,  $S_1 + S_2$ , we mean the set of vectors of the form  $z_1 + z_2$  with  $z_1 \in S_1$ ,  $z_2 \in S_2$ . Since

$$\dim (S_1 + S_2) = \dim S_1 + \dim S_2 - \dim (S_1 \cap S_2)$$

for any two subspaces  $S_1, S_2$ , Eqs. (A.3) imply that if  $\dim S_1 = q \geq 0$  then  $\dim S_1^\perp = s - q$ . A sum of complementary subspaces is said to be direct: Eqs. (A.3a,b) together imply that in fact every vector  $z \in S$  can be uniquely expressed in the form  $z = z_1 + z_2$  where  $z_1 \in S_1$  and  $z_2 \in S_1^\perp$ .

For further reference see, for example, Nering (1970, especially Secs. 1.3, 1.4, 4.4, 5.1, 5.4).

#### A.1. Proof of Lemma 1

We give a constructive proof. The construction will be used in the proof of Lemma 4, and serves as a model for the proof of Theorem 2.

ORIGINAL PAGE IS  
OF POOR QUALITY

-147-

If  $S = \{0\}$ , then  $\Pi = 0$  is a  $V$ -orthogonal projection onto  $S$  for all  $V$ . We therefore assume  $S \neq \{0\}$ , so that  $\dim S = s > 0$ .

Let  $S_1 = S \cap \text{Ker } V$ , with  $\dim S_1 = q$ , and let  $S_1^\perp$  be the orthogonal complement of  $S_1$  in  $S$ , defined by Eq. (A.2);  $\dim S_1^\perp = s - q$ . For now we assume  $q > 0$  and  $s - q > 0$ ; we return later to the case in which  $q = 0$  or  $s - q = 0$ . We show that the required projection can be expressed as the sum of two projections, one onto  $S_1$  and one onto  $S_1^\perp$ .

First we show that

$$y^T V y > 0 \text{ for all nonzero } y \in S_1^\perp. \quad (\text{A.4})$$

We have

$$\begin{aligned} S_1^\perp \cap \text{Ker } V &= (S \cap S_1^\perp) \cap \text{Ker } V \\ &= S_1^\perp \cap (S \cap \text{Ker } V) \\ &= S_1^\perp \cap S_1 = \{0\}, \end{aligned}$$

so  $V y \neq 0$  for all nonzero  $y \in S_1^\perp$ . Factoring  $V$  as  $V = V_1^T V_1$ , we therefore have  $V_1 y \neq 0$ , so that  $y^T V y = (V_1 y)^T (V_1 y) \neq 0$ , from which (A.4) follows since  $V$  is positive semidefinite.

It follows from (A.4) that there exists a  $V$ -orthonormal basis for  $S_1^\perp$ ,

$$S_1^\perp = \langle y_1, y_2, \dots, y_{s-q} \rangle, \quad (\text{A.5a})$$

$$y_i^T V y_j = \delta_{ij}, \quad i, j = 1, \dots, s - q. \quad (\text{A.5b})$$

We now define

$$\Pi_V = \sum_{i=1}^{s-q} y_i y_i^T V, \quad (\text{A.6})$$

and show that  $\Pi_V$  is a  $V$ -orthogonal projection onto  $S_1^\perp$ .

Range  $\Pi_V \subset S_1^\perp$ . If  $\underline{x} \in R^n$  then

$$\Pi_V \underline{x} = \sum_{i=1}^{s-q} (\underline{y}_i^T \underline{v} \underline{x}) \underline{y}_i \in S_1^\perp,$$

by Eqs. (A.6, A.5a).

Range  $\Pi_V \supset S_1^\perp$ . We want to show that if  $\underline{y} \in S_1^\perp$ , then there is a vector  $\underline{x} \in R^n$  such that  $\Pi_V \underline{x} = \underline{y}$ . In fact,  $\underline{x} = \underline{y}$  is such a vector, because from Eq. (A.5a) we have

$$\underline{y} = \sum_{j=1}^{s-q} \alpha_j \underline{y}_j$$

for some scalars  $\alpha_j$ , whence Eqs. (A.6, A.5b) give

$$\begin{aligned} \Pi_V \underline{y} &= \sum_{i=1}^{s-q} \sum_{j=1}^{s-q} \alpha_j \underline{y}_i \underline{y}_i^T \underline{v} \underline{y}_j \\ &= \sum_{i=1}^{s-q} \sum_{j=1}^{s-q} \alpha_j \underline{y}_i \delta_{ij} = \underline{y}. \end{aligned}$$

$\Pi_V^2 = \Pi_V$ . From Eqs. (A.6, A.5b) we have

$$\begin{aligned} \Pi_V^2 &= \sum_{i=1}^{s-q} \underline{y}_i \underline{y}_i^T \underline{v} \sum_{j=1}^{s-q} \underline{y}_j \underline{y}_j^T \underline{v} \\ &= \sum_{i=1}^{s-q} \underline{y}_i \sum_{j=1}^{s-q} \delta_{ij} \underline{y}_j^T \underline{v} = \Pi_V. \end{aligned}$$

$(V \Pi_V)^T = V \Pi_V$ . From Eq. (A.6) we have

$$(V \Pi_V)^T = \left( \sum_{i=1}^{s-q} \underline{v} \underline{y}_i \underline{y}_i^T \underline{v} \right)^T$$



ORIGINAL PAGE IS  
OF POOR QUALITY

-149-

$$= \sum_{i=1}^{s-q} v^T x_i x_i^T v = v^T \Pi_V ,$$

and the result follows since  $V^T = V$ .

Having shown that  $\Pi_V$  is a  $V$ -orthogonal projection onto  $S_1^1$ , we now let  $\{z_1, z_2, \dots, z_q\}$  be an orthonormal basis for  $S_1$ ,

$$S_1 = \langle z_1, z_2, \dots, z_q \rangle, \quad (\text{A.7a})$$

$$z_i^T z_j = \delta_{ij}, \quad i, j = 1, \dots, q, \quad (\text{A.7b})$$

and we define

$$\Pi_I = \sum_{i=1}^q z_i z_i^T. \quad (\text{A.8})$$

From the proof that  $\Pi_V$  is a  $V$ -orthogonal projection onto  $S_1^1$ , it is clear that  $\Pi_I$  is an  $(I-)$  orthogonal projection onto  $S_1$ .

Defining further

$$\Pi = \Pi_V + \Pi_I, \quad (\text{A.9})$$

we show that  $\Pi$  is a  $V$ -orthogonal projection onto  $S$ . We will make use of the facts that

$$x_i^T z_j = 0, \quad i = 1, \dots, s-q, \quad j = 1, \dots, q, \quad (\text{A.10a})$$

and

$$V z_i = 0, \quad i = 1, \dots, q; \quad (\text{A.10b})$$

the former equality follows from the definition of  $S_1^1$ , Eq. (A.2), while the latter follows from the fact that  $S_1 = S \cap \text{Ker } V$  is a subset of  $\text{Ker } V$ .

Range  $\Pi \subset S$ . If  $\underline{x} \in R^n$  then

$$\Pi \underline{x} = \Pi_V \underline{x} + \Pi_I \underline{x} \in S_1^\perp + S_1 ,$$

since  $\Pi_V \underline{x} \in S_1^\perp$  and  $\Pi_I \underline{x} \in S_1$  , and the result follows since  $S_1^\perp + S_1 = S$ , Eq. (A.3b).

Range  $\Pi \supset S$ . Suppose  $\underline{w} \in S$ . We show that  $\Pi \underline{w} = \underline{w}$ . According to Eq. (A.3b), there is a vector  $\underline{y} \in S_1^\perp$  and a vector  $\underline{z} \in S_1$  such that  $\underline{w} = \underline{y} + \underline{z}$ . Now  $\Pi_V \underline{z} = 0$  by Eqs. (A.6, A.7a, A.10b), and  $\Pi_I \underline{y} = 0$  by Eqs. (A.5a, A.8, A.10a). Therefore

$$\Pi \underline{w} = (\Pi_V + \Pi_I)(\underline{y} + \underline{z}) = \Pi_V \underline{y} + \Pi_I \underline{z} .$$

But  $\Pi_V \underline{y} = \underline{y}$  according to the proof that  $\text{Range } \Pi_V \supset S_1^\perp$ ; similarly,  $\Pi_I \underline{z} = \underline{z}$ . Therefore  $\Pi \underline{w} = \underline{y} + \underline{z} = \underline{w}$  .

$\Pi^2 = \Pi$ . Suppose  $\underline{x} \in R^n$ , and let  $\underline{w} = \Pi \underline{x}$ . Then  $\underline{w} \in S$ , since  $\text{Range } \Pi \subset S$ , and  $\Pi \underline{w} = \underline{w}$ , according to the proof that  $\text{Range } \Pi \supset S$ . Therefore

$$\Pi^2 \underline{x} = \Pi \underline{w} = \underline{w} = \Pi \underline{x} ,$$

i.e.,  $\Pi^2 \underline{x} = \Pi \underline{x}$  for all  $\underline{x} \in R^n$ , and therefore  $\Pi^2 = \Pi$ .

$(\Pi_V)^T = \Pi_I$ . From Eqs. (A.8, A.10b), it follows that  $\Pi_I = 0$ . Therefore  $\Pi = \Pi_V$  , and the result follows since we already showed that  $(\Pi_V)^T = \Pi_I$ .

This concludes the proof in case  $q > 0$  and  $s-q > 0$ . In summary, starting from arbitrary bases for  $S_1$  and  $S_1^\perp$ , one could use the

Gram-Schmidt process (A.1) to construct the bases in Eqs. (A.5, A.7), and then construct the projection  $\Pi$  by means of Eqs. (A.6, A.8, A.9).

In case  $q = 0$ , i.e.,  $S_1 = \{0\}$ , Eq. (A.3b) implies that  $S_1^\perp = S$  and  $\dim S_1^\perp = s - q = s > 0$ , so that  $\Pi_V$  in Eq. (A.6) is a  $V$ -orthogonal projection onto  $S$ . Similarly, if  $s - q = 0$ , then  $\Pi_I$  in Eq. (A.8) is a  $V$ -orthogonal projection onto  $S$ , for all  $V$ .

#### A.2. Proof of Lemma 2

Sufficiency. Let  $\Pi$  and  $\Lambda$  be two  $V$ -orthogonal projections onto  $S$ , and let  $\Delta = \Pi - \Lambda$ . We show that if  $S \cap \text{Ker } V = \{0\}$ , then  $\Delta = 0$ .

If  $\underline{x} \in \mathbb{R}^n$ , then  $\Lambda \underline{x} \in S$ , so Eq. (5.2) implies that  $\Pi \Lambda \underline{x} = \Lambda \underline{x}$ . Since  $\underline{x}$  is arbitrary, we have

$$\Pi \Lambda = \Lambda,$$

and similarly,

$$\Lambda \Pi = \Pi.$$

Therefore,

$$\Delta = \Pi - \Lambda = \Lambda \Pi - \Lambda = \Lambda(\Pi - I),$$

and

$$V\Delta = V\Lambda(\Pi - I).$$

We also have

$$\begin{aligned} V\Lambda &= (V\Lambda)^T = \Lambda^T V = (\Pi\Lambda)^T V \\ &= \Lambda^T \Pi^T V = \Lambda^T (V\Pi)^T = \Lambda^T V\Pi, \end{aligned}$$

so that

ORIGINAL PAGE IS  
OF POOR QUALITY

-152-

$$V\Delta = \Lambda^T V \Pi (\Pi - I) = \Lambda^T V (\Pi^2 - \Pi) = 0,$$

and therefore  $\Delta \underline{x} \in \text{Ker } V$  for every  $\underline{x} \in R^n$ . But  $\Delta \underline{x} = \Pi \underline{x} - \Lambda \underline{x} \in S$  for every  $\underline{x} \in R^n$ , since  $\Pi \underline{x} \in S$  and  $\Lambda \underline{x} \in S$  and  $S$  is a subspace. Therefore  $\Delta \underline{x} \in S \cap \text{Ker } V = \{0\}$ . That is,  $\Delta \underline{x} = 0$  for all  $\underline{x} \in R^n$ , whence  $\Delta = 0$ .

Necessity. Suppose that  $S \cap \text{Ker } V \neq \{0\}$  and let  $\Pi$  be a  $V$ -orthogonal projection onto  $S$ . We construct a matrix  $\Lambda \neq \Pi$  which is also a  $V$ -orthogonal projection onto  $S$ .

Let  $\underline{y} \in R^n$  be any nonzero vector such that  $\underline{y}^T \underline{w} = 0$  for all  $\underline{w} \in S$ , i.e.,  $\underline{y} \neq 0$  and  $\underline{y} \in S^\perp$ , the orthogonal complement of  $S$  in  $R^n$ . There are many such vectors  $\underline{y}$ : letting  $\dim S = s$ , Eqs. (A.3) imply that  $\dim S^\perp = n-s > 0$ , since  $S$  is a proper subspace of  $R^n$ .

Let  $\underline{z} \in S \cap \text{Ker } V$  with  $\underline{z} \neq 0$ . We claim that

$$\Lambda = \Pi + \underline{z} \underline{y}^T$$

is a  $V$ -orthogonal projection onto  $S$ . Obviously  $\Lambda \neq \Pi$ , since both  $\underline{y}$  and  $\underline{z}$  are nonzero.

Range  $\Lambda \subset S$ . If  $\underline{x} \in R^n$ , then

$$\Lambda \underline{x} = \Pi \underline{x} + (\underline{y}^T \underline{x}) \underline{z} \in S,$$

since  $\Pi \underline{x} \in S$ ,  $\underline{z} \in S$ , and  $S$  is a subspace.

Range  $\Lambda \supset S$ . Let  $\underline{w} \in S$ , so that  $\Pi \underline{w} = \underline{w}$ . We have also  $\underline{y}^T \underline{w} = 0$ , since  $\underline{y} \in S^\perp$ . Therefore

$$\Lambda \underline{w} = \Pi \underline{w} + (\underline{y}^T \underline{w}) \underline{z} = \underline{w},$$

ORIGINAL PAGE IS  
OF POOR QUALITY

-153-

i.e.,  $\Lambda \underline{x} = \underline{w}$  has solution  $\underline{x} = \underline{w}$  for all  $\underline{w} \in S$ .

$\Lambda^2 = \Lambda$ . As in the proof that  $\Pi^2 = \Pi$  in the proof of Lemma 1, Range  $\Lambda \subset S$  and  $\Lambda \underline{w} = \underline{w}$  for all  $\underline{w} \in S$  together imply that  $\Lambda^2 = \Lambda$ .

$(V\Lambda)^T = V\Lambda$ . We have

$$V\Lambda = V\Pi + (V\underline{z})\underline{v}^T = V\Pi$$

since  $\underline{z} \in \text{Ker } V$ , and the result follows since  $(V\Pi)^T = V\Pi$ .

A.3. Proof of Lemma 3

We show that the general solution of problem (5.5) is given by

$$\underline{x} = \Pi \underline{y} + \underline{z}, \quad (\text{A.11a})$$

where  $\Pi$  is any  $V$ -orthogonal projection onto  $S$  (such projections exist, by Lemma 1), and where  $\underline{z}$  is any vector such that

$$\underline{z} \in S \cap \text{Ker } V. \quad (\text{A.11b})$$

The lemma follows immediately from this result, for if  $S \cap \text{Ker } V = \{0\}$  then  $\underline{z} = 0$  and, according to Lemma 2,  $\Pi$  is unique, while if  $S \cap \text{Ker } V \neq \{0\}$  then neither  $\underline{z}$  nor  $\Pi$  is unique.

Let  $\Pi$  be a fixed  $V$ -orthogonal projection onto  $S$ , and define  $\gamma = \gamma(\underline{x})$  by

$$\gamma(\underline{x}) = (\underline{x} - \underline{y})^T V(\underline{x} - \underline{y}).$$

We have

ORIGINAL PAGE IS  
OF POOR QUALITY

-154-

$$\begin{aligned}\gamma(\underline{x}) &= [(\underline{x} - \Pi \underline{y}) + (\Pi \underline{y} - \underline{y})]^T V [(\underline{x} - \Pi \underline{y}) + (\Pi \underline{y} - \underline{y})] \\ &= (\underline{x} - \Pi \underline{y})^T V (\underline{x} - \Pi \underline{y}) + (\Pi \underline{y} - \underline{y})^T V (\Pi \underline{y} - \underline{y}) + 2(\underline{x} - \Pi \underline{y})^T V (\Pi \underline{y} - \underline{y}).\end{aligned}$$

The last term vanishes if  $\underline{x} \in S$ , for then  $\underline{x} = \Pi \underline{x}$  by Eq. (5.2), whence

$$\begin{aligned}(\underline{x} - \Pi \underline{y})^T V (\Pi \underline{y} - \underline{y}) &= (\Pi \underline{x} - \Pi \underline{y})^T V (\Pi \underline{y} - \underline{y}) \\ &= (\underline{x} - \underline{y})^T \Pi^T V (\Pi - I) \underline{y} = 0;\end{aligned}$$

the last equality follows from Eqs. (5.1b, 5.3) and the fact that  $V$  is symmetric,

$$\begin{aligned}\Pi^T V (\Pi - I) &= (V \Pi)^T (\Pi - I) = V \Pi (\Pi - I) \\ &= V (\Pi^2 - \Pi) = 0.\end{aligned}\tag{A.12}$$

Defining  $\underline{z} = \underline{z}(\underline{x})$  by

$$\underline{z} = \underline{x} - \Pi \underline{y},\tag{A.13}$$

we therefore have

$$\gamma(\underline{x}) = \underline{z}^T V \underline{z} + \beta \quad \text{if } \underline{x} \in S,$$

where

$$\beta = (\Pi \underline{y} - \underline{y})^T V (\Pi \underline{y} - \underline{y})$$

is independent of  $\underline{x}$ . Now  $\underline{z}^T V \underline{z} \geq 0$  since  $V$  is positive semidefinite, so

$$\gamma(\underline{x}) \geq \beta \quad \text{if } \underline{x} \in S.$$

Therefore  $\underline{x}$  is a solution of problem (5.5) if and only if

$$\gamma(\underline{x}) = \beta \quad \text{and} \quad \underline{x} \in S,$$

and this is the case if and only if

$$\underline{z}^T V \underline{z} = 0 \quad \text{and} \quad \underline{z} \in S; \quad (\text{A.14})$$

that the statements  $\underline{x} \in S$  and  $\underline{z} \in S$  are equivalent follows from (A.13) and the fact that  $S$  is a subspace.

The first condition in (A.14) is equivalent to  $\underline{z} \in \text{Ker } V$ , for if  $\underline{z}^T V \underline{z} = 0$  then, factoring  $V$  as  $V = V_1^T V_1$ , we have  $(V_1 \underline{z})^T (V_1 \underline{z}) = 0$ , whence  $V_1 \underline{z} = 0$  and  $V \underline{z} = V_1^T V_1 \underline{z} = 0$ ; obviously  $V \underline{z} = 0$  implies  $\underline{z}^T V \underline{z} = 0$ . Conditions (A.14) are therefore equivalent to (A.11b), so  $\underline{x}$  is a solution of problem (5.5) if and only if it is of the form (A.11), where  $\Pi$  is any  $V$ -orthogonal projection onto  $S$ .

#### A.4. Proof of Lemma 4

Let  $s = \dim S$ , and let  $C$  be an  $n \times s$  matrix whose  $s$  columns are an orthonormal basis for  $S$ ,

$$C = [\underline{w}_1, \underline{w}_2, \dots, \underline{w}_s], \quad \underline{w}_i^T \underline{w}_j = \delta_{ij}.$$

The  $(i, j)^{\text{th}}$  element of the matrix  $C^T C$  is  $\underline{w}_i^T \underline{w}_j$ , and therefore

$$C^T C = I. \quad (\text{A.15a})$$

We have also

$$C C^T = \sum_{i=1}^s \underline{w}_i \underline{w}_i^T$$

-156-

which, according to the proof of Lemma 1, is an orthogonal projection onto S. Since there is only one such projection, we therefore have

$$\Pi_I = CC^T. \quad (A.15b)$$

Now define

$$C_V = V^{-1/2}C.$$

From Eqs. (5.7), we have

$$(V^{-1/2})^T V V^{-1/2} = I,$$

and therefore

$$\begin{aligned} C_V^T V C_V &= (V^{-1/2}C)^T V (V^{-1/2}C) \\ &= C^T [(V^{-1/2})^T V V^{-1/2}] C \\ &= C^T C \\ &= I; \end{aligned}$$

that is, the columns of  $C_V$  are a V-orthonormal basis for S.

According to the proof of Lemma 1, and analogously with Eqs. (A.15), the matrix  $C_V C_V^T V$  is therefore a V-orthogonal projection onto S. There is only one such projection since V is positive definite, so

$$\Pi_V = C_V C_V^T V.$$

But then

$$\begin{aligned} \Pi_V &= (V^{-1/2} C) (V^{-1/2} C)^T V \\ &= V^{-1/2} C C^T (V^{-1/2})^T V \\ &= V^{-1/2} \Pi_I (V^{-1/2})^T V \\ &= V^{-1/2} \Pi_I V^{1/2}, \end{aligned}$$

since  $(V^{-1/2})^T V = V^{1/2}$ .



#### A.5. Proof of Theorem 1

The proof is similar to that of Lemma 3. The uniqueness part of the theorem follows immediately from Lemma 2. If  $A$  satisfies Eq. (5.21), then  $L_k = 0$  according to Eq. (5.20), and Lemma 2 implies uniqueness of the  $A$ -orthogonal projection,  $\Pi_k = \Pi$ ;  $K_k$  in Eq. (5.18) is therefore uniquely determined. On the other hand, if  $A$  does not satisfy Eq. (5.21), then  $\Pi_k$  and  $L_k$ , and therefore  $K_k$  and  $w_k^A$ , are not uniquely determined.

It therefore remains only to verify that the general solution of problem (5.17) is given by Eq. (5.18). We omit subscripts in the remainder of the proof; an observation time  $k$  is assumed.

Let  $\Pi$  be a fixed  $A$ -orthogonal projection matrix onto  $R$ ; that such a matrix exists is a consequence of Lemma 1. The constraint (5.17b) states that each column of  $K$  must lie in  $R$ , so it follows from Eq. (5.2) that the constraint is equivalent to requiring

$$\Pi K = K. \quad (A.16)$$

Indicating the dependence of  $n$  upon  $K$  by writing  $n = n(K)$ , we find a simple formula for  $n(\Pi K)$  from which, with Eq. (A.16), the general solution (5.18) will follow.

From Eq. (2.16), we have

$$n(\Pi K) = \text{trace} [A(\Pi K - K^{KB})C(\Pi K - K^{KB})^T + AZ], \quad (A.17)$$

where, according to Eqs. (2.14b, 2.15b, 2.20a),

$$C = HP^f H^T + R,$$

ORIGINAL PAGE IS  
OF POOR QUALITY

-158-

$$Z = P^f - P^f H^T C^{-1} H P^f ,$$

$$K^{KB} = P^f H^T C^{-1} .$$

We now show that Eq. (A.17) can be written

$$\begin{aligned} n(\Pi K) &= \text{trace } A[\Pi(K - K^{KB})] C[\Pi(K - K^{KB})]^T \\ &+ \text{trace } A[(I - \Pi)K^{KB}] C[(I - \Pi)K^{KB}]^T + \text{trace } AZ \end{aligned} \quad (A.18)$$

We expand the first term in Eq. (A.17) as,

$$\begin{aligned} A(\Pi K - K^{KB}) C(\Pi K - K^{KB})^T &= A[\Pi(K - K^{KB}) - (I - \Pi)K^{KB}] C[\Pi(K - K^{KB}) - (I - \Pi)K^{KB}]^T \\ &= A[\Pi(K - K^{KB})] C[\Pi(K - K^{KB})]^T + A[(I - \Pi)K^{KB}] C[(I - \Pi)K^{KB}]^T \\ &- A(I - \Pi)K^{KB} C(K - K^{KB})^T \Pi^T - A\Pi(K - K^{KB}) C(K^{KB})^T (I - \Pi)^T. \end{aligned} \quad (A.19)$$

Now,

$$\begin{aligned} \text{trace } A(I - \Pi)K^{KB} C(K - K^{KB})^T \Pi^T &= \text{trace } \Pi^T A(I - \Pi)K^{KB} C(K - K^{KB})^T \\ &= 0. \end{aligned} \quad (A.20a)$$

The first equality in (A.20a) follows from Eq. (2.11c), while the second follows from the fact that

$$\Pi^T A(I - \Pi) = 0 ;$$

cf. Eq. (A.12). Similarly, we have

$$\text{trace } A\Pi(K - K^{KB}) C(K^{KB})^T (I - \Pi)^T = 0. \quad (A.20b)$$

Inserting Eq. (A.19) into Eq. (A.17), and using Eqs. (A.20, 2.11b), yields Eq. (A.18).

The last two terms in Eq. (A.18) are independent of  $K$ . Analogously to the argument following Eqs. (2.18, 2.19), it follows that  $\eta(\Pi K)$  is minimized with respect to  $K$  if and only if

$$A_1 \Pi (K - K^{KB}) = 0, \quad (A.21a)$$

where  $A$  has been factored as  $A = A_1^T A_1$ . If Eq. (A.21a) holds, then

$$A \Pi (K - K^{KB}) = 0. \quad (A.21b)$$

On the other hand, if (A.21b) holds, then the first term on the right-hand side of Eq. (A.18) vanishes and  $\eta(\Pi K)$  is minimized: conditions (A.21a, A.21b) are equivalent. Therefore, a matrix  $K$  is a solution of problem (5.17) if and only if  $K$  satisfies Eqs. (A.16, A.21b), i.e., iff

$$\Pi K = K, \quad (A.22a)$$

$$A \Pi K = A \Pi K^{KB}. \quad (A.22b)$$

We seek solutions of Eqs. (A.22) of the form

$$K = \Pi K^{KB} + L, \quad (A.23)$$

where  $L$  is yet to be determined. Substituting Eq. (A.23) into Eqs. (A.22), and using Eq. (5.19b), we find that

$$\Pi L = L, \quad (\text{A.24a})$$

$$A \Pi L = 0. \quad (\text{A.24b})$$

Equation (A.24a) states that each column of  $L$  lies in  $R$ , and Eq. (A.24b) states that each column of  $\Pi L = L$  lies in the kernel of  $A$ ; that is, Eqs. (A.24) are equivalent to

$$\text{Range } L \subset R \cap \text{Ker } A. \quad (\text{A.25})$$

Equations (A.23, A.25), with  $\Pi$  being any  $A$ -orthogonal projection onto  $R$ , therefore represent the general solution of problem (5.17).

#### A.6. Proof of Lemma 5

If  $A$  is real then the submatrices  $A_j$  are real, and the formula

$$\hat{A}(\omega) = \sum_{j=-M/2+1}^{M/2} e^{2\pi i j \omega / M} A_j$$

immediately implies that the matrices  $\hat{A}(\omega)$  satisfy Eqs. (5.33a,b). Conversely, if the matrices  $\hat{A}(\omega)$  satisfy Eqs. (5.33a,b), then the inversion formula

$$A_j = \frac{1}{M} \sum_{\omega=-M/2+1}^{M/2} e^{-2\pi i j \omega / M} \hat{A}(\omega)$$

immediately implies that the  $A_j$  are real, and hence that  $A$  is real.

If  $A$  is symmetric and real, i.e.,  $A = A^T = A^*$ , then we have from  $\hat{A} = F A F^*$  that

$$\hat{A}^* = FA^*F^* = FAF^* = \hat{A} ,$$

which, with Eq. (5.30), implies Eq. (5.33c). Conversely, if Eqs. (5.33a,b,c) are satisfied, then  $A^T = A^*$ , as we have just shown, and  $\hat{A}^* = \hat{A}$ ; from  $A = F^*\hat{A}F$  we therefore have

$$A^T = A^* = F^*\hat{A}^*F = F^*\hat{A}F = A ,$$

i.e.,  $A$  is symmetric.

For positive semidefiniteness, it is clear from Eqs. (5.30, 5.32) that the following statements are equivalent:

$$\underline{x}^T A \underline{x} \geq 0, \quad \text{for all } \underline{x} \in R^n,$$

$$\underline{x}^T F^* \hat{A} F \underline{x} \geq 0, \quad \text{for all } \underline{x} \in R^n,$$

$$(F \underline{x})^* \hat{A} (F \underline{x}) \geq 0, \quad \text{for all } \underline{x} \in R^n,$$

$$\underline{y}^* \hat{A} \underline{y} \geq 0, \quad \text{for all } \underline{y} \text{ of the form } \underline{y} = F \underline{x}, \underline{x} \in R^n,$$

$$\underline{y}^*(\omega) \hat{A}(\omega) \underline{y}(\omega) \geq 0, \quad \text{for all complex 3-vectors } \underline{y}(\omega),$$

$$\text{and for all } \omega = -\frac{M}{2} + 1, \dots, \frac{M}{2}.$$

That the conditions in the last two statements are equivalent follows from the fact that if  $\underline{y} = F \underline{x}$  and  $\underline{x} \in R^n$  is arbitrary, then  $\underline{y}(\omega)$  is, for each  $\omega$ , an arbitrary complex 3-vector; conversely, if the last statement is true, then in particular it is true for arbitrary vectors satisfying  $\underline{y}(-\omega) = \overline{\underline{y}(\omega)}$  and  $\underline{y}(M/2) = \overline{\underline{y}(M/2)}$ , in which case  $\underline{x} = F^* \underline{y}$  is an arbitrary real  $n$ -vector.

A.7. Proof of Lemma 6

(5.39a)  $\Rightarrow$  (5.39b). Suppose there is an  $\omega$ , say  $\omega_*$ , such that

$$\hat{A}(\omega_*) \underline{r}_0(\omega_*) = 0 ;$$

we show that this implies  $R \cap \text{Ker } A \neq \{0\}$ . Suppose for now that  $\omega_* \neq M/2$ . Then from Eqs. (5.33a, 5.35a) we have also

$$\hat{A}(-\omega_*) \underline{r}_0(-\omega_*) = 0 .$$

Define the n-vector  $\underline{w} = F\hat{\underline{w}}$  by

$$\hat{\underline{w}}(\pm\omega_*) = \underline{r}_0(\pm\omega_*) ,$$

$$\hat{\underline{w}}(\omega) = 0 \text{ if } \omega \neq \pm\omega_* .$$

Then  $\underline{w} \neq 0$  and, according to Eq. (5.36), we have  $\underline{w} \in R$ . Clearly  $\hat{A}(\omega) \hat{\underline{w}}(\omega) = 0$  for all  $\omega$ , and therefore

$$0 = \hat{A}\hat{\underline{w}} = (FAF^*)(F\underline{w}) = F\underline{Aw} ,$$

whence  $\underline{Aw} = 0$  since  $F$  is nonsingular. Therefore  $\underline{w}$  is a nonzero vector in  $R \cap \text{Ker } A$ . If  $\omega_* = M/2$ , the same result obtains by setting

$$\hat{\underline{w}}(M/2) = \underline{r}_0(M/2) ,$$

$$\hat{\underline{w}}(\omega) = 0 \text{ if } \omega \neq M/2 .$$

-163-

(5.39b)  $\Rightarrow$  (5.39c). Suppose

$$\hat{A}(\omega) \underline{r}_0(\omega) \neq 0$$

for all  $\omega$ . Since  $\hat{A}^*(\omega) = \hat{A}(\omega)$  by Eq. (5.33c),  $\hat{A}(\omega)$  has a factorization

$$\hat{A}(\omega) = A_1^*(\omega) A_1(\omega).$$

Since  $\hat{A}(\omega) \underline{r}_0(\omega) \neq 0$ , we have  $A_1(\omega) \underline{r}_0(\omega) \neq 0$ , so

$$\underline{r}_0^*(\omega) \hat{A}(\omega) \underline{r}_0(\omega) = [A_1(\omega) \underline{r}_0(\omega)]^* [A_1(\omega) \underline{r}_0(\omega)] \neq 0,$$

which, according to Eq. (5.33d), implies that

$$\underline{r}_0^*(\omega) \hat{A}(\omega) \underline{r}_0(\omega) > 0.$$

(5.39c)  $\Rightarrow$  (5.39a). Suppose that  $R \cap \text{Ker } A \neq \{0\}$ ; we show that there is an  $\omega$  for which (5.39c) does not hold. Let

$$\underline{w} \in R \cap \text{Ker } A$$

with  $\underline{w} \neq 0$ . Since  $\underline{w} \in R$ , Eq. (5.36) implies that there is an  $\omega$ , say  $\omega_*$ , such that  $\hat{\underline{w}}(\omega_*) = \beta \underline{r}_0(\omega_*)$  with  $\beta \neq 0$ . Since  $A\underline{w} = 0$ , we have

$$\hat{\hat{\underline{w}}} = (FAF^*)(F\underline{w}) = F\underline{w} = 0.$$

Therefore

ORIGINAL PAGE IS  
OF POOR QUALITY

-164-

$$\hat{A}(\omega_*) \underline{x}_0(\omega_*) = \frac{1}{\beta} \hat{A}(\omega_*) \hat{\underline{w}}(\omega_*) = 0 ,$$

whence

$$\underline{x}_0^*(\omega_*) \hat{A}(\omega_*) \underline{x}_0(\omega_*) = 0 .$$

#### A.8. Proof of Theorem 2

That there exists a unique A-orthogonal projection onto  $R$  follows from Lemma 2, so we need only verify that  $\Pi$  defined by Eqs. (5.41) is indeed an A-orthogonal projection. This  $\Pi$  is certainly block circulant since it is defined by  $\Pi = F^* \hat{\Pi} F$ , with  $\hat{\Pi}$  block-diagonal.

Range  $\Pi \subset R$ . Let  $\underline{w} \in R^n$  and let  $\underline{z} = \Pi \underline{w}$ ; we want to show that  $\underline{z} \in R$ . We have

$$\hat{\underline{z}} = F \underline{z} = F \Pi \underline{w} = (F \Pi F^*) (F \underline{w}) = \hat{\Pi} \hat{\underline{w}} ,$$

so

$$\hat{\underline{z}}(\omega) = \hat{\Pi}(\omega) \hat{\underline{w}}(\omega) = \beta_0(\omega) \underline{x}_0(\omega) ,$$

where, according to Eq. (5.41c),

$$\beta_0(\omega) = \alpha_\omega [\underline{x}_0^*(\omega) \hat{A}(\omega) \hat{\underline{w}}(\omega)] .$$

Now  $\alpha_\omega$  is real, according to Eqs. (5.39c, 5.41d), so from Eqs. (5.33a,b, 5.35, 5.37) it follows that

$$\beta_0(-\omega) = \overline{\beta_0(\omega)} , \quad \omega = 0, 1, \dots, M/2 - 1$$



ORIGINAL PAGE IS  
OF POOR QUALITY

-165-

$$\beta_0\left(\frac{M}{2}\right) = \overline{\beta_0\left(\frac{M}{2}\right)}.$$

According to Eq. (5.36), therefore, we have  $\underline{z} \in R$ .

Range  $\Pi \supset R$ . Let  $\underline{w} \in R$ ; we show that  $\Pi \underline{x} = \underline{w}$  has solution  $\underline{x} = \underline{w}$ . Since  $\underline{w} \in R$ , Eq. (5.36) implies that

$$\hat{\underline{w}}(\omega) = \beta_0(\omega) \underline{x}_0(\omega)$$

for some scalars  $\beta_0(\omega)$ , whence we have from Eqs. (5.41c,d) that

$$\begin{aligned} \hat{\Pi}(\omega) \hat{\underline{w}}(\omega) &= \alpha_\omega \beta_0(\omega) \underline{x}_0(\omega) \underline{x}_0^*(\omega) \hat{A}(\omega) \underline{x}_0(\omega) \\ &= \beta_0(\omega) \underline{x}_0(\omega) = \hat{\underline{w}}(\omega). \end{aligned}$$

Therefore  $\hat{\Pi} \hat{\underline{w}} = \hat{\underline{w}}$  and

$$\Pi \underline{w} = (F^* \hat{\Pi} F)(F^* \hat{\underline{w}}) = F^* \hat{\Pi} \hat{\underline{w}} = F^* \hat{\underline{w}} = \underline{w}.$$

$\Pi^2 = \Pi$ . It follows immediately from Eqs. (5.41c,d) that

$$[\hat{\Pi}(\omega)]^2 = \hat{\Pi}(\omega),$$

so  $\hat{\Pi}^2 = \hat{\Pi}$  and

$$\Pi^2 = (F^* \hat{\Pi} F)(F^* \hat{\Pi} F) = F^* \hat{\Pi}^2 F = F^* \hat{\Pi} F = \Pi.$$

$(A\Pi)^T = A\Pi$ . From Eq. (5.41c) we have

$$[\hat{A}(\omega) \hat{\Pi}(\omega)]^* = [\alpha_\omega \hat{A}(\omega) \underline{x}_0(\omega) \underline{x}_0^*(\omega) \hat{A}(\omega)]^*$$

ORIGINAL PAGE IS  
OF POOR QUALITY

-166-

$$= \alpha_{\omega} \hat{A}(\omega) \underline{r}_0(\omega) \underline{r}_0^*(\omega) \hat{A}(\omega) = \hat{A}(\omega) \hat{\Pi}(\omega);$$

the second equality follows since  $\alpha_{\omega}$  is real and, according to Eq. (5.33c),  $\hat{A}^*(\omega) = \hat{A}(\omega)$ . Therefore we have

$$(\hat{A}\hat{\Pi})^* = \hat{A}\hat{\Pi}.$$

It follows from Eqs. (5.33a,b,5.35,5.41c) that

$$\hat{\Pi}(-\omega) = \overline{\hat{\Pi}(\omega)}, \quad \omega = 0, 1, \dots, M/2 - 1$$

$$\hat{\Pi}(\frac{M}{2}) = \overline{\hat{\Pi}(\frac{M}{2})},$$

so  $\Pi$  is real; since  $A$  is also real we therefore have

$$(A\Pi)^T = (A\Pi)^*.$$

Then

$$\begin{aligned} (A\Pi)^T &= (A\Pi)^* = (F^* \hat{A} F F^* \hat{\Pi} F)^* = (F^* \hat{A} \hat{\Pi} F)^* \\ &= F^* (\hat{A} \hat{\Pi})^* F = F^* \hat{A} \hat{\Pi} F = (F^* \hat{A} F) (F^* \hat{\Pi} F) \\ &= A\Pi. \end{aligned}$$

$\omega$	$c_0$	$c_{-1}$	$c_1$
1	7.51	-255.77	308.26
2	14.14	-182.95	228.81
3	16.89	-166.88	209.99
4	18.12	-161.00	202.87
5	18.76	-158.22	199.46
6	19.12	-156.70	197.58
7	19.35	-155.78	196.43
8	19.50	-155.18	195.68

TABLE 1. Phase speeds of solutions of the continuous system, Eqs. (3.1,3.3), in meters per second. The phase speeds are given by Eq. (3.22a), and are presented here for the first eight wave numbers. The speeds  $c_0$  are the Rossby wave phase speeds, while  $c_{-1}$  and  $c_1$  are, respectively, the phase speeds of westward-propagating and eastward-propagating inertia-gravity waves.

$\omega$	$c_0$	$c_{-1}$	$c_1$
1	7.53	-255.99	308.45
2	14.15	-183.01	228.87
3	16.89	-166.90	210.01
4	18.13	-161.00	202.88
5	18.76	-158.23	199.47
6	19.12	-156.70	197.58
7	19.35	-155.78	196.43
8	19.50	-155.18	195.68

TABLE 2. As in Table 1, but using the approximate formulas (3.25).

$\omega$	$c_0$	$c_{-1}$	$c_1$
1	7.44	-248.92	301.31
2	13.12	-164.92	208.45
3	13.73	-133.39	171.52
4	11.98	-107.91	141.65
5	9.17	- 82.00	110.85
6	5.95	- 54.49	76.45
7	2.79	- 26.22	38.13
8	0.00	0.00	0.00

TABLE 3. As in Table 1, but for the discrete system, Eqs. (4.7). The phase speeds are given by Eq. (4.34), and are obtained by first solving the eigenvalue problem, Eq. (4.27), and then solving Eq. (4.28) for the eigenfrequencies.

RUN	$u_{SL}$	$v_{SL}$	$v_{HA}$	$v_{LN}$	$\phi_{SL}$	$\phi_{HA}$	$\phi_{LN}$
$A_{KB}$	.031	.070	.311	.214	.045	.210	.117
$A_0$	.127	.302	.390	.334	.220	.297	.313
$A_{1/2}$	.144	.174	.371	.358	.070	.261	.194
$A_1$	.153	.163	.385	.412	.059	.262	.180
$A_{3/2}$	.167	.165	.398	.457	.062	.272	.201
$A_2$	.184	.172	.410	.493	.065	.285	.235
$B_{KB}$	.074	.092	.317	.223	.064	.217	.127
$B_0$	.075	.265	.371	.303	.183	.283	.286
$B_{1/2}$	.074	.113	.364	.313	.068	.263	.198
$B_1$	.074	.100	.381	.363	.053	.267	.173
$B_{3/2}$	.074	.099	.394	.394	.051	.275	.170
$B_2$	.074	.100	.404	.412	.051	.284	.174

TABLE 4. Summary of rms analysis errors at 10 days, for runs  $A_{KB}$  ,  $A_\alpha$  ,  $B_{KB}$  , and  $B_\alpha$  , for  $\alpha = 0, 1/2, 1, 3/2, 2$ .

RUN	$u_{SL}$	$v_{SL}$	$v_{HA}$	$v_{LN}$	$\phi_{SL}$	$\phi_{HA}$	$\phi_{LN}$
$A_{KB}$	.031	.070	.311	.214	.045	.210	.117
$A_{2,0}$	.073	.096	.374	.282	.055	.259	.166
$B_{KB}$	.074	.092	.317	.223	.064	.217	.127
$B_{5/4,1/4}$	.074	.098	.369	.287	.052	.256	.165

TABLE 5. Summary of rms analysis errors at 10 days, for runs  $A_{KB}$  ,  $A_{2,0}$  ,  $B_{KB}$  , and  $B_{5/4,1/4}$  .

# FIGURE CAPTIONS

Figure 1. An illustration of meteorological observations available at or near 1200 GMT, January 9, 1979. The various observing systems, as well as the error structures of data they provide, are described in Section 1.2. This figure is reproduced from the preface of Bengtsson et al. (1981), by permission of the publisher.

Figure 2. A schematic representation of three projections onto the slow-wave subspace  $R$ . As discussed in Section 5.5, the projections do not coincide because the fast-wave subspace  $G$  is not orthogonal to the slow-wave subspace. The points labeled  $\Pi_{\parallel} \underline{x}$ ,  $\Pi_{\perp} \underline{x}$ , and  $\Pi_E \underline{x}$  are, respectively, the parallel projection, the orthogonal projection, and the minimum-energy projection of a point  $\underline{x}$  onto the slow-wave subspace.

Figure 3. Time history of the state estimates  $\underline{w}_k^f$  at three locations, for the experiment using the standard KB filter. The selected locations are labeled SF (for San Francisco,  $x = -7\Delta x$ ), NY (for New York,  $x = 0 \Delta x$ ), and HA (for Hawaii,  $x = 5 \Delta x$ ). Figure 3a shows the  $u$ -component of velocity, Figure 3b shows the  $v$ -component of velocity, and Figure 3c shows the geopotential  $\phi$ . Notice the slow waves with a period of approximately 6 days, upon which are superimposed smaller-amplitude fast waves.

Figure 4. Same as Figure 3, but for the experiment with the modified KB filter. The fast waves have been completely eliminated and the state estimates evolve slowly.

Figure 5. Components of the expected rms estimation error, for the experiment with the standard KB filter. Figure 5a shows the expected rms error over land, Figure 5b over the ocean, and Figure 5c over the entire domain. The individual curves are labeled U, V, P and E, for



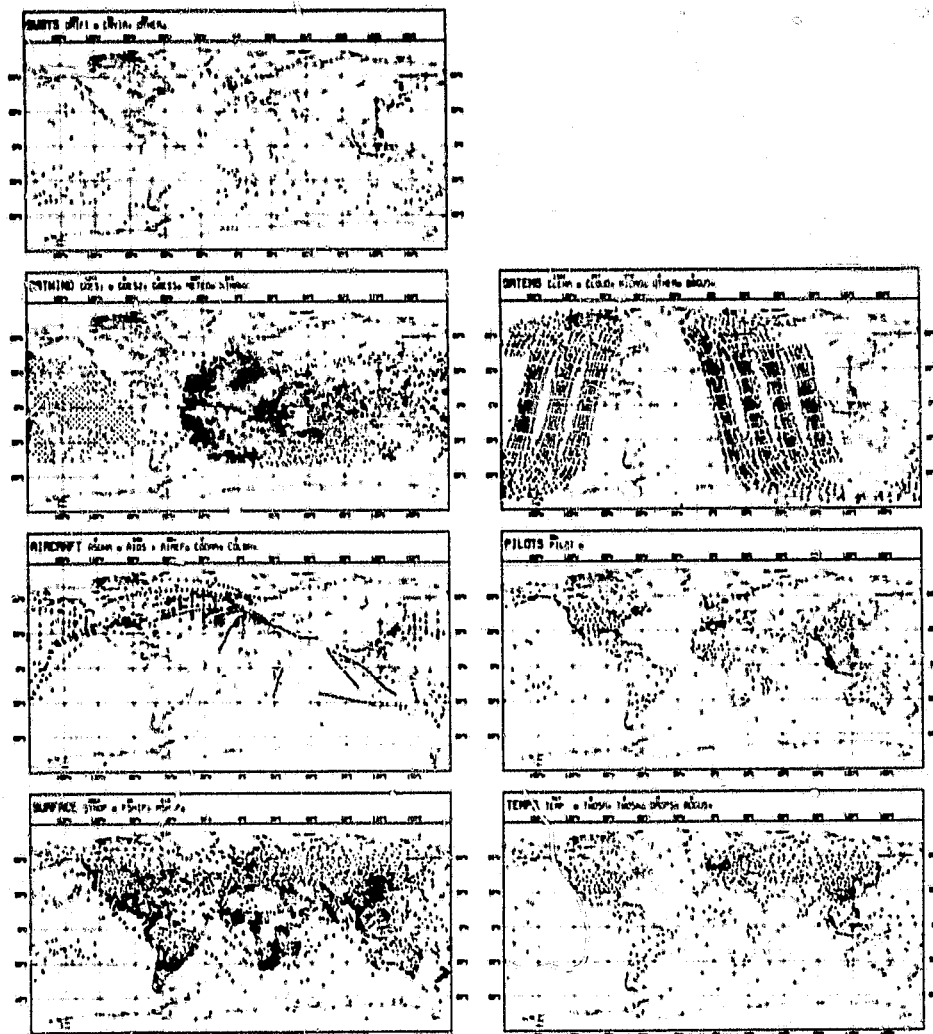
the expected rms error in  $u$ ,  $v$ ,  $\phi$  and the total energy, averaged over the indicated region. The error at synoptic times decreases immediately over land, and more gradually over the ocean. In between synoptic times, the error over land increases more sharply than the error over the ocean, due to advection of error from over the data-sparse ocean. Each curve converges rapidly to a periodic function.

Figure 6. Same as Figure 5, but for the experiment using the modified KB filter. Estimation errors in this case are nearly identical to those resulting from use of the standard KB filter, except that the  $u$ -component errors now increase slightly with time. This is due to the fact that, since the slow-wave subspace is quasigeostrophic, the modified filter allows almost no observational correction to be performed on the  $u$ -components.

Figure 7. Influence functions of selected observation stations at 10 days, or  $k = 480$  time steps, for the experiment with the standard KB filter. The influence functions of an observation station are obtained from columns of  $K_k^{KB}$ ; they show the weight give to an observation of  $u$ ,  $v$  or  $\phi$  at that station when updating points throughout the domain. Grid points are indicated by tick marks on the horizontal axis; the horizontal parallel lines and vertical dashed lines indicate the observed region, or land. The selected observation stations are SL (for Saint Louis,  $x = -3\Delta x$ ), SF and NY (see Figure 3). The nine panels, 7a-7i, give the influence of (a)  $u$  observations on  $u$  corrections, (b)  $v$  on  $u$ , (c)  $\phi$  on  $u$ , (d)  $u$  on  $v$ , (e)  $v$  on  $v$ , (f)  $\phi$  on  $v$ , (g)  $u$  on  $\phi$ , (h)  $v$  on  $\phi$ , (i)  $\phi$  on  $\phi$ . Particularities of the curves are discussed in Sec. 6.2.

Figure 8. Same as Figure 7, but at the first synoptic time,  $k = 24$  time steps. The influence functions here are much more symmetric than those in Figure 7. Comparison of these two figures allows one to distinguish between the effect of inhomogeneous data density and the effect of advection of information, as discussed in the text.

Figure 9. Plots of  $\phi-\phi$  and  $v-v$  forecast error correlation functions. Figures 9a,b show the correlation functions  $C_{1,i+j}^{\phi\phi}$  and  $C_{1,i+j}^{vv}$ , respectively, which are prescribed in OI, cf. Eqs. (7.10a,b). These two plots are generated by evaluating  $C_{1,i+j}^{\bullet\bullet}$  at the grid points  $x^j$ ,  $j = -8, -7, \dots, 7, 8$ ;  $C_{1,i+j}^{\bullet\bullet}$  is homogeneous, or independent of the base point  $x_1$ . Figures 9c,d show the true  $\phi-\phi$  and  $v-v$  forecast error correlation functions, respectively, computed from  $P_k^f$  at 10 days, for run  $A_1$ . These correlation functions are drawn for the base points SL ( $x^1 = -3 \Delta x$ ), HA ( $x^1 = 5 \Delta x$ ) and LN ( $x^1 = 8 \Delta x$ ). Figures 9e,f show the same correlation functions as Figures 9c,d, but for the initialized run  $B_1$ . Comparison of the prescribed and true correlation functions helps explain the results of the OI experiments which are summarized in Table 4.



Abbreviations used:

Airops	Standard wind observations from aircraft
Asdars, Aids	High quality wind observations from aircraft
Buoys	Surface pressure observations from drifting buoys
Colb	Constant level balloons
Drops	Radiosondes dropped from aircraft
Pilots	Wind measurements from ascending balloons
Satems	Temperature measurements from polar orbiting satellites
Satwind	Cloud drift wind measurements from geostationary satellites
Ships	Surface observations from ships
Synops	Surface observations from land
Temps	Temperature, humidity and wind measurements from radiosondes

Figure 1

ORIGINAL PAGE IS  
OF POOR QUALITY

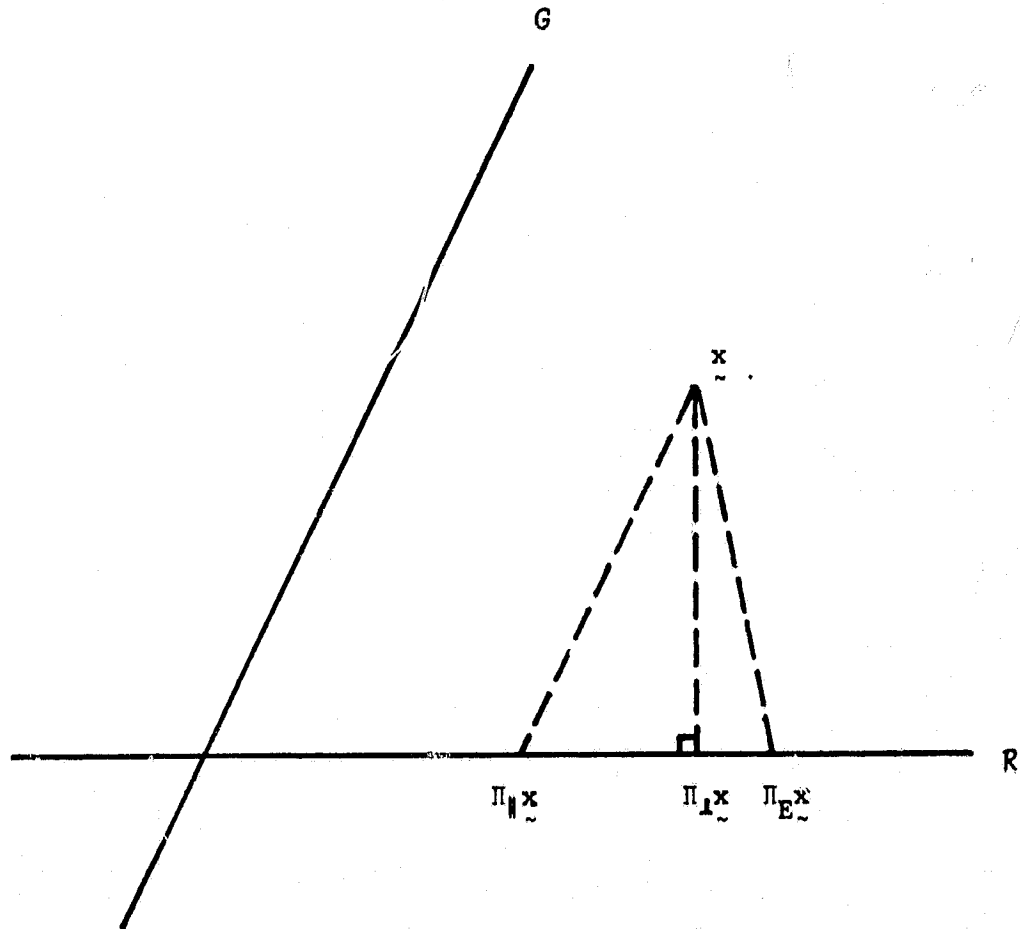


Figure 2

ORIGINAL PAGE IS  
OF POOR QUALITY

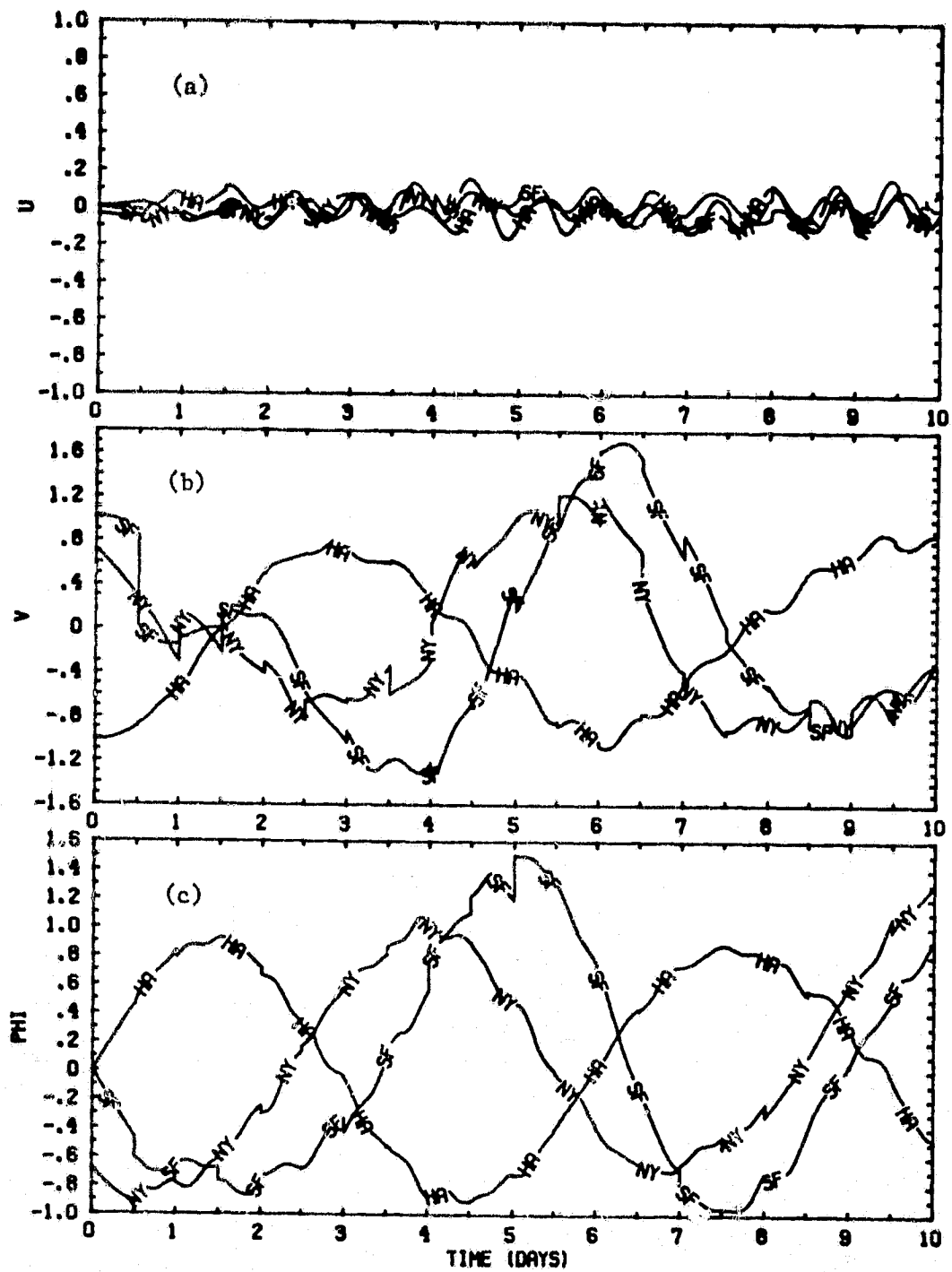


Figure 3

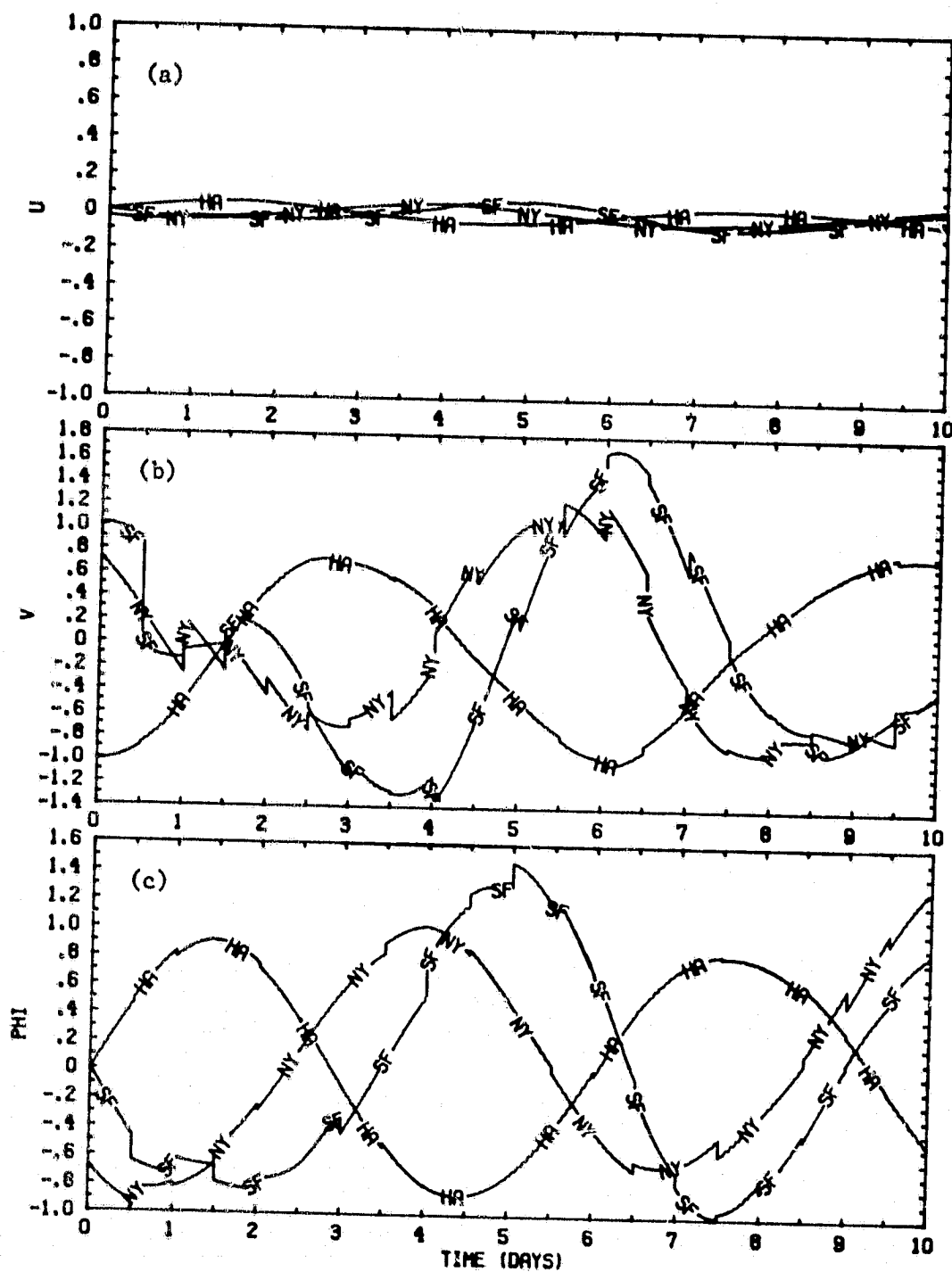


Figure 4

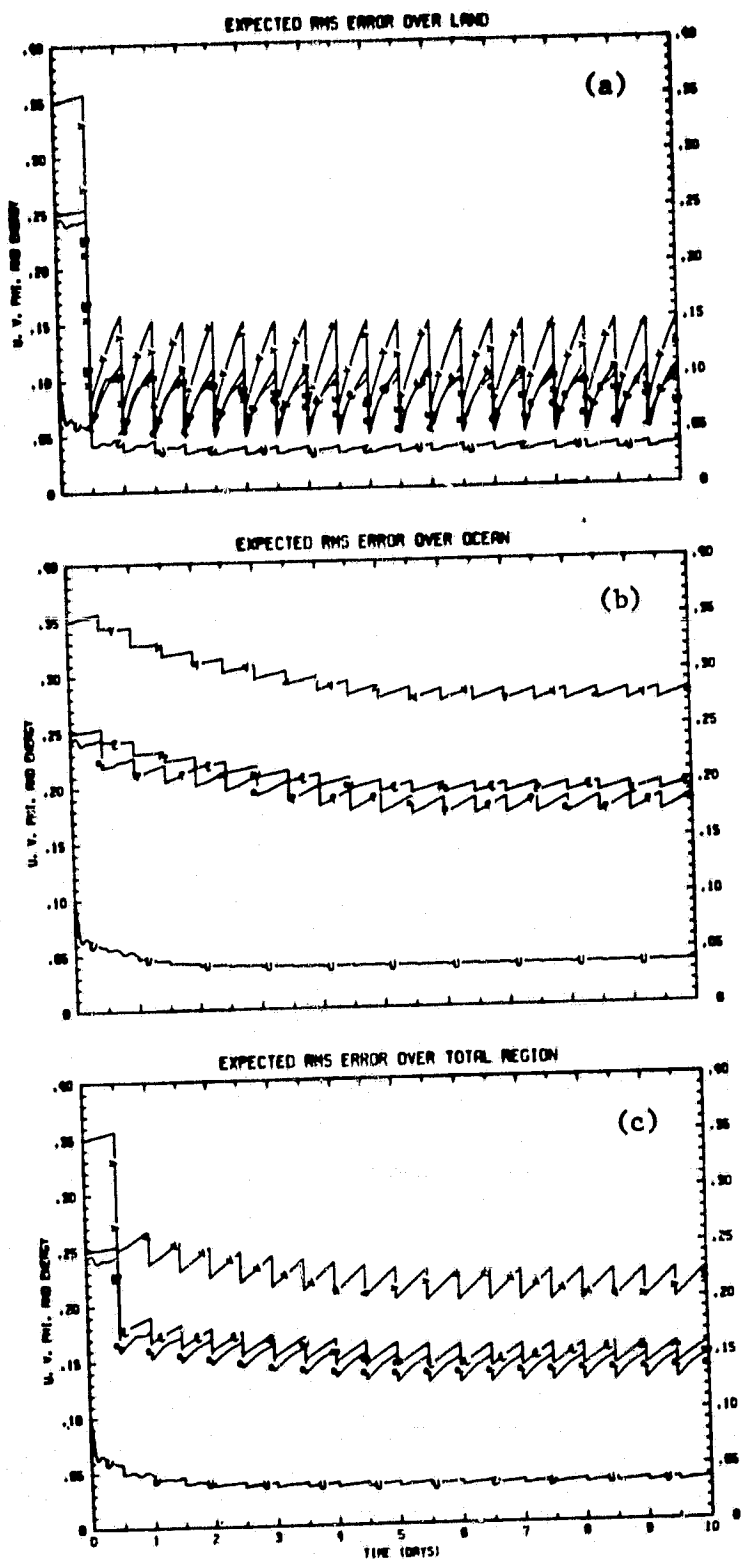


Figure 5

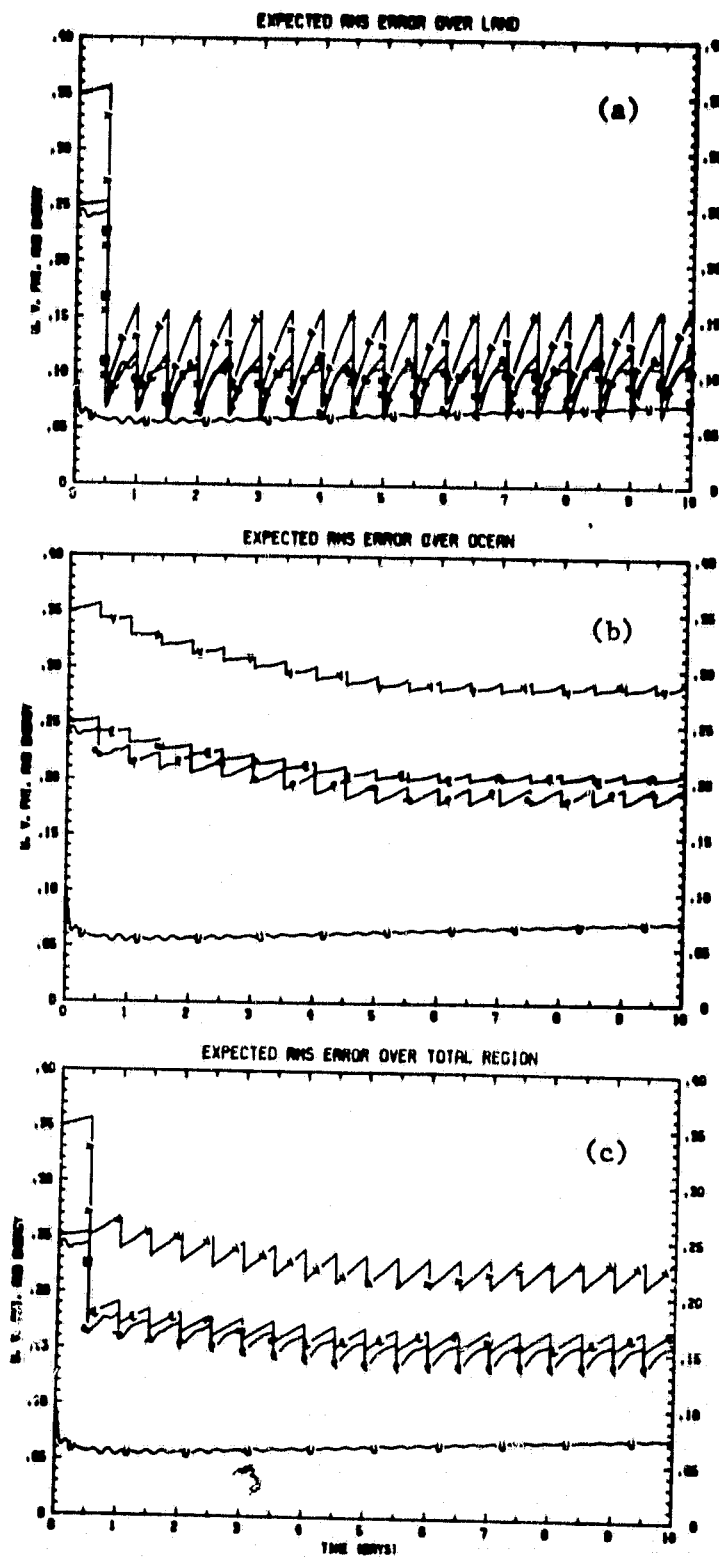


Figure 6



ORIGINAL PAGE IS  
OF POOR QUALITY

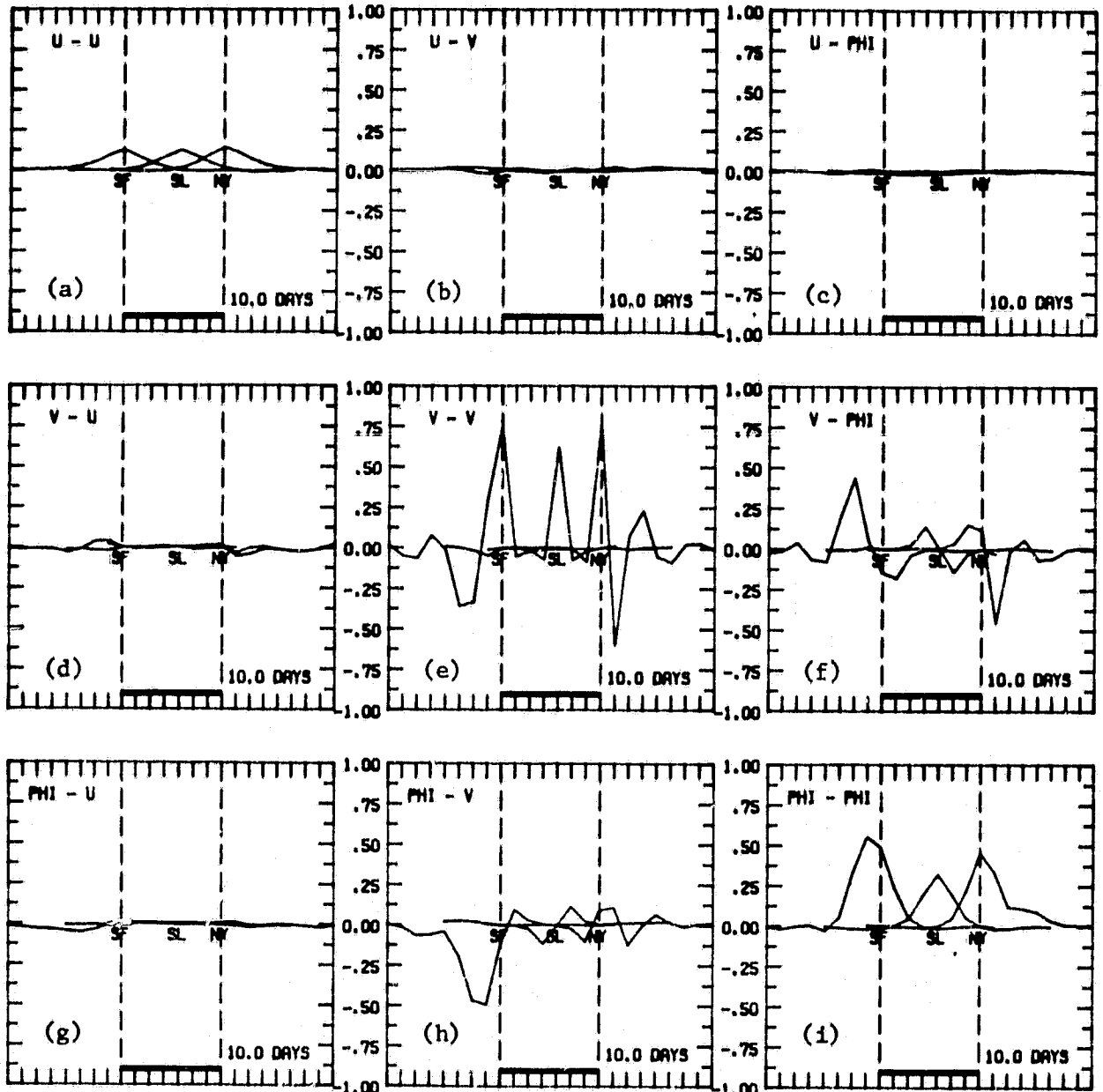


Figure 7

ORIGINAL PAGE IS  
OF POOR QUALITY

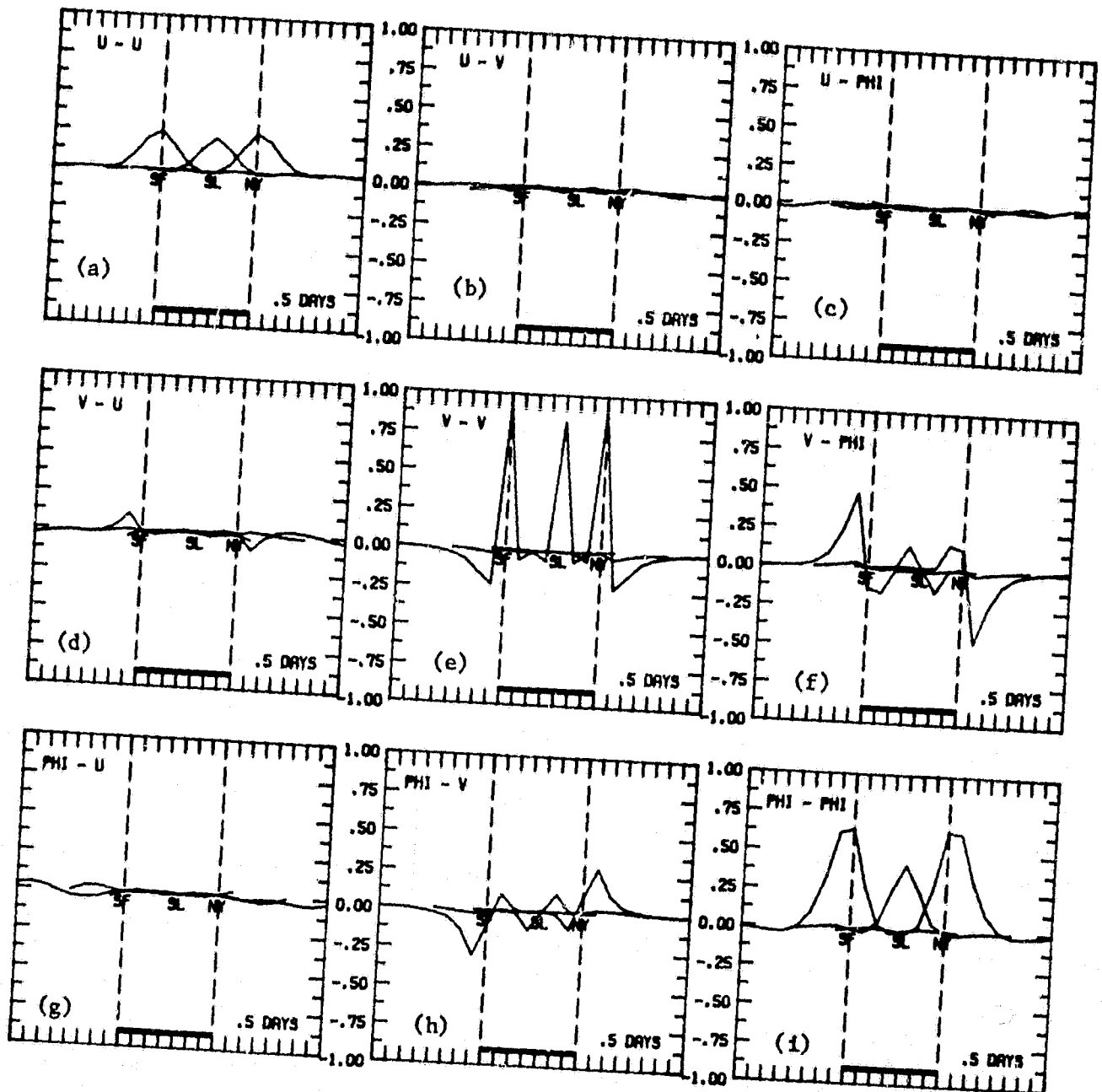


Figure 8

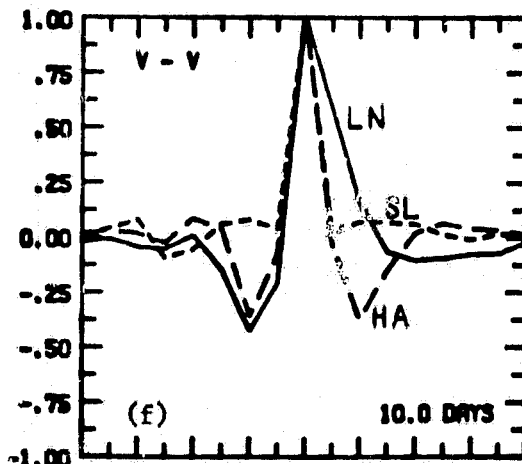
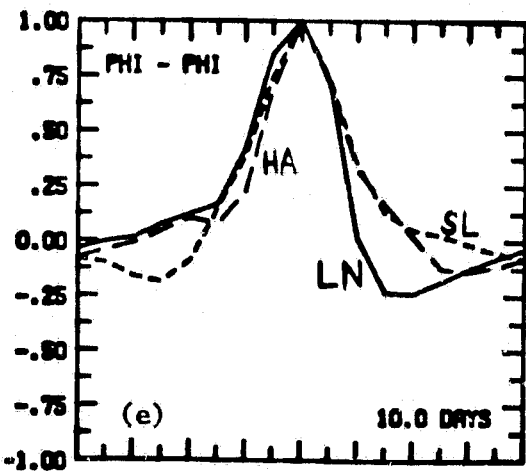
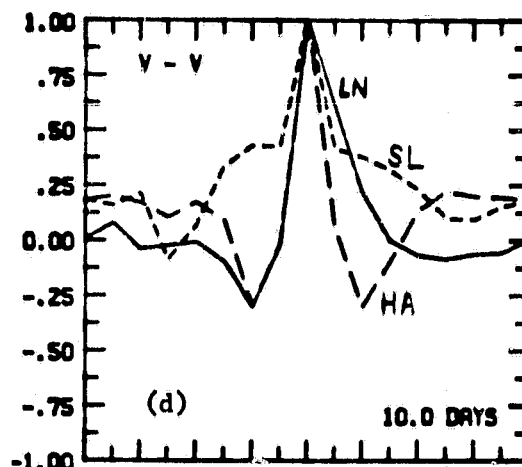
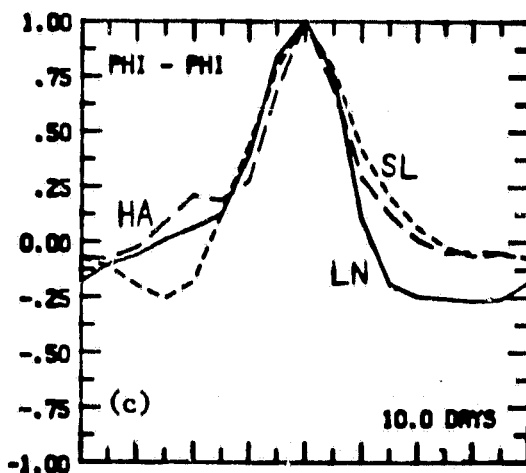
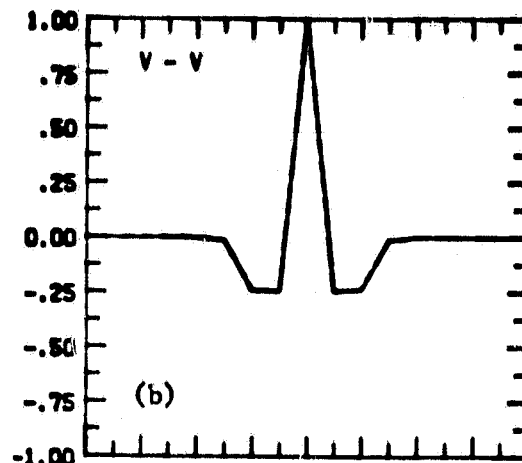
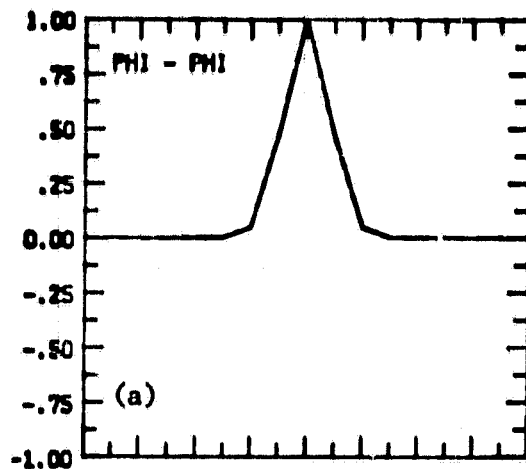


Figure 9